

The role of advanced imaging in Transcatheter Aortic Valve Implantation

**De rol van geavanceerde beeldvorming rondom
percutane aortaklepverving**

Apostolos Tzikas

ISBN 978-960-93-2840-1

The role of advanced imaging
in Transcatheter Aortic Valve Implantation

© 2011 Copyright of the published articles is with the corresponding journal or otherwise with the author. No part of this book may be reproduced, stored in a retrieval system, or transmitted in any form or by any means without the permission of the author or the corresponding journal.

Front cover: The Heart Nebula, in the constellation of Cassiopeia, is seen from NASA's Wide-field Infrared Survey Explorer, or WISE.

Produced in Thessaloniki, Greece by Ziti Publications

The role of advanced imaging in transcatheter aortic valve implantation

De rol van geavanceerde beeldvorming rondom
percutane aortaklepverving

Proefschrift

ter verkrijging van de graad van doctor aan de
Erasmus Universiteit Rotterdam
op gezag van de
rector magnificus

Prof.dr. H.G. Schmidt

en volgens besluit van het College voor Promoties.

De openbare verdediging zal plaatsvinden op
donderdag 21 april 2011 om 11:30 uur

door

Apostolos Tzikas
geboren in Thessaloniki, Griekenland



Promotiecommissie

Promotor: Prof.dr. P.W.J.C. Serruys

Overige leden:

Prof.dr. P.J. de Feyter

Prof.dr. F. Zijlstra

Dr. F.J. ten Cate

Copromotoren:

Dr. P.P.T. de Jaegere

Dr. M.L. Geleijnse

Financial support by the
Netherlands Heart Foundation
for the publication of this thesis
is gratefully acknowledged.

To Katerina and Zoi

Chapter 1. General introduction and outline of the thesis 9

Part I Pathophysiology of Aortic Stenosis

Chapter 2. Left ventricular twist and untwist in aortic stenosis 15

Chapter 3. Assessment of subendocardial ischemia in aortic stenosis: a study using speckle tracking echocardiography 29

Part II Imaging of the aortic root in the planning and during Transcatheter Aortic Valve Implantation

Chapter 4. Assessment of the aortic annulus by multi-slice computed tomography, contrast aortography and trans-thoracic echocardiography in patients referred for transcatheter aortic valve implantation 45

Chapter 5. Optimal projection estimation for transcatheter aortic valve implantation based on contrast aortography: validation of a prototype software 59

Part III Advanced imaging in the evaluation of Transcatheter Aortic Valve Implantation

Chapter 6. Determinants on MSCT of paravalvular aortic regurgitation after transcatheter aortic valve implantation 71

Chapter 7. Frequency of conduction abnormalities following transcatheter aortic valve implantation with the Medtronic-CoreValve and the effect on left ventricular ejection fraction 89

Chapter 8. Prosthesis-patient mismatch following transcatheter aortic valve implantation with the CoreValve Revalving System in patients with aortic stenosis 101

Chapter 9. Changes in mitral regurgitation after transcatheter aortic valve im-plantation	113
Chapter 10. Left ventricular mass regression one year after transcatheter aortic valve implantation	127
Summary and conclusions – Samenvatting en conclusies	141
Acknowledgements	147
List of publications	151
Curriculum vitae	155

Chapter 1

General introduction and outline of the thesis

Aortic stenosis, currently the most prevalent valvular heart disease in Europe [1], is an important public health problem, affecting thousands of patients every year. While surgical aortic valve replacement is still considered the “gold standard” treatment [2-4], recent innovations in transcatheter valve therapies have offered an attractive alternative: transcatheter aortic valve implantation (TAVI). In 2002, Cribier et al. announced the first human case description of a percutaneously implanted heart valve in a patient suffering from severe aortic stenosis [5]. Since then, the number of patients that undergo TAVI has increased exponentially. Preliminary early and midterm results following TAVI have been promising [6-9]. However, despite satisfactory hemodynamic results, TAVI procedures still face important safety issues such as paravalvular leaks, vascular complications, stroke, conduction disorders and the need for pacemaker implantation. Currently, TAVI is offered only to patients who are considered high risk candidates for surgical aortic valve replacement.

A fundamental characteristic of percutaneous interventions is the lack of direct visualization of the target organ/tissue. Consequently, interventional cardiology is greatly related to and depending on imaging. Especially in TAVI, which is entering the field of traditional valve surgery, the role of multimodality cardiac imaging is mandatory. Contrast aortography, multi slice computed tomography (MSCT), magnetic resonance imaging and echocardiography can provide a detailed characterisation of vascular anatomy, aortic root dimensions, aortic valve calcifications and left ventricular (LV) function. The use of these imaging techniques is invaluable for patient selection and planning of the procedure. In addition, some techniques can be used during the operation to guide the implantation, as well as after the procedure to evaluate the positioning and function of the prosthesis.

TAVI is a fascinating technology but it is still in its infancy. Further studies are needed in order to understand and modulate TAVI. The aim of the present thesis is to investigate the role of advanced cardiac imaging for TAVI.

In Part I (Chapters 2 and 3), we look into the pathophysiology of aortic stenosis using speckle tracking echocardiography, which is a new echocardiographic imaging modality that is able to relatively angle-independently quantify myocardial wall motion. In Chapter 2, LV rotation parameters are compared between patients with aortic stenosis and age-matched healthy controls. In Chapter 3, speckle tracking echocardiography is used for the assessment of subendocardial contractile function in aortic stenosis.

Part II (Chapters 4 and 5) comprises two papers related to the anatomy of the aortic root. Chapter 4 describes a comparison between MSCT, contrast aortography and trans-thoracic echocardiography in the assessment of the aortic annulus. In Chapter 5, we validate a prototype software which is designed to estimate the best fluoroscopic working view during TAVI.

Part III (Chapters 6 to 10) includes five publications related to the evaluation of patients following TAVI. In Chapter 6, MSCT is used to investigate the determinants of paravalvular aortic regurgitation. The vexing issue of conduction abnormalities following TAVI in relation to LV systolic function is explored in Chapter 7. Prosthesis-patient mis-

match after TAVI (i.e. the situation when the prosthetic valve is too small in relation to the patient's body size) is examined in Chapter 8. In Chapter 9, we investigate the changes in mitral regurgitation severity (which commonly accompanies aortic stenosis) following TAVI, and Chapter 10 shows the effects of TAVI on LV mass one year after the procedure.

REFERENCES

1. Lung B, Baron G, Butchart EG, Delahaye F, Gohlke-Bärwolf C, Levang OW, Tornos P, Vanoverschelde JL, Vermeer F, Boersma E, Ravaut P, Vahanian A. A prospective survey of patients with valvular heart disease in Europe: the Euro Heart Survey on Valvular Heart Disease. *Eur Heart J* 2003;24:1231-43.
2. Bonow RO, Carabello BA, Kanu C, de Leon AC Jr, Faxon DP, Freed MD, Gaasch WH, Lytle BW, Nishimura RA, O'Gara PT, O'Rourke RA, Otto CM, Shah PM, Shanewise JS, Smith SC Jr, Jacobs AK, Adams CD, Anderson JL, Antman EM, Faxon DP, Fuster V, Halperin JL, Hiratzka LF, Hunt SA, Lytle BW, Nishimura R, Page RL, Riegel B. ACC/AHA 2006 guidelines for the management of patients with valvular heart disease: a report of the American College of Cardiology/American Heart Association Task Force on Practice Guidelines (Writing Committee to Revise the 1998 Guidelines for the Management of Patients With Valvular Heart Disease). *Circulation* 2006;114:e84-e231.
3. Vahanian A, Alfieri O, Al-Attar N, Antunes M, Bax J, Cormier B, Cribier A, De Jaegere P, Fournial G, Kappetein AP, Kovac J, Ludgate S, Maisano F, Moat N, Mohr F, Nataf P, Pierard L, Pomar JL, Schofer J, Tornos P, Tuzcu M, van Hout B, Von Segesser LK, Walther T. Transcatheter valve implantation for patients with aortic stenosis: a position statement from the European association of cardio-thoracic surgery (EACTS) and the European Society of Cardiology (ESC), in collaboration with the European Association of Percutaneous Cardiovascular Interventions (EAPCI). *EuroIntervention* 2008;4:193-9.
4. Kvidal P, Bergström R, Hörte LG, Ståhle E. Observed and relative survival after aortic valve replacement. *J Am Coll Cardiol* 2000;35:747-56.
5. Cribier A, Eltchaninoff H, Bash A, Borenstein N, Tron C, Bauer F, Derumeaux G, Anselme F, Laborde F, Leon MB. Percutaneous transcatheter implantation of an aortic valve prosthesis for calcific aortic stenosis: first human case description. *Circulation* 2002;106:3006-8.
6. Grube E, Buellesfeld L, Mueller R, et al. Progress and current status of percutaneous aortic valve replacement: results of three device generations of the CoreValve Revalving system. *Circ Cardiovasc Interv* 2008;1:167-75.
7. Piazza N, Grube E, Gerckens U, et al. Procedural and 30-day outcomes following transcatheter aortic valve implantation using the third generation (18 Fr) corevalve revalving system: results from the multicentre, expanded evaluation registry 1-year following CE mark approval. *EuroIntervention* 2008;4:242-9.
8. Cribier A, Eltchaninoff H, Tron C, et al. Treatment of calcific aortic stenosis with the percutaneous heart valve: mid-term follow-up from the initial feasibility studies: the French experience. *J Am Coll Cardiol* 2006;47:1214-23.
9. Rodés-Cabau J, Webb JG, Cheung A, et al. Transcatheter aortic valve implantation for the treatment of severe symptomatic aortic stenosis in patients at very high or prohibitive surgical risk: acute and late outcomes of the multicenter Canadian experience. *J Am Coll Cardiol* 2010;55:1080-90.

Part

I

PATHOPHYSIOLOGY
OF AORTIC STENOSIS

Chapter 2

Left Ventricular Twist and Untwist in Aortic Stenosis

van Dalen BM

Tzikas A

Soliman OII

Kauer F

Heuvelman HJ

Vletter WB

Ten Cate FJ

Geleijnse ML

Int J Cardiol. 2009; in press

ABSTRACT

Background: To optimally exploit the potential added diagnostic and prognostic value of new left ventricular (LV) deformation parameters, better understanding of LV mechanics in aortic stenosis (AS) is warranted. We sought to determine a broad spectrum of LV rotation parameters in AS patients and age-matched healthy controls, in order to gain insight into the mechanical properties of the LV in AS.

Methods: The study comprised 48 AS patients with an aortic valve area $<2.0 \text{ cm}^2$ and LV ejection fraction $>50\%$, and 24 healthy – for age and gender matched – control subjects. LV peak systolic rotation (Rot_{max}), LV peak systolic twist ($\text{Twist}_{\text{max}}$), untwisting rate (*mean* diastolic untwisting velocity from $\text{Twist}_{\text{max}}$ to mitral valve opening), *peak* diastolic untwisting velocity, and *time-to-peak* diastolic untwisting velocity were determined by speckle tracking echocardiography.

Results: AS patients had normal basal Rot_{max} and increased apical Rot_{max} , resulting in increased $\text{Twist}_{\text{max}}$ ($13.4 \pm 4.0^\circ$ vs. $11.4 \pm 2.7^\circ$, $P < 0.05$). Apical Rot_{max} and $\text{Twist}_{\text{max}}$ correlated significantly to echo-Doppler indicators of AS severity. Time-to-peak diastolic untwisting velocity was increased ($20 \pm 10\%$ vs. $15 \pm 9\%$, $P < 0.05$) and untwisting rate was decreased ($-38 \pm 21^\circ/\text{s}$ vs. $-50 \pm 28^\circ/\text{s}$, $P < 0.01$) in AS patients.

Conclusions: $\text{Twist}_{\text{max}}$ increases proportionally to the severity of AS, which might serve as a compensatory mechanism to maintain systolic LV function. LV diastolic untwisting is delayed and the untwisting rate is reduced in AS.

INTRODUCTION

The timing of aortic valve replacement in patients with severe aortic stenosis (AS) is based on symptoms and left ventricular (LV) ejection fraction [1]. Newer LV deformation parameters, such as strain and rotation, may serve as better estimates of LV function [2]. However, to optimally exploit the added value of these new parameters, better understanding of LV mechanics in AS is warranted. In previous tagged magnetic resonance imaging (MRI) studies changes in LV rotation parameters in AS patients have been described [3–6]. However, these studies were limited by small numbers of patients [3–6] and not for age-matched control subjects [4–6]. Since LV rotation parameters are known to be influenced by age [7,8], the latter is a serious limitation. Speckle tracking echocardiography (STE) is a new imaging modality that is able to assess LV rotation [9,10]. The purpose of the current study was to determine a broad spectrum of LV rotation parameters in a large group of AS patients compared to age-matched healthy controls, in order to gain insight into the mechanical properties of the LV in AS. In addition, LV rotation parameters were correlated to echocardiographic indicators of AS severity.

METHODS

Study participants

The study population consisted of 46 consecutive patients (mean age 65 ± 14 year, 26 men) referred for echocardiography because of a murmur or follow-up of known AS, in sinus rhythm, with an aortic valve area $< 2.0 \text{ cm}^2$, normal LV ejection fraction ($> 50\%$), and good echocardiographic image quality that allowed for complete segmental assessment of LV rotation at both the basal and apical LV level, and without moderate to severe mitral regurgitation. During the enrolment of these 46 patients, 26 other patients (36%) were excluded because of suboptimal echocardiographic image quality not fulfilling this criterion or the presence of atrial fibrillation. Of the 46 included patients, 33 (72%) were symptomatic (dyspnoea in 23 [50%], angina in 12 [26%], and collapse in 1 [2%]). Mild mitral regurgitation was present in 14 patients (30%). The AS patients were compared to 23 healthy – for age and gender matched – control subjects in sinus rhythm, without hypertension, diabetes, or regular use of medication for cardiovascular disease, and with normal left atrial dimensions, LV dimensions, LV ejection fraction and LV diastolic function for age (in elderly subjects > 60 years an impaired relaxation pattern [grade 1 diastolic dysfunction, defined as: E/A ratio < 0.75 and E-wave velocity deceleration time > 240 ms] was not considered abnormal). Control subjects were recruited from our department

(personnel) or were family members or friends. The study protocol conformed to the ethical guidelines of the 1975 Declaration of Helsinki as reflected in a priori approval by the institution's review board and all subjects gave informed consent.

Echocardiography

Two-dimensional grayscale harmonic images were obtained in the left lateral decubitus position using a commercially available ultrasound system (iE33, Philips, Best, The Netherlands), equipped with a broadband (1–5 MHz) S5-1 transducer (frequency transmitted 1.7 MHz, received 3.4 MHz). All echocardiographic measurements were averaged from three heartbeats. From the M-mode recordings the following data were acquired: left atrial size, LV end-diastolic anteroseptal and inferolateral wall thickness, and LV end-diastolic and end-systolic dimension. LV mass was assessed with the two-dimensional area–length method [11]. LV ejection fraction was calculated from LV volumes by the modified biplane Simpson rule in accordance with the guidelines [11]. From the mitral-inflow pattern, peak early (E) and late (A) filling velocities, E/A ratio, and E-wave velocity deceleration time were measured. Tissue Doppler was applied end-expiratory in the pulsed-wave Doppler mode at the level of the inferoseptal side of the mitral annulus from an apical 4-chamber view. To acquire the highest wall tissue velocities, the angle between the Doppler beam and the longitudinal motion of the investigated structure was adjusted to a minimal level. The spectral pulsed-wave Doppler velocity range was adjusted to obtain an appropriate scale. The timing of the beginning and ending of the isovolumic relaxation time were determined using pulsed wave Doppler. Aortic valve areas were calculated by the continuity equation and also indexed by body surface areas, calculated using the Mosteller formula [12]. The severity of aortic and mitral regurgitation was determined according to the guidelines [13].

To optimize STE, images were obtained at a frame rate of 60 to 80 frames/s. Parasternal short-axis images at the LV basal level (showing the tips of the mitral valve leaflets) with the cross section as circular as possible were obtained from the standard parasternal position, defined as the long-axis position in which the LV and aorta were most in-line with the mitral valve tips in the middle of the sector. To obtain a short-axis image at the LV apical level (just proximal to the level with end-systolic LV luminal obliteration) the transducer was positioned 1 or 2 intercostal spaces more caudal as previously described by us [14]. From each short-axis image, three consecutive end-expiratory cardiac cycles were acquired and transferred to a QLAB workstation (Philips, Best, The Netherlands) for off-line analysis.

Speckle tracking analysis

Analysis of the datasets was performed using QLAB Advanced Quantification Software version 6.0 (Philips, Best, The Netherlands), which was recently validated against MRI for assessment of LV twist [10]. To assess LV rotation, six tracking points were placed man-

ually (after gain correction) on the mid-myocardium on an end-diastolic frame in each parasternal short-axis image. Tracking points were separated about 60° from each other and placed on 1 (30°, anteroseptal insertion into the LV of the right ventricle), 3 (90°), 5 (150°), 7 (210°), 9 (270°, inferoseptal insertion into the LV of the right ventricle), and 11 (330°) o' clock to fit the total LV circumference (Fig. 1).

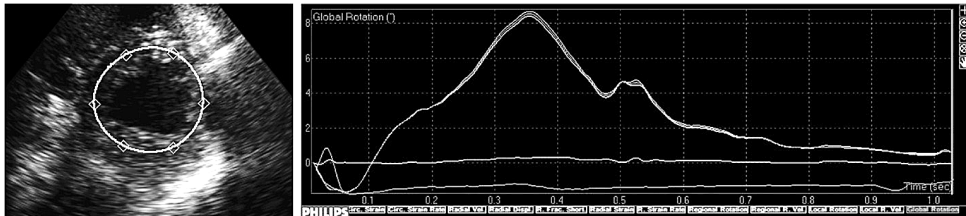


Figure 1. *Left.* Positioning of the tracking points at the left ventricular apical level. *Right.* Left ventricular rotation–time curve (x-axis: time in ms; y-axis: left ventricular apical rotation in degrees). The grey line represents left ventricular apical rotation (peak systolic rotation 8.2°), and the white line recruitment, which was not activated in this example. The electrocardiogram is displayed at the bottom.

Data were exported to a spreadsheet program (Excel, Microsoft Corporation, Redmond, WA) to determine LV peak systolic rotation during ejection (Rot_{max}), time to Rot_{max} (from R wave to Rot_{max}), instantaneous LV peak systolic twist ($Twist_{max}$, defined as the maximal value of instantaneous apical systolic rotation–basal systolic rotation), time to $Twist_{max}$ (from R wave to $Twist_{max}$), and LV untwisting at 5%, 10%, 15%, and 50% of diastole. The degree of untwisting was expressed as a percentage of maximum systolic twist:

$$\text{untwisting} = (Twist_{max} - Twist_t) / Twist_{max} \times 100\%$$

where $Twist_t$ is twist at time. Furthermore, peak systolic rotation velocity and peak diastolic de-rotation velocity, peak systolic twist velocity and peak diastolic untwist velocity, and the timing of these parameters were assessed. Normalized velocities were determined by correcting for Rot_{max} or $Twist_{max}$. Finally, untwisting rate was defined as the mean diastolic untwisting velocity from peak systolic twist to mitral valve opening and calculated as: (twist at mitral valve opening–peak systolic twist)/time interval from peak systolic twist to mitral valve opening. To adjust for intra- and intersubject differences in heart rate, the time sequence of systolic and diastolic events was normalized to the percentage of systolic and diastolic duration, respectively. End-systole was defined as the point of aortic valve closure. In each study it was verified that heart rate for the cardiac cycle in which the timing of aortic valve closure was assessed, was the same as the cardiac cycle used for analysis of LV rotation parameters.

Statistical analysis

Matching of controls and AS patients was achieved by randomly matching each control with two AS patients with the same sex and age ± 5 years. Measurements are presented as

mean±SD. Variables were compared using Student's t test, or Chi-square test when appropriate. Kolmogorov–Smirnov test with Lilliefors significance correction was used for testing normality of distribution. The homogeneity of variance in the data for AS patients and control subjects was checked with Levene's test. Relations between parameters were assessed using Pearson's and Spearman's test for parametric and nonparametric correlations. A P value <.05 was considered statistically significant. Intraobserver and interobserver variability for LV twist in our center are 6%±6% and 9%±5%, respectively [15].

RESULTS

Characteristics of the study population

In Table 1, the clinical and echocardiographic characteristics of the study population are shown. On average, AS was moderate-to-severe with a mean jet velocity of 3.9±0.9 m/s, a mean gradient of 41±20 mmHg, an aortic valve area of 1.0±0.5 cm², and an aortic valve

Table 1. *Clinical and echocardiographic characteristics of the study population.*

	Control subjects (n=23)	Aortic stenosis patients (n=46)	P value
Clinical characteristics			
Age, year	61±7	65±14	0.117
Male, n (%)	12 (54)	25 (54)	0.330
Heart rate, bpm	60±11	67±11	0.015
Hypertension, n (%)	0	9 (20)	0.054
Diabetes, n (%)	0	5 (11)	0.245
Coronary artery disease, n (%)	0	18 (39)	0.002
Echocardiographic characteristics			
Left atrial size, cm	3.8±0.5	4.4±0.9	0.004
Left ventricular mass, g	162±54	236±112	0.004
Left ventricular ejection fraction, %	60±8	56±8	0.054
E, cm/s	60±11	81±30	0.002
A, cm/s	69±17	89±30	<0.001
E/A ratio	1.1±0.3	1.0±0.5	0.381
Deceleration time, ms	185±29	239±85	0.004
Em septal, cm/s	8.0±1.9	5.3±2.5	<0.001
E/Em ratio	8.4±2.2	17.4±9.4	<0.001
Aortic valve			
Velocity, m/s	1.3±0.3	3.9±0.9	<0.001
Mean gradient, mmHg	4±2	41±20	<0.001
Valve area, cm ²	3.0±0.4	1.0±0.5	<0.001
Valve area indexed by BSA, cm ² /m ²	1.60±0.23	0.45±0.27	<0.001
Regurgitation grade (1–4), mean	0.0±0.0	1.1±0.9	<0.001

Values are means ± SD. E = peak early phase filling velocity, A= peak atrial phase filling velocity, Em=peak early diastolic wave velocity, BSA =body surface area.

area indexed by body surface area of $0.45 \pm 0.27 \text{ cm}^2/\text{m}^2$. Heart rate, left atrial size and LV mass were increased in AS patients as compared to control subjects. E-wave and A-wave velocities, the E-wave velocity deceleration time, and the E/Em ratio were increased in AS patients as well, whereas the E/A ratio was comparable.

Systolic LV rotation parameters

AS patients had normal basal Rot_{max} and increased apical Rot_{max} , resulting in increased $\text{Twist}_{\text{max}}$ (Fig. 2). Apical peak systolic rotation velocity and peak systolic twist velocity were increased in AS patients, although these differences were lost when the velocities were normalized for apical Rot_{max} and $\text{Twist}_{\text{max}}$, respectively. The time to-peak systolic twist velocity was decreased in AS patients (Table 2).

Diastolic LV rotation parameters

AS patients had decreased untwisting at 10% and 15% of diastole. Furthermore, AS patients had normal basal peak diastolic de-rotation velocity, and increased apical peak diastolic de-rotation velocity, resulting in increased peak diastolic untwisting velocity.

Table 2. *Systolic left ventricular rotation parameters in aortic stenosis patients and control subjects.*

	Control subjects (n=23)	Aortic stenosis patients (n=46)	P value
Left ventricular basal level			
Rotmax, degree	-3.9±1.6	-3.8±2.3	0.852
Peak systolic rotation velocity, °/s	-42±10	-46±15	0.252
Normalized peak systolic rotation velocity, s ⁻¹	11.4±2.4	10.7±5.0	0.528
Time to Rotmax, %	94±12	92±12	0.516
Time-to-peak systolic rotation velocity, %	47±10	46±18	0.805
Left ventricular apical level			
Rotmax, degree	7.5±2.2	9.7±2.5	<0.001
Peak systolic rotation velocity, °/s	52±11	67±18	<0.001
Normalized peak systolic rotation velocity, s ⁻¹	7.9±3.0	7.4±3.2	0.535
Time to Rotmax, %	95±5	95±8	1.000
Time-to-peak systolic rotation velocity, %	51±14	47±18	0.354
Left ventricular twist			
Twistmax, degree	11.4±2.7	13.4±4.0	0.034
Peak systolic twist velocity, °/s	69±17	81±22	0.025
Normalized peak systolic twist velocity, s ⁻¹	6.4±1.0	6.7±1.7	0.438
Time to Twistmax, %	96±5	97±6	0.494
Time-to-peak systolic twist velocity, %	56±11	45±14	0.002

Values are means±SD. Normalized rotation and twist velocities adjusted for Rot_{max} and $\text{Twist}_{\text{max}}$, respectively. Time to peak as a percentage of duration of systole. Rot_{max} =left ventricular peak systolic rotation during ejection, $\text{Twist}_{\text{max}}$ =instantaneous left ventricular peak systolic twist.

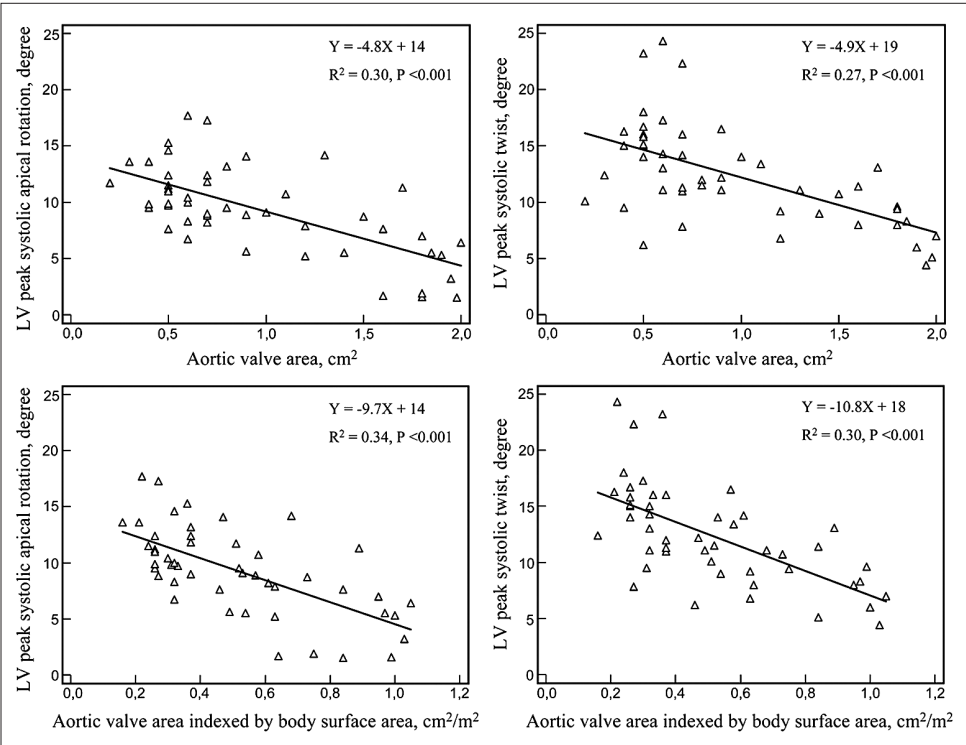
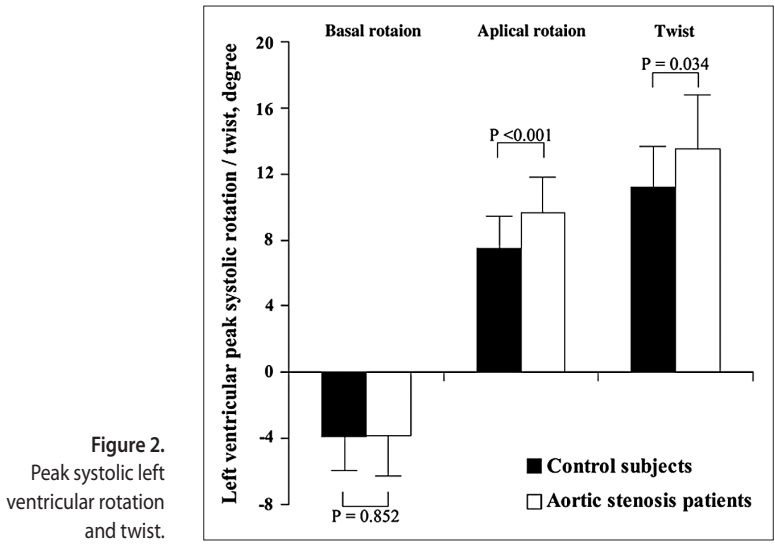


Figure 3. Linear regressions between aortic valve area and aortic valve area indexed by body surface area and left ventricular peak systolic apical rotation and twist.

However, again these differences were lost when apical peak diastolic de-rotation velocity and peak diastolic untwisting velocity were normalized for apical Rot_{max} and $Twist_{max}$, respectively. The time to-peak apical diastolic de-rotation velocity and time-to-peak diastolic untwisting velocity were increased in AS patients. Untwisting rate was decreased in AS patients (Table 3).

Table 3. Diastolic left ventricular rotation parameters in aortic stenosis patients and control subjects.

	Control subjects (n=23)	Aortic stenosis patients (n=46)	P value
Left ventricular basal level			
Peak diastolic de-rotation velocity, %/s	50±13	56±19	0.178
Normalized peak diastolic de-rotation velocity, s ⁻¹	-12.6±4.3	-12.5±10.3	0.965
Time-to-peak diastolic de-rotation velocity, %	17±11	23±14	0.077
Left ventricular apical level			
Peak diastolic de-rotation velocity, %/s	-62±23	-81±26	0.004
Normalized peak diastolic de-rotation velocity, s ⁻¹	-9.1±3.6	-9.4±5.2	0.805
Time-to-peak diastolic de-rotation velocity, %	11±7	22±13	<0.001
Left ventricular untwist			
Untwisting at 5% of diastole, %	14±6	12±8	0.294
Untwisting at 10% of diastole, %	30±13	22±15	0.033
Untwisting at 15% of diastole, %	43±17	32±18	0.017
Untwisting at 50% of diastole, %	70±10	68±14	0.544
Peak diastolic untwisting velocity, %/s	-89±22	-103±27	0.035
Normalized peak diastolic untwisting velocity, s ⁻¹	-8.7±2.4	-8.3±2.9	0.570
Time-to-peak diastolic untwisting velocity, %	15±9	20±10	0.042
Untwisting rate, %/s	-50±27	-37±21	0.031

Values are means±SD. Normalized de-rotation and untwist velocities adjusted for Rot_{max} and $Twist_{max}$, respectively. Time to-peak as a percentage of the duration of diastole.

Relations of LV rotation parameters to echocardiographic indicators of AS severity

Apical Rot_{max} and $Twist_{max}$ correlated positively to aortic valve jet velocity ($R^2=0.22$, and $R^2=0.21$, respectively, both $P=0.006$) and mean gradient ($R^2=0.19$, and $R^2=0.20$, respectively, both $P=0.005$), negatively to aortic valve area ($R^2=0.30$, and $R^2=0.27$, respectively, both $P<0.001$), and aortic valve area indexed by body surface area ($R^2=0.34$, and $R^2=0.30$, respectively, both $P<0.001$) (Fig. 3). To investigate the influence of the bimodally distributed patients group (relatively many patients had either severe or very mild AS) on these correlations, a separate analysis was performed in AS patients with an aortic valve area $<1.5\text{ cm}^2$. In this subgroup, all relationships remained identifiable (apical Rot_{max} and $Twist_{max}$ correlated positively to aortic valve jet velocity [$R^2=0.14$, $P=0.01$ and $R^2=0.13$, $P=0.02$, respectively] and mean gradient [both $R^2=0.12$, $P=0.02$], negatively to

aortic valve area [$R^2=0.20$, $P=0.006$ and $R^2=0.17$, $P=0.008$], and aortic valve area indexed by body surface area [$R^2=0.20$ and $R^2=0.19$, both $P=0.006$]. The only velocity parameter that was related to echocardiographic indicators of AS severity, was the time-to-peak apical de-rotation velocity (positively to aortic valve jet velocity [$R^2=0.24$, $P=0.008$], and aortic valve mean gradient [$R^2=0.18$, $P=0.02$], and negatively to aortic valve area [$R^2=0.20$, $P=0.007$] and aortic valve area indexed by body surface area [$R^2=0.22$, $P=0.009$]). LV mass was not related to any of the LV rotation parameters.

Mutual relations of LV rotation parameters

Basal and apical Rot_{max} correlated positively to basal ($R^2=0.61$, $P<0.001$) and apical ($R^2=0.46$, $P<0.001$) peak systolic rotation velocity, respectively, and to basal ($R^2=0.34$, $P=0.003$) and apical ($R^2=0.24$, $P<0.009$) peak diastolic de-rotation velocity, respectively. $\text{Twist}_{\text{max}}$ correlated positively to peak systolic twist velocity ($R^2=0.63$, $P<0.001$) and peak diastolic untwisting velocity ($R^2=0.45$, $P<0.001$).

DISCUSSION

This study sought to assess a broad spectrum of LV rotation parameters in a large group of AS patients compared to age-matched healthy controls and to correlate these parameters to echocardiographic indicators of AS severity. The main findings of this study are, 1) $\text{Twist}_{\text{max}}$ is increased in AS, driven by increased apical Rot_{max} , 2) this increased $\text{Twist}_{\text{max}}$ may facilitate maintenance of peak diastolic untwisting velocity, although overall untwisting is delayed and untwisting rate is decreased, and 3) apical Rot_{max} and $\text{Twist}_{\text{max}}$ are related to the severity of AS.

Systolic LV rotation in AS

LV twist is caused by the dynamic interaction between oppositely oriented subepicardial and subendocardial myocardial fibre helices and has an important role in LV ejection [16]. The direction of LV twist is governed by the subepicardial fibres, mainly owing to their longer arm of movement [17]. Subendocardial ischemia has long been recognized as an early sign of myocardial suffering from pressure overload caused by AS [18,19]. Apical Rot_{max} and $\text{Twist}_{\text{max}}$ were increased in AS patients, possibly because subendocardial ischemia diminishes the counteraction of the subendocardial myofibres. Another potential mechanism may be LV hypertrophy with an increased arm of force over which the subepicardial fibres work, although LV mass was not related to any of the LV rotation parameters in the current study. Nevertheless, both mechanisms may be expected to lead to increased basal Rot_{max} as well, supported by findings in a previous study in which increased basal Rot_{max} was found in hypertrophic cardiomyopathy patients [20]. The lack of increased basal Rot_{max} in the current study may be explained by stiffening of the atrioventricular valvular plane that might prevent basal Rot_{max} to increase.

The current study is the first to relate LV rotation parameters to echocardiographic indicators of AS severity. Apical Rot_{max} and $\text{Twist}_{\text{max}}$ correlated positively to aortic valve jet velocity and mean gradient, and negatively to aortic valve area and aortic valve area indexed by body surface area. This underlines the potential role of subendocardial ischemia as the cause of increased apical Rot_{max} and $\text{Twist}_{\text{max}}$ in AS since the severity of subendocardial ischemia is known to be related to the severity of AS [21]. We have previously shown that septal and lateral mitral annular velocities are reduced in patients with severe AS and normal LV ejection fraction [22]. Increased $\text{Twist}_{\text{max}}$ may serve as a compensatory mechanism to balance loss of LV myocardial contraction in other directions due to subendocardial ischemia. LV apical rotation, and in particular changes within one patient, may therefore provide an easy assessable marker of subendocardial ischemia. However, before large-scale clinical studies will be started, the relation between increased $\text{Twist}_{\text{max}}$ and subendocardial ischemia should be investigated in more detail, perhaps by using more objective measures of subendocardial ischemia, such as provided by contrast perfusion echocardiography.

In previous tagged MRI studies increased $\text{Twist}_{\text{max}}$ in AS patients has also been described [3–6]. However, these studies were limited by small numbers of patients [3–6] and not for age-matched control subjects [4–6]. It is well known that LV rotation parameters are influenced by age [7,8], so this latter is a serious limitation not present in our study. In other small tagged MRI studies, LV rotation parameters before and after aortic valve replacement were investigated [23,24]. Sandstede et al. [23] found that the compensating increased $\text{Twist}_{\text{max}}$ in AS patients declined with increasing LV hypertrophy and dilatation, and that aortic valve replacement led to normalization of $\text{Twist}_{\text{max}}$. The former may be a surprising finding since increasing LV hypertrophy would be expected to be accompanied by increasing subendocardial ischemia and a larger difference in lever arms between the subendocardial and subepicardial fibres, leading to a further increase in $\text{Twist}_{\text{max}}$. Sandstede et al. explained their finding by suggesting a reverse mechanism in which a smaller degree of compensating increased $\text{Twist}_{\text{max}}$ might result in more LV hypertrophy and dilatation. Biederman et al. [24] investigated the role of coronary artery disease and found that independent of the presence of concomitant coronary artery disease, $\text{Twist}_{\text{max}}$ decreased after aortic valve replacement. Finally, Tzemos et al. [25] studied women with congenital aortic stenosis and found that $\text{Twist}_{\text{max}}$ was increased in this population as well. Furthermore, during pregnancy, LV twist further increased in the antepartum period, except in those women who experienced functional deterioration requiring urgent aortic balloon valvuloplasty.

Diastolic LV rotation in AS

The LV myocardium adapts to increased pressure overload due to AS by hypertrophy of individual myocytes. In addition, this pathological hypertrophy is accompanied by interstitial and perivascular fibrosis, and thickening of the media of intramyocardial coronary

arteries [26]. Each of these factors in turn contributes to diastolic dysfunction commonly seen in AS patients [27,28]. In our study, LV untwist was delayed and the untwisting rate was reduced.

Normally, over 40% of diastolic LV untwisting has been completed after the first 15% of diastole, which contributes to the large pressure decrease during the isovolumic relaxation phase [29,30]. This early, rapid LV untwisting process may be supported by active and passive mechanisms. There is a temporal dispersion in endocardial and epicardial repolarization, with in early diastole still depolarized endocardial fibres (as opposite to the already repolarized epicardial fibres) that may actively untwist the LV (normally the action of these fibres are, as mentioned in the previous section, overruled by the epicardial fibres). However, the effective force of contraction of myocardial fibres is expected to be minimal during this part of the cardiac cycle. Nevertheless, dissimilarities of apparent stiffness of the endocardium and epicardium caused by differences in breakdown of actin-myosin cross-bridges may be of influence. Furthermore, high levels of stored potential energy from the active systolic twist are transformed into kinetic energy, adding a passive component to rapid early diastolic untwisting [31]. Subendocardial ischemia in AS patients may lead to loss of the active part of diastolic untwisting and the relaxation abnormality seen in AS patients may further compromise LV untwisting, evidenced by delayed and reduced early (and thus overall) LV untwisting. Surprisingly, peak diastolic untwisting velocity was higher in AS patients. This may be explained by the increased potential energy stored in the more twisted LV that will be released after all. This may lead to increased, but delayed, peak diastolic untwisting velocity, that may serve as a compensatory mechanism to help LV filling.

CONCLUSION

Twist_{\max} is increased in AS patients, proportionally to the severity of LV outflow obstruction. This increased Twist_{\max} might serve as a compensatory mechanism to maintain systolic function in the pressure overloaded LV. Conversely, LV untwist is delayed and the untwisting rate is reduced. However, the increase in Twist_{\max} may cause an (although delayed) increase in peak diastolic untwisting velocity that may partially compensate for the decrease in untwisting rate.

Acknowledgements

The authors of this manuscript have certified that they comply with the Principles of Ethical Publishing in the International Journal of Cardiology [32].

REFERENCES

1. Bonow RO, Carabello BA, Kanu C, et al. ACC/AHA 2006 guidelines for the management of patients with valvular Heart disease: a report of the American College of Cardiology/American Heart Association Task Force on Practice Guidelines (writing committee to revise the 1998 Guidelines for the Management of Patients With Valvular Heart Disease): developed in collaboration with the Society of Cardiovascular Anesthesiologists: endorsed by the Society for Cardiovascular Angiography and Interventions and the Society of Thoracic Surgeons. *Circulation* 2006;114:e84–e231.
2. Shaw SM, Fox DJ, Williams SG. The development of left ventricular torsion and its clinical relevance. *Int J Cardiol* 2008;130:319–25.
3. Delhaas T, Kotte J, van der Toorn A, Snoep G, Prinzen FW, Arts T. Increase in left ventricular torsion-to-shortening ratio in children with valvular aortic stenosis. *Magn Reson Med* 2004;51:135–9.
4. Nagel E, Stuber M, Burkhard B, et al. Cardiac rotation and relaxation in patients with aortic valve stenosis. *Eur Heart J* 2000;21:582–9.
5. Stuber M, Scheidegger MB, Fischer SE, et al. Alterations in the local myocardial motion pattern in patients suffering from pressure overload due to aortic stenosis. *Circulation* 1999;100:361–8.
6. Van Der Toorn A, Barenbrug P, Snoep G, et al. Transmural gradients of cardiac myofiber shortening in aortic valve stenosis patients using MRI tagging. *Am J Physiol Heart Circ Physiol* 2002;283:H1609–15.
7. van Dalen BM, Soliman OI, Vletter WB, Ten Cate FJ, Geleijnse ML. Age-related changes in the biomechanics of left ventricular twist measured by speckle tracking echocardiography. *Am J Physiol Heart Circ Physiol* 2008;295:H1705–11.
8. Notomi Y, Srinath G, Shiota T, et al. Maturational and adaptive modulation of left ventricular torsional biomechanics: Doppler tissue imaging observation from infancy to adulthood. *Circulation* 2006;113:2534–41.
9. Notomi Y, Lysyansky P, Setser RM, et al. Measurement of ventricular torsion by two-dimensional ultrasound speckle tracking imaging. *J Am Coll Cardiol* 2005;45: 2034–41.
10. Goffinet C, Chenot F, Robert A, et al. Assessment of subendocardial vs. subepicardial left ventricular rotation and twist using two-dimensional speckle tracking echocardiography: comparison with tagged cardiac magnetic resonance. *Eur Heart J* 2009;30:608–17.
11. Lang RM, Bierig M, Devereux RB, et al. Recommendations for chamber quantification: a report from the American Society of Echocardiography's Guidelines and Standards Committee and the Chamber Quantification Writing Group, developed in conjunction with the European Association of Echocardiography, a branch of the European Society of Cardiology. *J Am Soc Echocardiogr* 2005;18:1440–63.
12. Mosteller RD. Simplified calculation of body-surface area. *N Engl J Med* 1987;317: 1098.
13. Zoghbi WA, Enriquez-Sarano M, Foster E, et al. Recommendations for evaluation of the severity of native valvular regurgitation with two-dimensional and Doppler echocardiography. *J Am Soc Echocardiogr* 2003;16:777–802.
14. van Dalen BM, Vletter WB, Soliman OII, ten Cate FJ, Geleijnse ML. Importance of transducer position in the assessment of apical rotation by speckle tracking echocardiography. *J Am Soc Echocardiogr* 2008;21:895–8.

15. van Dalen BM, Soliman OI, Vletter WB, et al. Feasibility and reproducibility of left ventricular rotation parameters measured by speckle tracking echocardiography. *Eur J Echocardiogr* 2009;10:669–76.
16. Ingels Jr NB, Hansen DE, Daughters 2nd GT, Stinson EB, Alderman EL, Miller DC. Relation between longitudinal, circumferential, and oblique shortening and torsional deformation in the left ventricle of the transplanted human heart. *Circ Res* 1989;64:915–27.
17. Taber LA, Yang M, Podszus WW. Mechanics of ventricular torsion. *J Biomech* 1996;29:745–52.
18. Buckberg G, Eber L, Herman M, Gorlin R. Ischemia in aortic stenosis: hemodynamic prediction. *Am J Cardiol* 1975;35:778–84.
19. Vincent WR, Buckberg GD, Hoffman JI. Left ventricular subendocardial ischemia in severe valvar and supra-valvar aortic stenosis. A common mechanism. *Circulation* 1974;49:326–33.
20. van Dalen BM, Kauer F, Soliman OI, et al. Influence of the pattern of hypertrophy on left ventricular twist in hypertrophic cardiomyopathy. *Heart* 2009;95:657–61.
21. Smucker ML, Tedesco CL, Manning SB, Owen RM, Feldman MD. Demonstration of an imbalance between coronary perfusion and excessive load as a mechanism of ischemia during stress in patients with aortic stenosis. *Circulation* 1988;78:573–82.
22. Galema TW, Yap SC, Geleijnse ML, et al. Early detection of left ventricular dysfunction by Doppler tissue imaging and N-terminal pro-B-type natriuretic peptide in patients with symptomatic severe aortic stenosis. *J Am Soc Echocardiogr* 2008;21:257–61.
23. Sandstede JJ, Johnson T, Harre K, et al. Cardiac systolic rotation and contraction before and after valve replacement for aortic stenosis: a myocardial tagging study using MR imaging. *AJR Am J Roentgenol* 2002;178:953–8.
24. Biederman RW, Doyle M, Yamrozik J, et al. Physiologic compensation is supranormal in compensated aortic stenosis: does it return to normal after aortic valve replacement or is it blunted by coexistent coronary artery disease? An intramyocardial magnetic resonance imaging study. *Circulation* 2005;112:1429–36.
25. Tzemos N, Silversides CK, Carasso S, Rakowski H, Siu SC. Effect of pregnancy on left ventricular motion (twist) in women with aortic stenosis. *Am J Cardiol* 2008;101: 870–3.
26. Ouzounian M, Lee DS, Liu PP. Diastolic Heart failure: mechanisms and controversies. *Nat Clin Pract Cardiovasc Med* 2008;5:375–86.
27. Lorell BH, Grossman W. Cardiac hypertrophy: the consequences for diastole. *J Am Coll Cardiol* 1987;9:1189–93.
28. Gabay J, Donato M, Pascua A, Gelpi RJ, Grinfeld L. Effects of isometric exercise on the diastolic function in patients with severe aortic stenosis with or without coronary lesion. *Int J Cardiol* 2005;104:52–8.
29. Courtois M, Kovacs Jr SJ, Ludbrook PA. Transmitral pressure-flow velocity relation. Importance of regional pressure gradients in the left ventricle during diastole. *Circulation* 1988;78:661–71.
30. van Dalen BM, Soliman OI, Vletter WB, ten Cate FJ, Geleijnse ML. Insights into left ventricular function from the time course of regional and global rotation by speckle tracking echocardiography. *Echocardiography* 2009;26:371–7.
31. Rademakers FE, Buchalter MB, Rogers WJ, et al. Dissociation between left ventricular untwisting and filling. Accentuation by catecholamines. *Circulation* 1992;85:1572–81.
32. Coats AJ. Ethical authorship and publishing. *Int J Cardiol* 2009;131:149–50.

Chapter 3

Assessment of Subendocardial Contractile Function in Aortic Stenosis: a Study using Speckle Tracking Echocardiography

van Dalen BM

Tzikas A

Soliman OI

Kauer F

Heuvelman HJ

Vletter WB

Ten Cate FJ

Geleijnse ML

Submitted

ABSTRACT

Aims: Angina and an electrocardiographic strain pattern are potential manifestations of subendocardial ischemia in aortic stenosis (AS). Left ventricular (LV) twist is known to increase proportionally to the severity of AS, which may be a result of loss of the inhibiting effect of the subendocardial fibres due to subendocardial dysfunction. It has also been shown that the ratio of LV twist to circumferential shortening of the endocardium (twist-to shortening ratio, TSR) is a reliable parameter of subendocardial dysfunction. The aim of the present study was to investigate whether these markers are increased in AS patients with angina and/or electrocardiographic strain.

Methods and Results: The study comprised 60 AS patients with an aortic valve area $<2.0 \text{ cm}^2$ and LV ejection fraction $>50\%$, and 30 healthy – for age and gender matched – control subjects. LV rotation parameters were determined by speckle tracking echocardiography. Compared to control subjects, AS patients had comparable peak systolic LV basal rotation and increased peak systolic LV apical rotation, resulting in increased peak systolic LV twist. Comparison of patients without angina and strain ($n=22$), with either angina or strain ($n=28$), and with both angina and strain ($n=8$), showed highest peak systolic LV apical rotation (9.2 ± 3.2 vs. 10.5 ± 3.2 vs. 13.0 ± 3.4 degree, $P<0.05$), peak systolic LV twist (12.1 ± 4.2 vs. 14.0 ± 4.4 vs. 19.1 ± 5.1 degree, $P<0.001$), and TSR (0.5 ± 0.2 vs. 0.7 ± 0.3 vs. 0.8 ± 0.3 degree / %, $P<0.001$), in patients with more signs of subendocardial ischemia. In a multivariate linear regression model only severity of AS and the presence of angina and/or strain could be identified as independent predictors of peak systolic LV twist and TSR.

Conclusion: Peak systolic LV twist and TSR are increased in AS patients and related to the severity of AS and symptoms (angina) or electrocardiographic signs (strain) compatible with subendocardial ischemia.

INTRODUCTION

Angina in aortic stenosis (AS) patients with normal coronary arteries is most likely a result of subendocardial ischemia, caused by increased myocardial oxygen demand and increased systolic impedance to coronary flow as a result of perivascular compression and a reduction in diastolic perfusion time [1]. Identification of subendocardial ischemia is important because it may ultimately lead to subendocardial fibrosis and other structural changes that are likely to influence the patient's morbidity and mortality [2]. Another potential manifestation of subendocardial ischemia is an electrocardiographic strain pattern. Strain has been associated with adverse events in a variety of populations [3-5], and an electrocardiogram is recommended yearly in the asymptomatic adolescent or young adult with moderate to severe AS [6]. The pathophysiology of strain remains incompletely understood, although it has been linked to increased LV mass and myocardial oxygen demand [7,8]. Unfortunately, strain is not very sensitive to identify subendocardial ischemia [9]. Therefore, a search for a reliable noninvasive quantitative tool able to assess subendocardial ischemia seems warranted.

Left ventricular (LV) twist results from the dynamic interaction of counteracting muscle fibres arranged in subendocardial and subepicardial spiral loops [10]. The direction of LV twist is governed by the subepicardial fibres, mainly owing to their longer arm of movement (Figure 1) [11]. Recently, our group has shown that LV twist increases proportionally to the severity of AS, which may be a result of a complete or partial loss of the inhibiting effect of the subendocardial fibres due to subendocardial dysfunction [12]. It has also been shown by others that the ratio of LV twist to circumferential shortening of the endocardium (twist-to shortening ratio, TSR) is a reliable parameter of subendocardial dysfunction [13-16]. The aim of the present study was to investigate whether these markers are increased in AS patients with angina and/or strain.

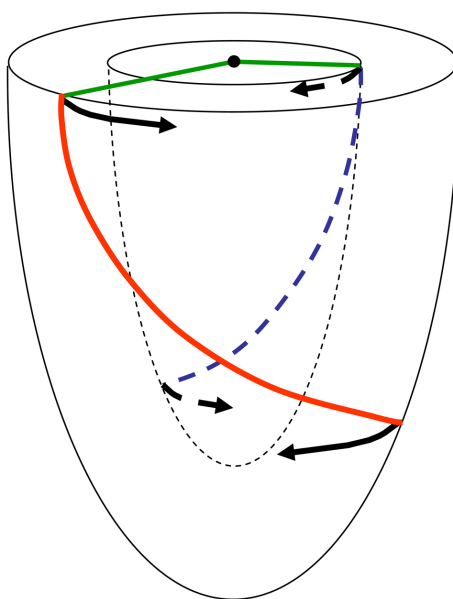


Figure 1. Left ventricular twist results from the dynamic interaction of counteracting muscle fibres arranged in subendocardial (blue dotted line) and subepicardial (red line) spiral loops. The direction of LV twist is governed by the subepicardial fibres, mainly owing to their longer arm of movement (green line).

METHODS

Study participants

The study population consisted of 60 AS patients (mean age 66 ± 15 year, 32 men) referred for echocardiography because of a murmur or follow-up of known AS, in sinus rhythm, with an aortic valve area $< 2.0 \text{ cm}^2$, normal LV ejection fraction ($> 50\%$), and good echocardiographic image quality that allowed for complete segmental assessment of LV rotation at both the basal and apical LV level. The presence of coronary artery disease was determined by coronary angiography in a subgroup of patients ($n=48$). AS patients were compared to 30 healthy – for age and gender matched – control subjects in sinus rhythm, without hypertension, diabetes, or regular use of medication for cardiovascular disease, and with normal left atrial dimensions, LV dimensions, and LV ejection fraction. Control subjects were recruited from our department (personnel) or were family members or friends. All subjects gave informed consent and the institutional review board approved the study. An electrocardiographic ‘strain pattern’ was defined as high lateral precordial voltages in association with ST-T-depression in V5-V6 [5,17]. In case of a left bundle branch block, electrocardiographic strain could not be determined.

Echocardiography

Two-dimensional grayscale harmonic images were obtained in the left lateral decubitus position using a commercially available ultrasound system (iE33, Philips, Best, The Netherlands), equipped with a broadband (1-5MHz) S5-1 transducer (frequency transmitted 1.7MHz, received 3.4MHz). All echocardiographic measurements were averaged from three heartbeats. From the M-mode recordings the following data were acquired: left atrial size, LV end-diastolic anteroseptal and inferolateral wall thickness, and LV end-diastolic and endsystolic dimension. LV mass was assessed with the two-dimensional area-length method [18]. LV ejection fraction was calculated from LV volumes by the modified biplane Simpson rule in accordance with the guidelines [18]. From the mitral-inflow pattern, peak early (E) and late (A) filling velocities, E/A ratio, and E-velocity deceleration time were measured. Tissue Doppler was applied end-expiratory in the pulsed-wave Doppler mode at the level of the inferoseptal side of the mitral annulus from an apical 4-chamber view. To acquire the highest wall tissue velocities, the angle between the Doppler beam and the longitudinal motion of the investigated structure was adjusted to a minimal level. The spectral pulsed-wave Doppler velocity range was adjusted to obtain an appropriate scale. Aortic valve areas were calculated by the continuity equation and also indexed by body surface areas, calculated using the Mosteller formula [19]. The severity of aortic regurgitation was determined according to the guidelines [20].

To optimize STE, images were obtained at a frame rate of 60 to 80 frames/s. Parasternal short-axis images at the LV basal level (showing the tips of the mitral valve leaflets) with the cross section as circular as possible were obtained from the standard parasternal position,

defined as the long-axis position in which the LV and aorta were most in-line with the mitral valve tips in the middle of the sector. To obtain a short-axis image at the LV apical level (just proximal to the level with end-systolic LV luminal obliteration) the transducer was positioned 1 or 2 intercostal spaces more caudal as previously described by us [21]. From each short-axis image, three consecutive end-expiratory cardiac cycles were acquired and transferred to a QLAB workstation (Philips, Best, The Netherlands) for off-line analysis.

Speckle tracking analysis

Analysis of the datasets was performed using QLAB Advanced Quantification Software version 6.0 (Philips, Best, The Netherlands), which was recently validated against magnetic resonance imaging for assessment of LV twist [22]. To assess LV rotation, six tracking points were placed manually (after gain correction) on the mid-myocardium (to assess endocardial circumferential shortening [end-systolic length segment / end-diastolic length segment] on the endocardium) on an end-diastolic frame in each parasternal short-axis image. Tracking points were separated about 60° from each other and placed on 1 (30°, anteroseptal insertion into the LV of the right ventricle), 3 (90°), 5 (150°), 7 (210°), 9 (270°, inferoseptal insertion into the LV of the right ventricle), and 11 (330°) o' clock to fit the total LV circumference.

Data were exported to a spreadsheet program (Excel, Microsoft Corporation, Redmond, WA) to determine LV peak systolic rotation during the isovolumic relaxation phase (Rot_{early}), LV peak systolic rotation during ejection (Rot_{max}), and instantaneous LV peak systolic twist ($Twist_{max}$, defined as the maximal value of instantaneous apical systolic rotation – basal systolic rotation). Finally, twist-to-shortening ratio (TSR) was calculated as mean ΔLV twist / Δ mean of LV basal and apical endocardial circumferential shortening during ejection (Figure 2) [23].

Statistical Analysis

Matching of controls and AS patients was achieved by randomly matching each control with two aortic stenosis patients with the same sex and age \pm 5 year. Measurements are presented as mean \pm SD. Variables were compared using Student's *t* test, Chi-square test, or ANOVA when appropriate. Kolmogorov-Smirnov test with Lilliefors significance correction was used for testing normality of distribution. The homogeneity of variance in the data for AS patients and control subjects was checked with Levene's test. Relations between parameters were assessed using Pearson's and Spearman's test for parametric and nonparametric correlations.

ANCOVA was used to analyze the association between LV twist or TSR and angina and/or an electrocardiographic strain after adjusting for potential confounding variables, including age, LV mass, coronary artery disease, and severity of AS. A P value $<$.05 was considered statistically significant. Intraobserver and interobserver variability for LV twist in our center are 6% \pm 6% and 9% \pm 5%, respectively [24].

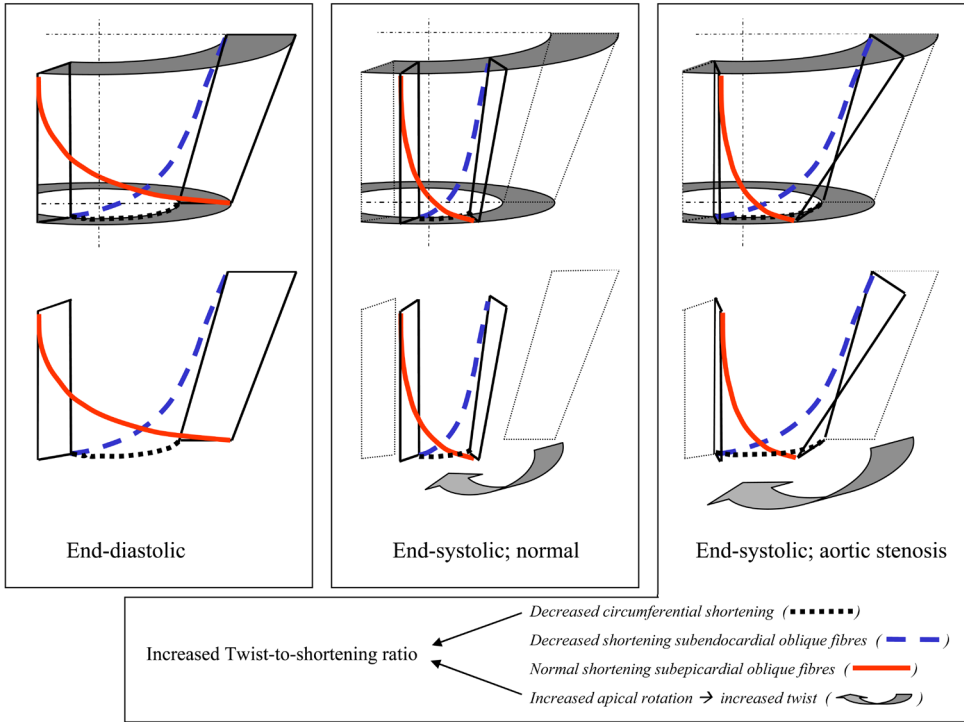


Figure 2. Twist-to-shortening ratio is determined by the ratio of left ventricular twist and subendocardial shortening. In the normal heart, systolic endocardial circumferential shortening (black dotted line) is accompanied by shortening of oblique subepicardial (red line) and subendocardial (blue dotted line) myofibres. Because of their longer lever arms, the subepicardial fibres dominate and lead to left ventricular apical rotation and twist in a counterclockwise direction (arrow). In aortic stenosis patients subendocardial contractile dysfunction may lead to decreased systolic endocardial circumferential shortening (black dotted line), and loss of counteracting shortening of subendocardial oblique fibres (blue dotted line). The latter will lead to increased left ventricular apical rotation and twist (arrow), which, together with the decreased endocardial circumferential shortening, will lead to an increased twist-to-shortening ratio in aortic stenosis.

RESULTS

Characteristics of the study population

In Table 1, the clinical and echocardiographic characteristics of the study population are shown. On average, AS was moderate-to-severe with a mean jet velocity of 3.8 ± 0.9 m/s, a mean gradient of 40 ± 19 mmHg, an aortic valve area of 0.9 ± 0.5 cm², and an aortic valve area indexed by body surface area of 0.4 ± 0.2 cm²/m². Symptoms of either dyspnea (33 [55%]), angina (15 [25%]), or collapses 2 [3%]) were present in 37 (62%) AS patients. A right or left bundle branch block was identified in 5 (8%) and 2 (3%) AS patients, respectively. In 23 (40%) out of 58 AS patients without a left bundle branch block, a strain pattern could be identified.

Table 1. Characteristics of the study population.

	Aortic stenosis patients (n = 60)	Control subjects (n = 30)
Clinical characteristics		
Age, year	66±15	61±14
Male, n (%)	32 (53)	16 (53)
Heart rate, beats per minute	67±12**	60±11
Systolic blood pressure, mmHg	138±17	130±14
Diastolic blood pressure, mmHg	77±7	76±9
Dyspnea / Angina / Collaps, n (%)	33 (55)*** / 15 (25)** / 2 (3)	0 / 0 / 0
Coronary artery disease, n (%) ⁽¹⁾	20 (42)	0
Electrocardiographic characteristics		
Right bundle branch block, n (%)	5 (8)	0
Left bundle branch block, n (%)	2 (3)	0
Strain pattern, n (%) ⁽²⁾	23 (40%)***	0
Echocardiographic characteristics		
Left atrial size, cm	4.3±0.9**	3.9±0.4
Left ventricular mass, g	224±108**	165±51
E/A ratio	1.1±0.6	1.0±0.2
Deceleration time, ms	231±85*	192±26
E/Em ratio	17.0±9.3***	7.9±3.4
Aortic valve		
Velocity, m/s	3.8±0.9***	1.2±0.3
Mean gradient, mmHg	40±19***	4±2
Valve area, cm ²	0.9±0.5***	3.0±0.3
Valve area indexed by BSA, cm ² /m ²	0.4±0.2***	1.6±0.2
Regurgitation grade (1-4), mean	1.1±0.9***	0.0±0.0

⁽¹⁾ Data for 48 patients with available coronary angiography. ⁽²⁾ Strain pattern in 58 patients without left bundle branch block. E = peak early phase filling velocity, A = peak atrial phase filling velocity, Em = peak early diastolic wave velocity, BSA = body surface area. *P <0.05, **P <0.01, ***P <0.001 versus control subjects.

LV rotation parameters in AS patients and control subjects

Compared to control subjects, AS patients had comparable basal Rot_{max} (-3.7 ± 3.1 vs. -4.0 ± 1.9 degree, $P=NS$), and increased apical Rot_{max} (10.2 ± 3.4 vs. 8.0 ± 2.2 degree, $P<0.01$), resulting in increased $Twist_{max}$ (13.6 ± 4.2 vs. 11.4 ± 3.1 degree, $P<0.01$). In a high proportion of AS patients, counterclockwise basal Rot_{early} and clockwise apical Rot_{early} were absent (65% and 47% respectively), whereas in all but one control subjects both parameters were measurable ($P<0.001$). In the AS patients with available basal and apical Rot_{early} reduced values were seen compared to control subjects (0.8 ± 0.6 vs. 1.1 ± 0.4 degree, and -0.5 ± 0.6 vs. -0.8 ± 0.5 degree, respectively, both $P<0.05$). TSR was increased in AS patients (0.6 ± 0.3 vs. 0.4 ± 0.1 degree / %, $P<0.01$) (Figure 2, Table 2). Furthermore, TSR was related to apical Rot_{max} ($R^2=0.37$, $P<0.01$) and $Twist_{max}$ ($R^2=0.39$, $P<0.01$).

Table 2. Left ventricular rotation parameters in aortic stenosis patients and control subjects.

	Aortic stenosis patients (n = 60)	Control subjects (n = 30)
Basal Rot _{max} , degree	-3.7 ± 3.1	-4.0 ± 1.9
Basal Rot _{early} absent, n (%)	39 (65) **	0 (0)
degree ⁽¹⁾	0.8 ± 0.6*	1.1 ± 0.4
Apical Rot _{max} , degree	10.2 ± 3.4*	8.0 ± 2.2
Apical Rot _{early} absent, n (%)	28 (47) **	1 (3)
degree ⁽¹⁾	-0.5 ± 0.6*	-0.8 ± 0.5
Twist _{max} , degree	13.6 ± 4.2*	11.4 ± 3.1
Twist-to-shortening ratio, degree / %	0.6 ± 0.3*	0.4 ± 0.1

⁽¹⁾ Data for patients with a present basal or apical Rot_{early}. Rot_{max} = left ventricular peak systolic rotation during ejection, Rot_{early} = left ventricular early peak of systolic rotation during isovolumic contraction phase, Twist_{max} = instantaneous left ventricular peak systolic twist. *P < 0.05, *P < 0.01, **P < 0.001 versus control subjects.

Relation of angina, electrocardiographic strain, and LV rotation parameters to other clinical characteristics

Patients were subdivided into 3 groups according to the presence of angina and strain (both angina and strain absent, n=22; either angina or strain present, n=28; both angina and strain present, n=8; patients with left bundle branch block excluded, n=2) (Table 3). Age and the presence of coronary artery disease were comparable between AS patients with or without angina and/or strain. Conversely, LV mass was increased in patients with both angina and strain (276±95 g) as compared to patients with either angina or strain (233±83 g) and patients without angina and strain (184±41 g, P<0.01). Furthermore, comparison of these groups, revealed a trend toward higher aortic valve velocity and gradient and a significant smaller aortic valve area in patients with more signs of subendocardial ischemia (P<0.05).

LV mass was not related to any of the LV rotation parameters in AS, whereas age was only significantly related to TSR (R²=0.19, P<0.05). Investigation of the 48 AS patients with available coronary angiography did not reveal any differences in LV rotation parameters between patients with (n=23) and without (n=25) coronary artery disease. Apical Rot_{max}, Twist_{max}, and TSR correlated positively to aortic valve jet velocity (R²=0.20, R²=0.19, and R²=0.22, respectively, all P<0.01) and mean gradient (R²=0.18, R²=0.18, and R²=0.19, respectively, all P<0.01), and negatively to aortic valve area (R²=0.28, R²=0.26, and R²=0.25, respectively, all P<0.001) and aortic valve area indexed by body surface area (R²=0.30, R²=0.29, R²=0.19, and R²=0.29, respectively, all P<0.001).

Table 3. *Echocardiographic indicators of aortic stenosis severity and left ventricular rotation parameters in patients with and without angina or an electrocardiographic strain pattern.*

	No angina or electrocardiographic strain pattern (n = 22)	Angina or electrocardiographic strain pattern (n = 28)	Angina and electrocardiographic strain pattern (n = 8)	F (ANOVA)
Age, year	63±13	67±19	72±18	2.22
Left ventricular mass, g	184±41	233±83	276±95	5.32**
Available coronary angiogram, n (%)	21 (95)	20 (71)	7 (88)	NS (Chi-Square)
Coronary artery disease, n (%) ⁽¹⁾	8 (38)	12 (60)	3 (43)	NS (Chi-Square)
Severity aortic stenosis				
Velocity, m/s	3.6±0.9	4.0±0.8	4.2±0.5	1.99
Mean gradient, mmHg	36±20	45±19	48±11	2.30
Valve area, cm ²	1.1±0.6	0.7±0.4	0.6±0.3	3.50*
Valve area indexed by BSA, cm ² /m ²	0.5±0.3	0.4±0.2	0.3±0.1	1.16
LV rotation parameters				
Basal Rot _{max} degree	-3.6±3.6	-3.7±3.1	-3.9±3.2	0.32
Basal Rot _{early} absent, n (%)	19 (86)	15 (54)	5 (63)	NS (Chi-Square)
degree ⁽²⁾	0.9±0.6	0.7±0.5	0.6±0.3	2.34
Apical Rot _{max} degree	9.2±3.2	10.5±3.2	13.0±3.4	4.33*
Apical Rot _{early} absent, n (%)	11 (50)	12 (43)	5 (63)	NS (Chi-Square)
degree ⁽²⁾	-0.6±0.4	-0.3±0.4	-0.2±0.2	6.81**
Twist _{max} degree	12.1±4.2	14.0±4.4	19.1±5.1	7.96***
Twist-to-shortening ratio, degree / %	0.5±0.2	0.7±0.3	0.8±0.3	9.07***

⁽¹⁾ Data for 42 patients with available coronary angiography. ⁽²⁾ Data for patients with a present basal or apical Rot_{early}. NS = not significant, other abbreviations as in Table 2. *P <0.05, **P <0.01, ***P <0.001 between age-groups (analysis of variance).

Relation of angina and electrocardiographic strain to LV rotation parameters in AS patients

Comparison of patients without angina and strain, with either angina or strain, and with both angina and strain, showed highest apical Rot_{max}, Twist_{max}, and TSR, and lowest Rot_{early} in patients with more signs of subendocardial ischemia (Table 3).

Multivariate analysis

In a multivariate linear regression model using ANCOVA, only severity of AS and the presence of angina and/or strain could be identified as independent predictors of Twist_{max} and TSR (both P<0.05).

DISCUSSION

The most important conclusion of the current study is that apical Rot_{max} , $\text{Twist}_{\text{max}}$, and TSR are increased in AS patients and related to the severity of AS and symptoms (angina) or electrocardiographic signs (strain) compatible with subendocardial ischemia.

Assessment of subendocardial contractile function in AS

In the normal heart, myocardial fibre helices in the inner and outer layers of the wall exert opposite torques. Torques caused by the outer layers are larger than torques due to the inner layers because of the longer lever (Figure 1). This causes LV twist to occur in favour of the outer layers. In AS patients, increased myocardial oxygen demand and relative impairment of coronary flow to the subendocardium may result in subendocardial ischemia. During subendocardial ischemia the counteracting torque of the inner layers is diminished and therefore LV twist increases [25,26], proportionally to AS severity [12,13]. Added to reduced subendocardial fibre shortening that is seen during ischemia, the absolute value of the slope of the relation between LV twist and endocardial circumferential shortening is expected to increase [13-16,23,27], as is shown in this study. Both increased $\text{Twist}_{\text{max}}$ and the decreased circumferential shortening it may compensate for, are caused by subendocardial contractile dysfunction, making the TSR a potentially sensitive marker of subendocardial ischemia [23,27]. Since the severity of subendocardial ischemia and the increase in LV twist are both known to be related to the severity of AS [28], LV rotation parameters may have an important role as markers of subendocardial ischemia. The decreased basal and apical $\text{Rot}_{\text{early}}$ in AS (that was even completely absent in a high proportion of patients in our study), are likely to be caused by subendocardial contractile dysfunction as well since normal counterclockwise basal $\text{Rot}_{\text{early}}$ and clockwise apical $\text{Rot}_{\text{early}}$ are caused by the predominant mechanical activity that develops along the subendocardial helical direction during the isovolumic contraction phase [10,29].

According to current guidelines, angina in patients with severe AS is a class I indication for aortic valve replacement [6]. This indication is largely based on the 1968 publication by Ross and Braunwald [30], in which the mean survival of 5 years after the onset of angina in severe AS was based on data retrieved from post-mortem studies and observations on patients with severe AS not undergoing aortic valve replacement for several reasons, leading to significant selection bias [31-33]. Angina in AS is most likely caused by subendocardial ischemia resulting from increased myocardial oxygen demand and relative impairment of coronary flow to the subendocardium. Although history-taking is a valuable, fast and easy diagnostic tool, the inherent subjectivity of symptoms may limit its use in clinical decision-making. Furthermore, patients may deny symptoms because they significantly reduce their activities. Therefore it may be better to study a more objective sign of subendocardial ischemia, such as the TSR.

To further prevent sudden cardiac death and irreversible LV damage, it is also advocated to perform aortic valve replacement in asymptomatic patients at high-risk, based on aortic valve calcification severity, rate of stenosis progression, response to exercise testing, and LV ejection fraction [6,34]. According to the ischemic cascade, angina is the final step, and thus often not present [35]. Before angina develops, electrical and functional changes occur in the ischemic endocardium that may guide earlier aortic valve replacement. However, it is well known that a surface electrocardiogram can also remain completely normal in the presence of subendocardial ischemia [36]. One of the earliest signs of perfusion abnormalities are alterations in contractile function [35]. In the current study and other studies [37] it has been shown that abnormalities in longitudinal and circumferential contraction and rotation precede changes in LV ejection fraction. In future large-scale studies it should be investigated whether such abnormalities, and in particular the TSR, in asymptomatic patients with severe AS identify patients at high-risk for sudden cardiac death and irreversible LV damage. However, it should be noticed that unlike angina and strain, which can be assessed in virtually all patients, reliable assessment of the TSR relies on echocardiographic image quality [24] and the ability of two-dimensional echocardiography to image the true LV apex [21,22]. This may limit the use of the TSR in clinical practice at this moment.

REFERENCES

1. Rajappan K, Rimoldi OE, Dutka DP, Ariff B, Pennell DJ, Sheridan DJ, Camici PG. Mechanisms of coronary microcirculatory dysfunction in patients with aortic stenosis and angiographically normal coronary arteries. *Circulation* 2002;105:470-6.
2. Lund O, Nielsen TT, Emmertsen K, Flo C, Rasmussen B, Jensen FT, Pilegaard HK, Kristensen LH, Hansen OK. Mortality and worsening of prognostic profile during waiting time for valve replacement in aortic stenosis. *Thorac Cardiovasc Surg* 1996;44:289-95.
3. Verdecchia P, Schillaci G, Borgioni C, Ciucci A, Gattobigio R, Zampi I, Porcellati C. Prognostic value of a new electrocardiographic method for diagnosis of left ventricular hypertrophy in essential hypertension. *J Am Coll Cardiol* 1998;31:383-90.
4. Drazner MH, Rame JE, Marino EK, Gottdiener JS, Kitzman DW, Gardin JM, Manolio TA, Dries DL, Siscovick DS. Increased left ventricular mass is a risk factor for the development of a depressed left ventricular ejection fraction within five years: the Cardiovascular Health Study. *J Am Coll Cardiol* 2004;43:2207-15.
5. Hering D, Piper C, Horstkotte D. Influence of atypical symptoms and electrocardiographic signs of left ventricular hypertrophy or ST-segment/T-wave abnormalities on the natural history of otherwise asymptomatic adults with moderate to severe aortic stenosis: preliminary communication. *J Heart Valve Dis* 2004;13:182-7.
6. Bonow RO, Carabello BA, Kanu C, de Leon AC, Jr., Faxon DP, Freed MD, Gaasch WH, Lytle BW, Nishimura RA, O'Gara PT, O'Rourke RA, Otto CM, Shah PM, Shanewise JS, Smith SC, Jr., Jacobs AK, Adams CD, Anderson JL, Antman EM, Faxon DP, Fuster V, Halperin JL, Hiratzka LF, Hunt SA, Lytle BW, Nishimura R, Page RL, Riegel B. ACC/AHA 2006 guidelines for the management of patients with valvular heart disease: a report of the American College of Cardiology/American Heart Association Task Force on Practice Guidelines (writing committee to revise the 1998 Guidelines for the Management of Patients With Valvular Heart Disease): developed in collaboration with the Society of Cardiovascular Anesthesiologists: endorsed by the Society for Cardiovascular Angiography and Interventions and the Society of Thoracic Surgeons. *Circulation* 2006;114:e84-231.
7. Okin PM, Devereux RB, Nieminen MS, Jern S, Oikarinen L, Viitasalo M, Toivonen L, Kjeldsen SE, Julius S, Dahlöf B. Relationship of the electrocardiographic strain pattern to left ventricular structure and function in hypertensive patients: the LIFE study. Losartan Intervention For End point. *J Am Coll Cardiol* 2001;38:514-20.
8. Okin PM, Devereux RB, Fabsitz RR, Lee ET, Galloway JM, Howard BV. Quantitative assessment of electrocardiographic strain predicts increased left ventricular mass: the Strong Heart Study. *J Am Coll Cardiol* 2002;40:1395-400.
9. Rahimtoola SH. Valvular heart disease: a perspective on the asymptomatic patient with severe valvular aortic stenosis. *Eur Heart J* 2008;29:1783-90.
10. Ingels NB, Jr., Hansen DE, Daughters GT, 2nd, Stinson EB, Alderman EL, Miller DC. Relation between longitudinal, circumferential, and oblique shortening and torsional deformation in the left ventricle of the transplanted human heart. *Circ Res* 1989;64:915-27.
11. Taber LA, Yang M, Podszus WW. Mechanics of ventricular torsion. *J Biomech* 1996;29:745-52.
12. van Dalen BM, Tzikas A, Soliman OI, Heuvelman HJ, Vletter WB, ten Cate FJ, Geleijnse ML. Left ventricular twist and untwist in aortic stenosis. *Int J Cardiol* 2009; in press.

13. Aelen FW, Arts T, Sanders DG, Thelissen GR, Muijtjens AM, Prinzen FW, Reneman RS. Relation between torsion and cross-sectional area change in the human left ventricle. *J Biomech* 1997;30:207-12.
14. Arts T, Meerbaum S, Reneman RS, Corday E. Torsion of the left ventricle during the ejection phase in the intact dog. *Cardiovasc Res* 1984;18:183-93.
15. Arts T, Veenstra PC, Reneman RS. Epicardial deformation and left ventricular wall mechanisms during ejection in the dog. *Am J Physiol* 1982;243:H379-90.
16. Delhaas T, Kotte J, van der Toorn A, Snoep G, Prinzen FW, Arts T. Increase in left ventricular torsion-to-shortening ratio in children with valvular aortic stenosis. *Magn Reson Med* 2004;51:135-9.
17. Ganame J, Mertens L, Eidem BW, Claus P, D'Hooge J, Havemann LM, McMahon CJ, Elayda MA, Vaughn WK, Towbin JA, Ayres NA, Pignatelli RH. Regional myocardial deformation in children with hypertrophic cardiomyopathy: morphological and clinical correlations. *Eur Heart J* 2007;28:2886-94.
18. Lang RM, Bierig M, Devereux RB, Flachskampf FA, Foster E, Pellikka PA, Picard MH, Roman MJ, Seward J, Shanewise JS, Solomon SD, Spencer KT, Sutton MS, Stewart WJ. Recommendations for chamber quantification: a report from the American Society of Echocardiography's Guidelines and Standards Committee and the Chamber Quantification Writing Group, developed in conjunction with the European Association of Echocardiography, a branch of the European Society of Cardiology. *J Am Soc Echocardiogr* 2005;18:1440-63.
19. Mosteller RD. Simplified calculation of body-surface area. *N Engl J Med* 1987;317:1098.
20. Zoghbi WA, Enriquez-Sarano M, Foster E, Grayburn PA, Kraft CD, Levine RA, Nihoyanopoulos P, Otto CM, Quinones MA, Rakowski H, Stewart WJ, Waggoner A, Weissman NJ. Recommendations for evaluation of the severity of native valvular regurgitation with two-dimensional and Doppler echocardiography. *J Am Soc Echocardiogr* 2003;16:777-802.
21. van Dalen BM, Vletter WB, Soliman OII, ten Cate FJ, Geleijnse ML. Importance of transducer position in the assessment of apical rotation by speckle tracking echocardiography. *J Am Soc Echocardiogr* 2008;21:895-898.
22. Goffinet C, Chenot F, Robert A, Pouleur AC, de Waroux JB, Vancrayenest D, Gerard O, Pasquet A, Gerber BL, Vanoverschelde JL. Assessment of subendocardial vs. subepicardial left ventricular rotation and twist using two-dimensional speckle tracking echocardiography: comparison with tagged cardiac magnetic resonance. *Eur Heart J* 2009;30:608-17.
23. Van Der Toorn A, Barenbrug P, Snoep G, Van Der Veen FH, Delhaas T, Prinzen FW, Maessen J, Arts T. Transmural gradients of cardiac myofiber shortening in aortic valve stenosis patients using MRI tagging. *Am J Physiol Heart Circ Physiol* 2002;283:H1609-15.
24. van Dalen BM, Soliman OI, Vletter WB, Kauer F, van der Zwaan HB, Ten Cate FJ, Geleijnse ML. Feasibility and reproducibility of left ventricular rotation parameters measured by speckle tracking echocardiography. *Eur J Echocardiogr* 2009;10:669-76.
25. van Dalen BM, Soliman OI, Vletter WB, Ten Cate FJ, Geleijnse ML. Age-related changes in the biomechanics of left ventricular twist measured by speckle tracking echocardiography. *Am J Physiol Heart Circ Physiol* 2008;295:H1705-11.
26. Bertini M, Nucifora G, Marsan NA, Delgado V, van Bommel RJ, Boriani G, Biffi M, Holman ER, Van der Wall EE, Schalij MJ, Bax JJ. Left ventricular rotational mechanics in acute myocardial infarction and in chronic (ischemic and nonischemic) heart failure patients. *Am J Cardiol* 2009;103:1506-12.

27. Lumens J, Delhaas T, Arts T, Cowan BR, Young AA. Impaired subendocardial contractile myofiber function in asymptomatic aged humans, as detected using MRI. *Am J Physiol Heart Circ Physiol* 2006;291:H1573-9.
28. Smucker ML, Tedesco CL, Manning SB, Owen RM, Feldman MD. Demonstration of an imbalance between coronary perfusion and excessive load as a mechanism of ischemia during stress in patients with aortic stenosis. *Circulation* 1988;78:573-82.
29. van Dalen BM, Soliman OI, Vletter WB, ten Cate FJ, Geleijnse ML. Insights into left ventricular function from the time course of regional and global rotation by speckle tracking echocardiography. *Echocardiography* 2009;26:371-7.
30. Ross J, Jr., Braunwald E. Aortic stenosis. *Circulation* 1968;38:61-7.
31. Kumpe CW, Bean WB. Aortic stenosis; a study of the clinical and pathologic aspects of 107 proved cases. *Medicine (Baltimore)* 1948;27:139-85.
32. Mitchell AM, Sackett CH, Hunzicker WJ, Levine SA. The clinical features of aortic stenosis. *Am Heart J* 1954;48:684-720.
33. Contratto AW, Levine SA. Aortic stenosis with special reference to angina pectoris and syncope. *Ann Intern Med* 1937;10:1636-1653.
34. Vahanian A, Baumgartner H, Bax J, Butchart E, Dion R, Filippatos G, Flachskampf F, Hall R, Jung B, Kasprzak J, Nataf P, Tornos P, Torracca L, Wenink A. Guidelines on the management of valvular heart disease: The Task Force on the Management of Valvular Heart Disease of the European Society of Cardiology. *Eur Heart J* 2007;28:230-68.
35. Nesto RW, Kowalchuk GJ. The ischemic cascade: temporal sequence of hemodynamic, electrocardiographic and symptomatic expressions of ischemia. *Am J Cardiol* 1987;59:23C30C.
36. Monroe RG, Gamble WJ, LaFarge CG, Kumar AE, Stark J, Sanders GL, Phornphutkul C, Davis M. The Anrep effect reconsidered. *J Clin Invest* 1972;51:2573-83.
37. Galema TW, Yap SC, Geleijnse ML, van Thiel RJ, Lindemans J, ten Cate FJ, Roos-Hesselink JW, Bogers AJ, Simoons ML. Early detection of left ventricular dysfunction by Doppler tissue imaging and N-terminal pro-B-type natriuretic peptide in patients with symptomatic severe aortic stenosis. *J Am Soc Echocardiogr* 2008;21:257-61.

Part

II

IMAGING OF THE AORTIC ROOT
IN THE PLANNING AND DURING
TRANSCATHETER AORTIC VALVE
IMPLANTATION

Chapter 4

Assessment of the Aortic Annulus by Multislice Computed Tomography, Contrast Aortography, and Trans-Thoracic Echocardiography in Patients Referred for Transcatheter Aortic Valve Implantation

Tzikas A
Schultz CJ
Piazza N
Moelker A
Van Mieghem NM
Nuis RJ
van Geuns RJ
Geleijnse ML
Serruys PW
de Jaegere PPT

ABSTRACT

Objective: We sought to determine the level of agreement and the reproducibility of trans-thoracic Echocardiography (TTE), contrast aortography (CA) and multislice computed tomography (MSCT) for the assessment of the aortic annulus, in patients referred for Transcatheter Aortic Valve Implantation (TAVI).

Background: Correct measurement of the aortic annulus is important for TAVI.

Methods: The dimensions of the aortic annulus were measured using TTE, CA and MSCT in 70 patients with severe aortic stenosis, referred for TAVI. Agreement between imaging techniques and interobserver variability was assessed using the Bland -Altman method and a linear regression model.

Results: The MSCT Coronal view provided the largest mean annulus diameter (26.3 mm) followed by CA (24.4 mm), MSCT Mean (23.7 mm), TTE (22.6 mm), and MSCT Sagittal (21.8 mm) view. Differences in the annulus measurements were significant: MSCT Coronal view versus CA (mean, 95% confidence interval, Pearson's correlation) 2.0 mm, -1.9 to 6.0 mm, $r=0.72$, CA versus MSCT Mean 0.2 mm, -3.3 to 3.7 mm, $r=0.76$, MSCT Mean versus TTE 1.3 mm, -2.9 to 5.5 mm, $r=0.61$, TTE versus MSCT Sagittal view 0.9 mm, -3.6 to 5.4 mm, $r=0.59$, CA versus TTE 1.5 mm, -3.0 to 5.9 mm, $r=0.57$. Interobserver variability was: TTE (mean, 95% confidence interval, Pearson's correlation) 0.29 mm, -4.2 to 4.8 mm, $r=0.57$, CA 0.14 mm, -3.5 to 3.8 mm, $r=0.77$, MSCT Mean 0.20 mm, -1.4 to 1.8 mm, $r=0.95$.

Conclusions: We found significant differences in the dimensions of the aortic annulus measured by MSCT, CA, and TTE. Interobserver variability for TTE and CA was substantially higher compared with MSCT.

INTRODUCTION

Transcatheter Aortic Valve Implantation (TAVI) is increasingly being used to treat elderly or high-risk patients with aortic stenosis [1,3]. In current clinical practice, eligibility for treatment and sizing of the bioprosthesis is predominantly based upon the measurements of the aortic annulus by trans-thoracic (TTE) or trans-esophageal (TEE) echocardiography. Yet, some investigators advocate the use of multi-slice computed tomography (MSCT) since it may provide more accurate morphologic and quantitative details of the aortic annulus, whereas others use contrast aortography (CA) since it is an inherent part of the procedure [4,8]. Given the intrinsic differences between these various imaging techniques and their potential value in either the planning, execution or evaluation of the procedure, we sought to determine the level of agreement and the reproducibility of TTE, CA and MSCT for the assessment of the dimensions of the aortic annulus in patients with aortic stenosis referred for TAVI.

METHODS

Patient population

The study population comprises 70 patients with severe aortic stenosis who were referred for TAVI and who underwent a TTE, a MSCT and a CA of adequate quality during the evaluation process. They stem from a series of 97 consecutive patients of whom 27 were rejected from the current study because of either inadequate image quality (TTE 9 patients, CA 2 patients, MSCT 8 patients) or inability of calibration (CA 8 patients). The inclusion and exclusion criteria for TAVI have been described in detail elsewhere [2]. Briefly patients were included if they had severe native valvular aortic stenosis with an area $<1 \text{ cm}^2$ or $<0.6 \text{ cm}^2/\text{m}^2$, with or without aortic regurgitation and were deemed high risk surgical candidates by the Heart Team (specifically, an interventional cardiologist and a cardiothoracic surgeon).

Trans-thoracic echocardiography

TTE was performed with the patient in the left lateral decubitus position, by using a Philips iE33 or a Sonos 7500 system (Philips, Best, The Netherlands). Complete echocardiographic studies were performed for each patient in a standard fashion and were saved as loops or still images for off-line analysis with the QURAD software package (Curad BV, Wijk Bij Duurstede, The Netherlands). The diameter of the aortic annulus was obtained in the parasternal long-axis view, by using the zoom mode and standard 2D caliper

measurements (Figure 1A). All measurements were obtained in mid-systole, coinciding with the onset of the T wave on the surface electrocardiogram. This offers optimal visualization of the aortic valve leaflets with the annulus at its largest diameter [9]. Specifically, the distance between the aortic leaflet insertions on the anterior versus the posterior aortic wall was measured after choosing the frame in which correct positioning of the caliper was not biased by artifacts such as shadows or a blurred image. The effective orifice area was calculated using the continuity equation approach. Aortic regurgitation was assessed semiquantitatively according to the current guidelines [10].

Contrast aortography

CA was performed in all patients with a 20-ml bolus of contrast (Visipaque® 320 mg/l/ml, GE Health Care, Eindhoven, The Netherlands), given at a rate of 20 ml/sec through a



Figure 1. Methodology for the assessment of the aortic annulus.

Panel A: Trans-Thoracic Echocardiography, parasternal long axis view (the white dotted arrow indicates the aortic annulus). Panel B: Contrast Aortography, anterior–posterior view (the white dotted arrow indicates the aortic annulus). Panels C to F: Multislice Computed Tomography oblique sagittal (C), oblique coronal (D), and axial view (E–F). The black arrow indicates the aortic annulus in the MSCT Sagittal view and the black dotted arrow indicates the aortic annulus in the MSCT Coronal view. The white arrow heads are indicating the positions of the most caudal attachments of the three leaflets. On a clock face these are located at 12 (right leaflet), 5 (left leaflet), and 8 o'clock (noncoronary leaflet). It can be seen on the axial image that the coronal cut-plane cuts through the annulus from 10 to 4 o'clock whereas the sagittal plane cuts through the annulus from 1 to 7 o'clock. The sagittal and coronal windows were selected as shown to cut through the centre of the annulus. This is verified during the analysis on the axial view.

6-F marker pigtail catheter (Super Torque MB®, Cordis, Miami Lakes, FL), positioned in the nadir of the noncoronary sinus. The X-ray C-arm was positioned in such way that all three aortic sinuses were depicted in one line, corresponding to the MSCT Coronal view. All angiograms were analyzed with the Rubo Dicom Viewer 2.0 software package (Rubo Medical Imaging BV, The Netherlands). The radiographic markers, spaced by 1 cm on the pigtail catheter, were used for calibration purposes. The aortic annulus diameter was measured in mid-systole (onset of the T wave) at the level of leaflet insertion to the aortic wall (Figure 1B).

Multislice computed tomography

The MSCT acquisition protocol has been described before [11,12]. In brief, all patients were scanned using dual source CT (Somatom Definition, Siemens Medical Solutions, Forchheim, Germany) with a 2×detector collimation of 32×0.6 mm² and a z-axis flying focal spot, a rotation time of 330 ms, tube voltage of 120 kV, and with variable pitch adjusted to heart rate. Typically, a contrast bolus of 50–60 ml Visipaque 320 mg/ml was injected in an antecubital vein at a flow rate of 5.0 ml/ sec, followed by a second contrast bolus of 30–40 ml at 3.0 ml/sec. Bolus tracking was used as a trigger. Images were reconstructed in end-systole as follows: single segmental reconstruction algorithm; slice thickness 1.5 mm; increment 0.4 mm; medium-to-smooth convolution kernel (B26f). The resulting spatial resolution was 0.6–0.7 mm in-plane and 0.4–0.5 mm through-plane, and a temporal resolution of 83 ms. Radiation doses ranged from 8 to 20 mSv depending on body habitus and table speed.

MSCT images were analyzed on a Siemens *Circulation* workstation. The sagittal and coronal windows were adjusted so that an axial cut was obtained through the aortic root (Figure 1C,D), wherein the most caudal floor of the three aortic leaflet attachments could be seen simultaneously (Figure 1E) [13]. The aortic annulus was defined as the base of the aortic root where the lowest point of all three native leaflets could be seen on one axial image. The sagittal diameter of the annulus (MSCT Sagittal) was defined along the attachment line of the left and noncoronary leaflets and through the centre of the annulus with the coronal diameter (MSCT Coronal) orthogonal to it (Figure 1F). A mean diameter between the coronal and sagittal view was calculated for each patient [MSCT Mean = (MSCT Coronal + MSCT Sagittal) / 2].

Interobserver variability

Four observers (three cardiologists and one radiologist, experienced in imaging related to TAVI) did the analyses. They were blinded to the other respective measurements. The interobserver variability was determined as follows: TTE: First observer (A.T.) analyzed all 70 echocardiograms and a second observer (N.P.) analyzed 45 randomly chosen echocardiograms. CA: First observer (N.P.) analyzed all 70 angiograms and a second observer (A.T.) analyzed 45 randomly chosen angiograms. MSCT: First observer (C.S.)

analyzed all 70 scans and a second observer (A.M.) analyzed 48 randomly chosen scans. Interobserver variability was assessed by using the Bland -Altman methodology and a linear regression model [14].

Treatment strategy

Treatment strategy for TAVI was assessed in 61 patients who were treated with the Medtronic Core-Valve System™ (Medtronic-CoreValve Inc., Minneapolis, MN), on the basis of the diameters derived from the various imaging modalities used in this study and the manufacturer's matrix: 26 mm inflow prosthesis to be implanted in a 23-27 mm annulus and 29 mm prosthesis in a 23-27 mm annulus.

Statistical analysis

Variables are presented as mean ± standard deviation (SD) or, in case of a non-Gaussian distribution, as median and interquartile range (IQ-range). Comparisons of different measurements in the same patient were done using the Student t-test for paired data or, in case of non-Gaussian distribution using the Wilcoxon rank test for two related samples. Agreement between MSCT, TTE and CA, and interobserver variability was assessed by linear regression analyses and the Bland-Altman methodology [14]. The limits of agreement are represented by four standard deviations (+2SD to -2SD) of the differences (95% confidence interval). Two-tailed tests were used for all the analyses. Statistical analysis was done using SPSS 16.0. Statistical significance was defined as P<0.05.

RESULTS

The baseline patient characteristics and echocardiographic indices are shown in the Table 1. Sixty-one patients received a Medtronic-CoreValve (26 mm inflow; 22 patients, 29 mm inflow; 39 patients) and 2 patients received an Edwards SAPIEN Valve (Edwards Lifesciences, Irvine, CA). One patient underwent surgical valve replacement, two were rejected for valve replacement and the remaining 4 are on the waiting list for TAVI. TAVI with the Medtronic-CoreValve was successful in 58 out of 61 patients. Two patients died during the procedure, one because of LVOT rupture and one due to asystole after balloon valvuloplasty. Another patient with severe congenital kyphoscoliosis died 14 days after TAVI because of severe aortic regurgitation. There was no valve embolization and no dissection of the ascending aorta. The mean trans-aortic gradient (mean±SD) decreased from 48±15 to 8±3 mm Hg. The effective orifice area [median (IQ range)] increased from 0.56 (0.44-0.80) to 1.58 (1.33-2.03) cm². Paravalvular aortic regurgitation was seen in 49 patients (trivial to mild in 34 patients and mild to moderate in 15 patients).

The dimensions of the aortic annulus are summarized in Figure 2. The MSCT Coronal view provided the largest mean diameter (26.3 mm) followed by CA (24.4 mm), MSCT Mean (23.7 mm), TTE (22.6 mm) and MSCT Sagittal (21.8 mm) view. Paired sample sta-

Table 1. Baseline Patient Characteristics and Echocardiographic Indices (n=70).

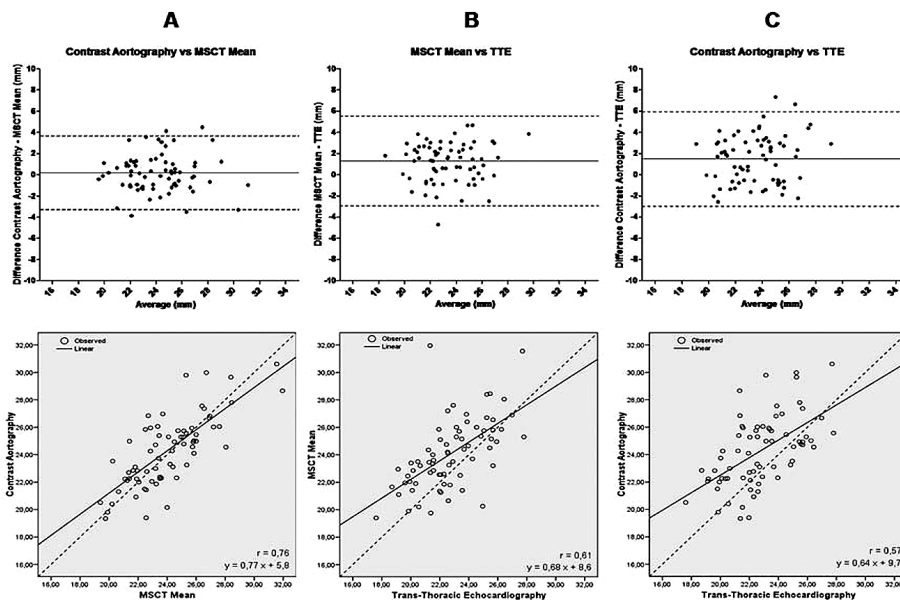
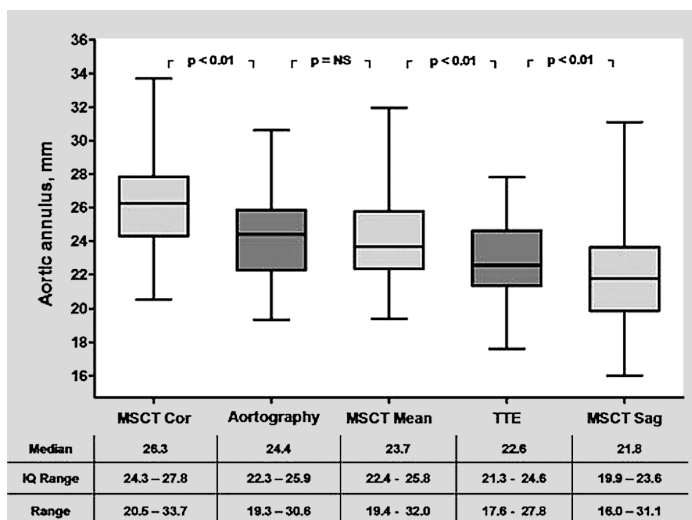
Age (y)	82 (80–86)
Male	36 (51)
Height (cm)	167±9
Weight (kg)	74±13
Body Mass Index (kg/m ²)	26 (24–29)
Body Surface Area (m ²)	1.84±0.20
Antecedents	
Cerebro-vascular events	17 (24)
Acute myocardial infarction	16 (23)
Percutaneous coronary intervention	16 (23)
Coronary artery bypass	18 (26)
Comorbidity	
Atrial fibrillation	14 (20)
Diabetes	15 (21)
Chronic obstructive pulmonary disease	19 (27)
Renal disease	8 (11)
Peripheral vascular disease	5 (7)
NYHA class III–IV	52 (74)
Logistic EuroScore	11 (8–16)
Echocardiography	
LV ejection fraction (%)	53±17
Peak AV gradient (mm Hg)	77±25
Mean AV gradient (mm Hg)	46±15
Aortic valve area (cm ²)	0.60 (0.49–0.79)
Aortic valve area indexed (cm ² /m ²)	0.33 (0.26–0.43)
Aortic regurgitation grade III–IV	24 (34)
Mitral regurgitation grade III–IV	10 (14)

Variables are presented as n (%), mean ± SD or median (interquartile range).
 NYHA, New York Heart Association; LV, left ventricular; AV, aortic valve.

tistical analysis revealed a significant difference in the aortic annulus diameter between all imaging modalities, except for the comparison of the means between CA and MSCT Mean. Using the Bland–Altman method and a linear regression model, best agreement was also found between CA and MSCT Mean (mean difference 0.2 mm, SD of differences 1.8 mm, $y = 0.77x + 5.8$, $r = 0.76$, Figure 3).

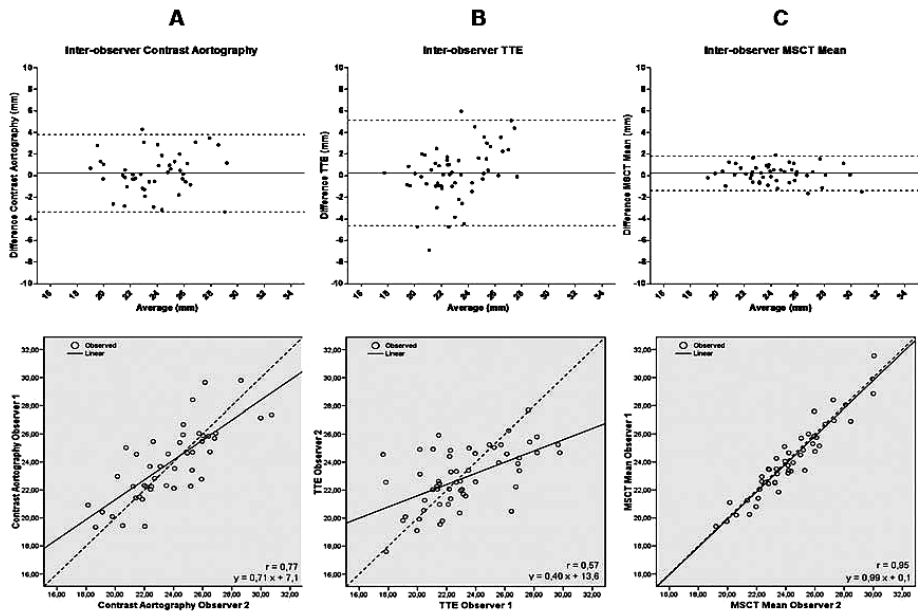
The interobserver variability is shown in Figure 4. TTE was found to be the least reproducible technique in the quantification of the aortic annulus (SD of difference = 2.25 mm, $y = 0.40x + 13.6$, $r = 0.57$). MSCT was found to be the most reproducible; MSCT Mean in particular revealed the lowest interobserver variability (SD of difference = 0.81 mm, $y = 0.99x + 0.1$, $r = 0.95$).

Figure 2. Aortic annulus diameters (mm). The *P* values at the top represent the results of statistical analysis (NS, non-significant). MSCT, multislice computed tomography; TTE, trans-thoracic Echocardiography; IQ, interquartile.



	CA - MSCT Mean	MSCT Mean - TTE	CA - TTE
Dif, mm	0.2	1.3	1.5
SD	1.8	2.2	2.3
95% CI	-3.3 – 3.7	-2.9 – 5.5	-3.0 – 5.9
r	0.76	0.61	0.57

Figure 3. Agreement between imaging modalities. Bland -Altman and corresponding linear regression analysis plots comparing A: Contrast Aortography -MSCT Mean, B: MSCT Mean -TTE, C: Contrast Aortography -TTE, MSCT, multislice computed tomography; TTE, trans-thoracic Echocardiography; Dif, mean difference in mm, SD, standard deviation in mm; CI, confidence interval in mm; r, Pearson's correlation coefficient.



	Aortography	TTE	MSCT Mean
Dif, mm	0.14	0.29	0.20
SD	1.84	2.25	0.81
95% CI	-3.5 – 3.8	-4.2 – 4.8	-1.4 – 1.8
r	0.77	0.57	0.95

Figure 4. Interobserver variability of each technique. Bland-Altman and corresponding linear regression analysis plots. A: Contrast Aortography, B: Trans-Thoracic Echocardiography, C: MSCT Mean. Abbreviations are as shown in Figure 3.

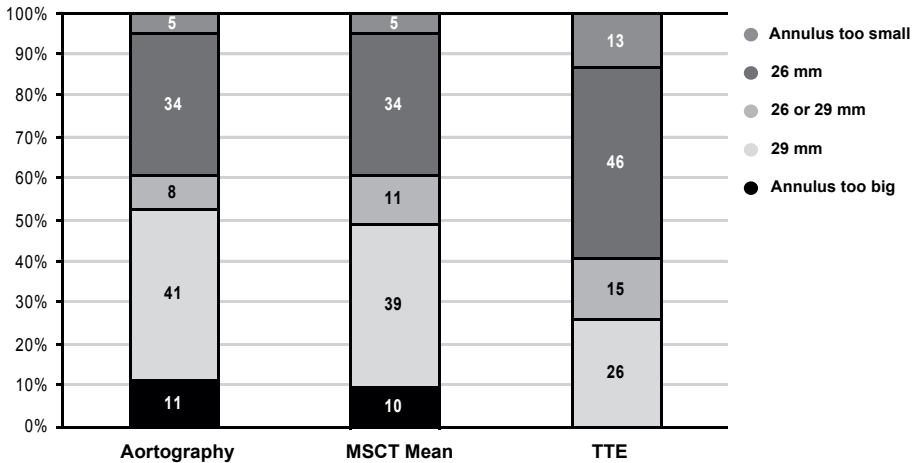


Figure 5. Changes in treatment strategy that would occur if the aortic annulus dimensions were measured only by MSCT or Contrast Aortography or TTE. Abbreviations are as shown in Figure 3.

Treatment strategy according to the manufacturer's guidelines was assessed in 61 patients who received a Medtronic-CoreValve. When using the MSCT Coronal and Sagittal view 36% and 28% of the patients should have been excluded from treatment due to an annulus being too large or too small respectively. By CA, MSCT Mean and TTE, 16%, 15%, and 13% of patients should have been rejected (Figure 5). Following TAVI, sizing based on CA, MSCT Mean and TTE was in agreement with the operator's choice in 69%, 70%, and 57% of patients, respectively (Figure 6). There was no association between under-and/or over-sizing of the prosthesis and paravalvular aortic regurgitation. Finally, under-sizing and/or over-sizing were not associated with device embolization.

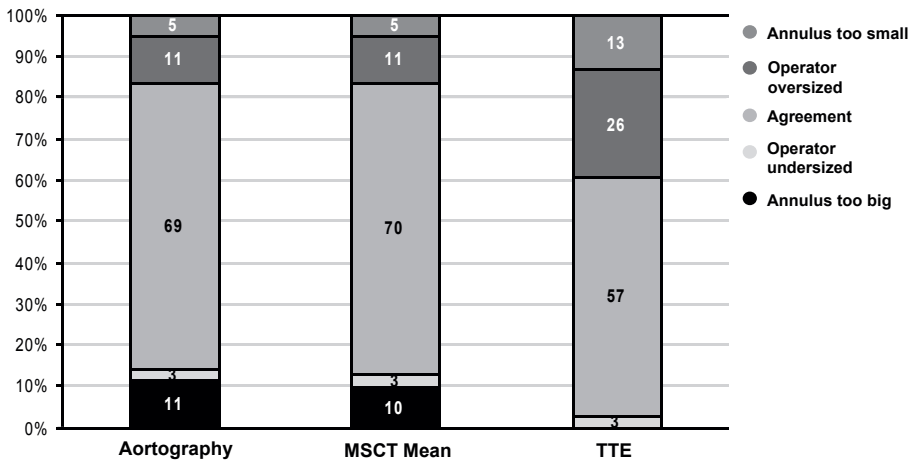


Figure 6. Agreement on sizing between MSCT, Contrast Aortography and TTE and the operator's choice. Abbreviations are as shown in Figure 3.

DISCUSSION

In this study, we found a significant difference in the dimensions of the aortic annulus measured by MSCT, CA, and TTE in patients with aortic stenosis referred for TAVI. We also found a substantial interobserver variability in the measurement of the aortic annulus dimensions by TTE, while MSCT proved to be the most reproducible technique.

The aortic annulus is described as a virtual ring formed by joining the basal attachments of aortic valvular leaflets [15]. Several studies have shown that in many patients the aortic annulus has an oval shape and, thereby, the use of a single diameter to describe it may lead in under- or over-estimation of its dimensions [5–8]. With respect to these observations, the differences in the measurements obtained by the MSCT Coronal and Sagittal view are not surprising (Figure 1F). This also holds for the differences between CA and TTE since the former corresponds to MSCT Coronal and the latter to MSCT Sagittal view. However, the oval anatomy does not fully explain the observed differences. As demonstrated by

Piazza et al, measurements made by two-dimensional (2D) techniques using the basal attachments of the leaflets do not transect the full diameter of the outflow tract but instead a tangent cut across the aortic root [15]. This is the case with CA in which the annulus is defined by the shadowgram showing the opening of the aortic leaflets (usually the basal attachment of the noncoronary and the left leaflet; Figure 1B). As a result, CA underestimates the annulus when compared to MSCT Coronal view. Finally, it should be noted that the MSCT “mean” annulus diameter can be also extrapolated from the annulus area or the annulus circumference after making simple calculations. However, in a previous study published by our group, the way of calculation did not influence the final result [12]. Thereby, we chose to use the simplest way to calculate the MSCT Mean annulus diameter.

In a study comparing the aortic annulus measurements in 26 patients, Wood et al. reported mean differences between MSCT Coronal, MSCT Sagittal, TTE and CA that were similar to our study [7]. However, the 95% confidence interval (CI) of the differences for all comparisons was more narrowed than in the present study. Yet, the Bland Altman plots depicting the $-2SD$ to $+2SD$ of the mean differences on the Y-axis reveal a much larger variation which is consistent with the findings of this study.

Recently, in a study involving 45 patients, Messika-Zeitoun et al. reported analogous mean differences between TTE and MSCT Long-axis (equivalent to MSCT Coronal), MSCT Short-axis (equivalent MSCT Sagittal), and MSCT Mean for the assessment of the aortic annulus [8]. In this study, another MSCT view was introduced (3-chamber view) and, using this view, the mean annulus measurements were similar to the ones obtained by TTE ($P=0.73$). However, the Pearson’s correlation was only moderate ($r=0.71$) and the reported interobserver variability for the MSCT 3-chamber view was two times higher than the MSCT Mean. The latter may be explained by the lack of a precise methodology for reconstruction of the MSCT 3-chamber view.

The clinical implications of the differences in the measurements of the aortic annulus are important. Patients can be denied therapy when using one technique or undergo TAVI when using another, whereas different imaging modalities may suggest different sizes of bioprostheses. In our current clinical practice, we use MSCT for the evaluation of TAVI candidates and for sizing purposes. In case of contraindications for MSCT (e.g., renal insufficiency), we combine the findings of TTE, CA, and TEE, bearing in mind that CA may overestimate and TTE may underestimate the annulus. For example, if the annulus measurement obtained by TTE is 23 mm (which is a cutoff value for the use of 26 mm or 29 mm inflow Medtronic-Core-Valve) we select a large valve, whereas if the same measurement is obtained by CA we prefer a small bioprosthesis.

At variance with surgical aortic valve replacement, TAVI does not allow a direct quantification of the aortic annulus. Given the importance of the correct measurement of the aortic annulus in patients scheduled to undergo TAVI, the findings of this study raise the question which imaging modality should be used in the planning of the procedure in order to ensure appropriate patient selection, procedure safety, proper valve function, and

durability [16,17]. Echocardiography plays a central role in evaluating patients with valvular heart disease. However, in contrast with Messika-Zeitoun et al., we consider MSCT as the reference technique for the assessment of the aortic root and for prosthesis sizing. Obviously, MSCT has several disadvantages, namely radiation exposure, iodine injection, accessibility, and cost, but it is currently the only technique that combines 3D capabilities with high spatial and temporal resolution and, moreover, it is less invasive than TEE. It is true that MSCT requires a detailed acquisition–analysis protocol and experienced operators. We anticipate that in the future 3D TEE and 3D CA will achieve higher resolution and may replace MSCT for the assessment of the aortic root anatomy.

Limitations

This study is limited by the relatively small number of observations and by the fact that it was performed in a single center. Both limitations preclude the generalizability of the findings. In addition, this study lacks the power to define which imaging modality should be considered the “gold standard” for the assessment and quantification of the aortic annulus. Finally, TEE readings were not compared to CA, MSCT or TTE because TEE was available in a limited number of patients.

CONCLUSIONS

In this study, we found significant differences in the dimensions of the aortic annulus measured by MSCT, CA, and TTE, in patients referred for TAVI. Interobserver variability for TTE and CA was substantially higher compared with MSCT.

REFERENCES

1. Cribier A, Eltchaninoff H, Tron C, Bauer F, Agatiello C, Nercolini D, Tapiero S, Litzler PY, Bessou JP, Babaliaros V. Treatment of calcific aortic stenosis with the percutaneous aortic valve: Mid-term follow-up from the initial feasibility studies: The French experience. *J Am Coll Cardiol* 2006;47:1214–1223.
2. Piazza N, Grube E, Gerckens U, den Heijer P, Linke A, Luha O, Ramondo A, Ussia G, Wenaweser P, Windecker S, Laborde JC, de Jaegere P, Serruys PW. Procedural and 30-day outcomes following transcatheter aortic valve implantation using the third generation (18 Fr) corevalve revalving system: Results from the multicentre, expanded evaluation registry 1-year following CE mark approval. *EuroIntervention* 2008;4:242–249.
3. Webb JG, Altwegg L, Boone RH, Cheung A, Ye J, Lichtenstein S, Lee M, Masson JB, Thompson C, Moss R, Carere R, Munt B, Nietlispach F, Humphries K. Transcatheter aortic valve implantation: Impact on clinical and valve-related outcomes. *Circulation* 2009;119:3009–3016.
4. Chin D. Echocardiography for transcatheter aortic valve implantation. *Eur J Echocardiogr* 2009;10:i21–9.
5. Ng AC, Delgado V, van der Kley F, Shanks M, van de Veire NR, Bertini M, Nucifora G, van Bommel RJ, Tops LF, de Weger A, Tavilla G, de Roos A, Kroft LJ, Leung DY, Schuijf J, Schalij MJ, Bax JJ. Comparison of aortic root dimensions and geometries before and after transcatheter aortic valve implantation by 2- and 3-dimensional transesophageal echocardiography and multislice computed tomography. *Circ Cardiovasc Imaging* 2010;3:94–102.
6. Tops LF, Wood DA, Delgado V, Schuijf JD, Mayo JR, Pasupati S, Lamers FP, van der Wall EE, Schalij MJ, Webb JG, Bax JJ. Noninvasive evaluation of the aortic root with multislice computed tomography implications for transcatheter aortic valve replacement. *JACC Cardiovasc Imaging* 2008;1:321–330.
7. Wood DA, Tops LF, Mayo JR, Pasupati S, Schalij MJ, Humphries K, Lee M, Al Ali A, Munt B, Moss R, Thompson CR, Bax JJ, Webb JG. Role of multislice computed tomography in transcatheter aortic valve replacement. *Am J Cardiol* 2009;103:1295–1301.
8. Messika-Zeitoun D, Serfaty JM, Brochet E, Ducrocq G, Lepage L, Detaint D, Hyafil F, Himbert D, Pasi N, Laissy JP, Jung B, Vahanian A. Multimodal assessment of the aortic annulus diameter: Implications for transcatheter aortic valve implantation. *J Am Coll Cardiol* 2010;55:186–194.
9. Veronesi F, Corsi C, Sugeng L, Mor-Avi V, Caiani EG, Weinert L, Lamberti C, Lang RM. A study of functional anatomy of aortic-mitral valve coupling using 3D matrix transesophageal echocardiography. *Circ Cardiovasc Imaging* 2009;2:24–31.
10. Zoghbi WA, Enriquez-Sarano M, Foster E, Grayburn PA, Kraft CD, Levine RA, Nihoyanopoulos P, Otto CM, Quinones MA, Rakowski H, Stewart WJ, Waggoner A, Weissman NJ; American Society of Echocardiography. Recommendations for evaluation of the severity of native valvular regurgitation with two-dimensional and Doppler echocardiography. *J Am Soc Echocardiogr* 2003;16:777–802.
11. Schultz C, Weustink A, Piazza N, Otten A, Mollet N, Krestin G, van Geuns RJ, de Feyter P, Serruys PW, de Jaegere P. Geometry and degree of apposition of the CoreValve ReValving system with multislice computed tomography after implantation in patients with aortic stenosis. *J Am Coll Cardiol* 2009;54: 911–918.

12. Schultz C, Moelker A, Piazza N, Tzikas A, Otten A, Nuis RJ, van Geuns RJ, de Feyter P, Krestin G, Serruys PW, de Jaegere P. 3D evaluation of the aortic annulus using multislice computer tomography. Are manufacturer's guidelines for sizing helpful? *Eur Heart J*. 2009 [Epub ahead of print].
13. Schultz CJ, Moelker AD, Tzikas A, Rossi A, van Geuns RJ, de Feyter PJ, Serruys PW, de Jaegere PP. Cardiac CT: Necessary for precise sizing for transcatheter aortic implantation. *EuroIntervention* 2010;6 Suppl G:G6–G13.
14. Bland JM, Altman DG. Statistical methods for assessing agreement between two methods of clinical measurement. *Lancet* 1986;1:307–310.
15. Piazza N, de Jaegere P, Schultz C, Becker P, Serruys PWJS, Anderson R. Anatomy of the aortic valvar complex and its implications for transcatheter implantation of the aortic valve. *Circ Cardiovasc Intervent* 2008;1:74–81.
16. Thubrikar M, Piepgrass WC, Shaner TW, Nolan SP. The design of the normal aortic valve. *Am J Physiol* 1981;241: H795– H801.
17. Zegdi R, Ciobotaru V, Noghin M, Sleilaty G, Lafont A, Latre«mouille C, Deloche A, Fabiani JN. Is it reasonable to treat all calcified stenotic aortic valves with a valved stent? Results from a human anatomic study in adults. *J Am Coll Cardiol* 2008;51:579–584.

Chapter 5

Optimal Projection Estimation for Transcatheter Aortic Valve Implantation Based on Contrast-Aortography: Validation of a Prototype Software

Tzikas A
Schultz C
Van Mieghem NM
de Jaegere PP
Serruys PW

ABSTRACT

We investigate the accuracy of a new software system (C-THV, Paieon) designed to calculate the optimal projection (OP) view for transcatheter aortic valve implantation (TAVI) based on two aortograms, and its agreement with the operator's choice. An optimal **fluoroscopic working** view projection with all three aortic cusps depicted in one line, is crucial during TAVI. In our institution selection of the OP is based on multislice computed tomography (MSCT). Seventy-three consecutive patients referred for TAVI were divided into two groups. For the first group (53 patients, retrospective cohort) we compared the OP views estimated by C-THV with the ones estimated by MSCT. For the second group (20 patients, prospective cohort), we compared the OP views estimated by C-THV with the operator's choice during TAVI. For the retrospective cohort, the mean absolute difference (mean \pm SD) between C-THV and MSCT was 6.6 ± 4.9 degrees. In 77% of the cases the mean difference between C-THV and MSCT was <10 degrees. For the prospective cohort, the mean absolute difference (mean \pm SD) between C-THV and the operator's choice was 5.5 ± 3.4 degrees. A mean difference of <10 degrees was found in 90% of the cases. In this study we found that the C-THV software estimated the OP view for TAVI with good accuracy. The level of agreement between C-THV and either the MSCT or the operator's choice was deemed satisfactory, with the vast majority of observed differences being <10 degrees.

INTRODUCTION

Recent innovations in transcatheter aortic valve implantation (TAVI) led to a widespread proliferation of transcatheter treatment strategies for aortic valve disease. Currently, the two leading technologies are the Medtronic CoreValve SystemTM (Medtronic, Minneapolis, MN) and the Edwards SAPIEN valve (Edwards Lifesciences, Irvine, CA) [1,3]. Both bioprostheses are implanted under fluoroscopic guidance (transesophageal echocardiography is sometimes also used for additional monitoring). A good fluoroscopic working view projection provides essential anatomical landmarks and is crucial during implantation of the device. Positioned too high the bioprosthesis may embolize to the aorta, whereas a very low implantation may lead to significant paravalvular aortic regurgitation. Moreover, positioning of the bioprosthesis occurs in relation to the diseased aortic valve and should take into account the proximity of the conduction system, mitral valve and coronary arteries. A too high position might jeopardize the ostia of the coronary arteries, whereas a too low implantation could induce electrical conduction abnormalities or interfere with normal mitral valve physiology. In the optimal projection (OP) view all three aortic cusps are depicted in one line. Therefore, the OP ameliorates the intrinsic limitation of fluoroscopy to produce only two-dimensional images and the inaccuracies related to the parallax effect.

The OP during the implantation procedure is reached by orienting the C-arm so that the X-ray beam is orthogonal to the axial plane of the aortic valve annulus, and is unique for each patient. In our institution selection of the OP is based on a multi-slice computed tomography (MSCT), obtained before the procedure [4,5]. MSCT can generate a 3D anatomical reconstruction of the aortic root from which a range of gantry angulations in the plane of the aortic valve can be determined [4-8]. In this study, we investigate the accuracy of a new software system (C-THV, Paieon) designed to calculate the OP based on two angiographic views of the aortic root. In addition, we study the agreement between the OP views estimated by the C-THV with the view that was chosen by the operator during the procedure.

METHODS

Patient population and study design

The study population consists of 73 consecutive patients with severe aortic stenosis referred for TAVI. Patients were divided into two groups. The first group comprised 53 patients that were treated before the introduction of the C-THV software in the catheterization laboratory, and the second comprised 20 patients that were treated while the C-THV

was available. For the first group, we compared the OP view estimated with the retrospective use of C-THV on contrast aortography versus the OP views estimated by MSCT (retrospective cohort). For the second group, we assessed prospectively the agreement between the OP view that was estimated by C-THV and operator's decision on the OP view during the procedure (prospective cohort).

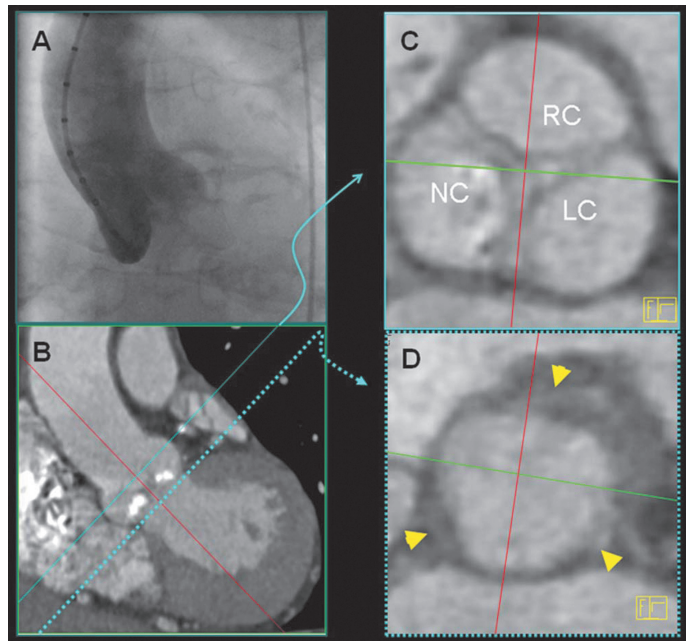
Multislice computed tomography (MSCT)

Details regarding acquisition and analysis of MSCT scans have been previously described [4,5]. Briefly, the three orthogonal viewing planes were oriented so that the most caudal attachments of all three aortic leaflets could be seen simultaneously in one axial image (Figure 1). The OP was estimated using the coronal window (which corresponds to contrast aortography). By rotating the cut plane in the axial window multiple viewing angles axial to the aortic valve can be obtained through 360 degrees. In order to avoid very steep cranial or caudal angulations of the C-arm, a single OP view was extrapolated from the MSCT analysis and was available in the catheterization laboratory, ranging from left anterior oblique (LAO) 0 to 20 degrees, with corresponding cranial–caudal angulations that were less than 20 degrees.

Contrast-aortography, C-THV Software

Diagnostic contrast-aortography views, recorded before the implantation, were analyzed using a prototype version of the C-THV software (Paieon). The OP curve (Figure

Figure 1. Obtaining the optimal projection by multi-slice projection by multi-slice computed tomography. The three orthogonal analysis windows are arranged so that the nadir of all three aortic leaflets are seen in one axial image (D, yellow arrowheads). The axial image is then parallel shifted to the level of the sinuses (C), where the sagittal cut-plane is then rotated on the axial image so that it cuts through the coaptation line of the noncoronary (NC) and left coronary (LC) leaflets, dividing the right coronary (RC) sinus into two halves. The coronal window (B) then provides the C-arm angulations for the angiographic view (A), where all three sinuses can be seen on one line with the NC to the left the RC in the middle and the LC to the right.



2) consists of an unlimited number of pairs of C-arm angulations which are orthogonal to the axial plane of the aortic valve, and is calculated using two aortograms. The operator marks the aortic direction on the first aortogram (Figure 3A). For the purpose of selecting the second projection, the available projections are graded by the software using a color coded area map (Figure 3B). The green and blue areas represent projections producing ideal and acceptable OP curves, respectively, whereas projections in the black area are automatically rejected. The operator selects the second projection based on the map

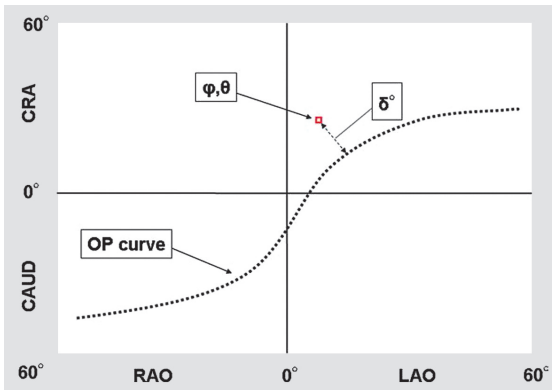


Figure 2. The optimal projection curve –the optimal projection curve consists of an unlimited number of pairs of C-arm angulations which are orthogonal to the axial plane of the aortic valve. Red box, for any given pair of C-arm angulations (ϕ , θ) a difference in degrees (δ) can be calculated using a mathematical model (see text).

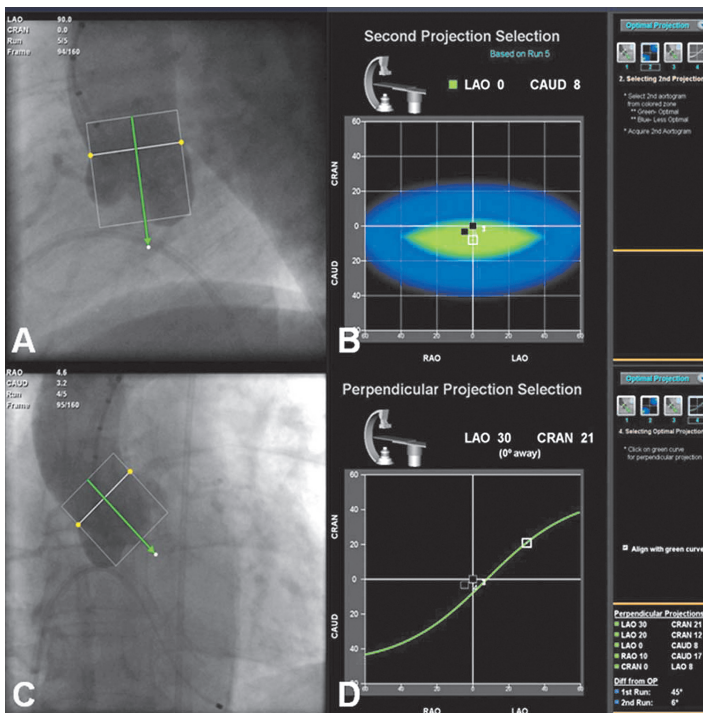


Figure 3. Estimation of the optimal projection view using the CTHV software -The Optimal Projection (OP) view is derived from the OP curve. A: Marking of the aortic direction on the first aortogram. B: Color coded area map on which all available aortograms are displayed and graded; green zone is ideal, blue zone is acceptable. The operator chooses the second aortogram. C: Marking of the aortic direction on the second aortogram. D: The OP curve is calculated and the operator can choose the OP among several projections that are orthogonal to the axial plane of the aortic valve.

and marks the aortic direction on the selected aortogram (Figure 3C). Finally, the software calculates the OP curve (Figure 3D). During the analyses with the C-THV software the operator was unaware of the OP views that were estimated by MSCT. It should be noted that the C-arm angulations for the two aortograms that are recommended by the manufacturer of the C-THV software are an LAO 30 Cranial 20 and a right anterior oblique (RAO) 20 caudal 30. However, in this study this particular recommendation was not followed because the first group of patients was studied retrospectively and because for the second group the TAVI strategy remained the same regardless of the on site availability of the C-THV software.

Level of agreement: C-THV versus MSCT and C-THV versus operator's choice

In order to assess the agreement between the OP views suggested by C-THV on contrast aortography and the ones estimated by MSCT (for the retrospective cohort), we calculated the angular difference between them, for each patient. Analogously, to assess the agreement between the C-THV and the operator's choice (prospective cohort) we calculated the angular difference between the OP views estimated by the CTHV software on contrast aortography and the final working view that was used by the operator during the procedure. It should be noted that in 19 out of the 20 prospectively studied cases an OP based on MSCT was still provided to the operator before the procedure. The C-THV was also available but as a secondary tool, which was still considered to be under evaluation.

Mathematical calculation of the angular deviation of the C-arm position from the OP curve

Using φ to denote the C-arm LAO/RAO angle and θ for the cranial/caudal angle, the C-arm position is denoted as (φ, θ) (Figure 2). Each C-arm position (φ, θ) defines a direction in space (unit vector) which we denote as (x_1, y_1, z_1) , where $x_1 = \sin(\varphi) \cos(\theta)$, $y_1 = \sin(\theta)$, and $z_1 = \cos(\varphi) \cos(\theta)$. Then we denote as (x_2, y_2, z_2) the direction in space perpendicular to the plane of the annulus that was calculated by the C-THV software. The angular deviation of the C-arm position from the OP curve (δ), calculated in degrees, is given by the formula $\delta^\circ = 90^\circ - \cos^{-1}(x_1x_2 + y_1y_2 + z_1z_2)$ [9].

Statistical Analysis

Variables are presented as the mean \pm standard deviation (SD) or, if the distribution was not Gaussian, as the median and interquartile range (IQ range). The independent samples t-test was used for comparisons between measurements. Statistical analysis was done using SPSS 16.0. Statistical significance was defined as $P < 0.05$.

RESULTS

The baseline patient characteristics are shown in Table 1.

Table 1. *Baseline Characteristics (n=73).*

Age (yrs), median [IQ range]	81 [78–85]
Male, n (%)	33 (45)
Height (cm), mean \pm SD	167 \pm 9
Weight (kg), median [IQ range]	70 [62–86]
Body mass index (kg/m ²), median [IQ range]	26 [23–29]
Body surface area (m ²), median [IQ range]	1.79 [1.69–2.03]

Table 2. *Agreement Between C-THV and MSCT (Retrospective Cohort, n=53).*

	Total	Ideal zone	Acceptable zone	P
n (%)	53	31 (58)	22 (42)	
Difference (°), mean \pm SD	6.6 \pm 4.9	5.3 \pm 3.8	8.6 \pm 5.7	0.014
Difference <10°, n (%)	41 (77)	26 (84)	15 (68)	0.202

Retrospective Cohort: Agreement Between C-THV and MSCT (n=53)

For the retrospective cohort, the mean absolute difference (mean \pm SD) between C-THV and MSCT was 6.6 \pm 4.9 degrees (Table 2). If the second projection was located in the ideal zone (58%) the mean difference was 5.3 \pm 3.8 degrees. If the second projection was located in the acceptable zone (42%) the mean difference was 8.6 \pm 5.7 degrees ($P = 0.014$). In 77% of the cases the mean difference between C-THV and MSCT was less than 10 degrees (ideal zone 84%, acceptable zone 68%).

Table 3. *Agreement Between C-THV and Operator's Choice (Prospective Cohort, n=20).*

	Total	Ideal zone	Acceptable zone	P
n (%)	20	11 (55)	9 (45)	
Difference (°), mean \pm SD	5.5 \pm 3.4	4.6 \pm 3.0	6.6 \pm 3.7	0.214
Difference <10°, n (%)	18 (90)	11 (100)	7 (78)	0.189

Prospective Cohort: Agreement Between C-THV and Operator's Choice (n=20)

For the prospective cohort, the mean absolute difference (mean \pm SD) between C-THV and the operator's choice was 5.5 \pm 3.4 degrees (Table 3). The mean differences were 4.6 \pm 3.0 and 6.6 \pm 3.7 degrees if the second projection was located in the ideal and acceptable zone, respectively. A mean difference of less than 10 degrees was found in 90% of the cases (ideal zone 100%, acceptable zone 78%).

In the majority of cases (64 out of 73, 88%) one of the two projections was LAO 90, cranial 0, due to biplane recordings. This projection was far from the corresponding OP curve [median (IQ range): 42 (38-51) degrees]. The second projection varied but on average it was located closer to the OP curve [median (IQ range): 13 (7-21) degrees]. The mean analysis time (mean±SD) with the C-THV software was 8±2 minutes.

DISCUSSION

In this study we found that the C-THV software estimated the OP view for TAVI with good accuracy. For both the retrospectively and prospectively studied group the level of agreement between C-THV and either the MSCT or the operator's choice was satisfactory, with the vast majority of observed differences being less than 10 degrees.

The capability of MSCT to provide high quality 3D imaging of the aortic root has been well established [6,8]. Before the introduction of MSCT for the evaluation of TAVI candidates the OP was estimated empirically, requiring an excess of contrast agent and radiation, and often resulting in suboptimal working projections while performing TAVI. In our institution, since 2007, MSCT has become the standard reference technique for the estimation of the OP. However, MSCT itself increases the radiation exposure, and a contrast agent is commonly used. In addition, MSCT is always acquired preoperatively and can be affected by variations in patient position (more an issue with trans-apical procedures). Obviously, the potential advantages of a dedicated software requiring only two aortograms for the estimation of the OP for TAVI are important, especially if TAVI would be offered to younger patients and given the limited availability of MSCT in some medical centers.

In the retrospectively studied group, the C-THV software provided OP views approaching the projections that were suggested by MSCT. Of note, the agreement was good despite the fact that in the majority of cases one of the two projections was an LAO 90 cranial 0. This projection is usually far from the OP curve and, therefore, the aortic annulus appears almost as a circular structure, facing the operator and overlaying the aortic sinuses. That makes the marking of the aortic direction more difficult and may explain the difference of >10 degrees which was found in some patients. The use of that projection is not recommended but if it is the only one available, as in our study, the operator should align the markings of the aortic root direction more tangentially to the right than to the left aortic wall (Figure 3A). In addition, marking of the aortic direction is preferable during systole when the aortic annulus is better visualized. In the prospectively studied group, the accuracy of the C-THV software was even better, especially if the second projection that was used was located in the ideal zone. Again, most of the times, the first projection was an LAO 90 Cranial 0. In addition, the choice of the OP was still based almost exclusively on MSCT, the C-THV tool being under evaluation. Despite such a suboptimal use of the CTHV its accuracy for the estimation of the OP for TAVI was deemed satisfactory.

Study Limitations

Although the findings of this study demonstrate the feasibility of C-THV in estimating the OP for TAVI, the impact on procedural success and clinical outcome could not be investigated because C-THV was used in parallel with the standard TAVI procedure, with no impact on the decision making. In addition, the cut-of values (e.g. <10 degrees) that were used to grade the software's accuracy may seem arbitrary. For that reason absolute differences are also reported in order to allow independent conclusions. Finally, for the reasons mentioned above, the recommendations of the manufacturer regarding the suggested angulations of the two aortograms were not strictly followed. Thereby, it can be anticipated that the accuracy of the software might further improve in case of a more "optimal" use.

CONCLUSIONS

In this study we found that the C-THV software estimated the OP view for TAVI with good accuracy. The level of agreement between C-THV and either the MSCT or the operator's choice was deemed satisfactory, with the vast majority of observed differences being less than 10 degrees.

Acknowledgments

The authors thank Rafi Brada for his essential contribution in the preparation of the present manuscript.

REFERENCES

1. Piazza N, Grube E, Gerckens U, den Heijer P, Linke A, Luha O, Ramondo A, Usia G, Wenaweser P, Windecker S, Laborde JC, de Jaegere P, Serruys PW. Procedural and 30-day outcomes following transcatheter aortic valve implantation using the third generation (18 Fr) CoreValve Revalving System: Results from the multicentre, expanded evaluation registry 1-year following CE mark approval. *EuroIntervention* 2008;4:242–249.
2. Cribier A, Eltchaninoff H, Tron C, Bauer F, Agatiello C, Nercolini D, Tapiero S, Litzler PY, Bessou JP, Babaliaros V. Treatment of calcific aortic stenosis with the percutaneous heart valve: mid-term follow-up from the initial feasibility studies: The French experience. *J Am Coll Cardiol* 2006;47:1214–1223.
3. Webb JG, Pasupati S, Humphries K, Thompson C, Altwegg L, Moss R, Sinhal A, Carere RG, Munt B, Ricci D, Ye J, Cheung A, Lichtenstein SV. Percutaneous transarterial aortic valve replacement in selected high-risk patients with aortic stenosis. *Circulation* 2007;116:755–763.
4. Schultz C, Weustink A, Piazza N, Otten A, Mollet N, Krestin G, van Geuns RJ, de Feyter P, Serruys PW, de Jaegere P. Geometry and degree of apposition of the CoreValve ReValving system with multislice computed tomography after implantation in patients with aortic stenosis. *J Am Coll Cardiol* 2009;54:911–918.
5. Schultz C, Moelker A, Piazza N, Tzikas A, Otten A, Nuis RJ, van Geuns RJ, de Feyter P, Krestin G, Serruys PW, de Jaegere P. 3D evaluation of the aortic annulus using multislice computer tomography: Are manufacturer's guidelines for sizing helpful? *Eur Heart J* 2010 31:849–856.
6. Tops LF, Wood DA, Delgado V, Schuijf JD, Mayo JR, Pasupati S, Lamers FP, van der Wall EE, Schalij MJ, Webb JG, Bax JJ. Noninvasive evaluation of the aortic root with multislice computed tomography implications for transcatheter aortic valve replacement. *JACC Cardiovasc Imaging* 2008;1:321–330.
7. Messika-Zeitoun D, Serfaty JM, Brochet E, Ducrocq G, Lepage L, Detaint D, Hyafil F, Himbert D, Pasi N, Laissy JP, Lung B, Vahanian A. Multimodal assessment of the aortic annulus diameter: implications for transcatheter aortic valve implantation. *J Am Coll Cardiol* 2010;55:186–194.
8. Kurra V, Kapadia SR, Tuzcu EM, Halliburton SS, Svensson L, Roselli EE, Schoenhagen P. Pre-procedural imaging of aortic root orientation and dimensions: Comparison between X-ray angiographic planar imaging and 3-dimensional multidetector row computed tomography. *JACC Cardiovasc Interv* 2010;3: 105–113.
9. Wollschliager H, Lee P, Zeiher A, Solzbach U, Bonzel T, Just HJ. Mathematical tools for spatial computations with biplane isocentric x-ray equipment. *Biomed Techn (Berl)* 1986;31:101–106.

Part III

ADVANCED IMAGING
IN THE EVALUATION
OF TRANSCATHETER
AORTIC VALVE IMPLANTATION

Chapter 6

Determinants on MSCT of Paravalvular Aortic Regurgitation after Transcatheter Aortic Valve Implantation using the Medtronic Corevalve Prosthesis

Schultz CJ

Tzikas A

Moelker A

Rossi A

Nuis RJ

Van Mieghem NM

Krestin G

de Feyter P

Serruys PW

de Jaegere PP

Submitted

ABSTRACT

Background: To investigate the causes of paravalvular aortic regurgitation (PAR) after the implantation of the Medtronic CoreValve prosthesis (MCRS).

Methods and Results: 56 patients underwent MSCT before TAVI with a MCRS and PAR was assessed with transthoracic echocardiography (TTE) between 5 and 10 days after TAVI. The aortic annulus smallest and largest orthogonal diameters and the mean diameter from the area were determined on MSCT on an axial image at the nadir of all 3 native leaflets. PAR was related to relevant anatomical structures on MSCT according to a clockface in the orientation of the parasternal short axis view on TTE.

PAR ≥ 1 was present in 25% of the patients and was associated with a larger annulus, a lower degree of oversizing and with a more aortic root calcification. On MSCT post TAVI malapposition was seen predominantly at the aorto-mitral fibrous continuity and the aspect of the largest diameter of the aortic annulus on the inside curve of the ascending aorta. PAR was predominantly seen at these two anatomic locations and less frequent in the area that contains the ventricular membranous septum and the area between the non- and right coronary sinus.

Conclusions: Mild to moderate PAR is common after TAVI. The availability of additional (larger) prosthesis sizes in combination with improved sizing based on mean annulus diameter (e.g. D_{CSA}) may help to reduce PAR.

INTRODUCTION

Transcatheter Aortic Valve Implantation (TAVI) is increasingly being performed to alleviate symptoms of severe aortic stenosis in patients at high surgical risk [1-6]. Despite promising clinical results, TAVI is associated with a high incidence of (mostly mild) paravalvar aortic regurgitation of which the long terms effects are unknown [7].

Whereas surgical aortic valve replacement (SAVR) prostheses are sewn into the decalcified aortic annulus, both the commercially available TAVI prostheses rely on the apposition of a section of the frame to the base of the aortic root in order to assure a stable position [1,2]. This part of the frame is covered with a protective skirt to prevent paravalvular aortic regurgitation. Achieving a good seal may rely on procedural factors such as accurate sizing and correct positioning of the prosthesis in addition to adequate predilatation of the native stenotic valve [7]. It may also be affected by anatomical factors such as the non-circular shape of the aortic annulus and the degree of calcification of the aortic leaflets, which are pushed aside to make space for the prosthesis.

The purpose of this study was to investigate the causes of aortic regurgitation related to anatomy and prosthesis-anatomy interaction after the implantation of the Medtronic CoreValve prosthesis, using a combination of multislice computer tomography (MSCT) and transthoracic echocardiography (TTE).

METHODS

This study complies with the declaration of Helsinki. The study population consists of 56 patients who had an implantation of a Medtronic CRS valve because of severe valvular aortic stenosis. Consecutive patients who underwent a preprocedure MSCT and a TTE >5 but <10 days post implantation were included. Details of the selection process for TAVI, procedure and valve have been described in detail elsewhere [8]. MSCT was repeated in 34 of these 56 patients post procedure at >5 days post TAVI.

MSCT protocol pre-procedure

The MSCT acquisition protocol has been described before [9,10]. In brief all patients were scanned using dual source CT (Somatom Definition, Siemens Medical Solutions, Forchheim, Germany). A non-contrast calcification score acquisition was performed before contrast MSCT. The contrast MSCT scanning parameters were: 2× detector collimation of 32×0.6 mm with a z-axis flying focal spot, rotation time 330 ms, tube voltage 120 kV, with variable pitch adjusted to heart rate. The scan ranged from the top of the aortic arch to the diaphragm. The volume of iodinated contrast material was adapted to the ex-

pected scan time. A contrast bolus (50-60 ml Visipaque® 320 mg l/ml, GE Health Care, Eindhoven, The Netherlands) was injected in an antecubital vein at a flow rate of 5.0 ml/s followed by a second contrast bolus of 30-40 at 3.0 ml/s. Bolus tracking was used to trigger the start of the scan. Reconstructions were made in end systole using a single-segmental reconstruction algorithm with slice thickness 1.5 mm; increment 0.4 mm; medium-to-smooth convolution kernel (B26f) resulting in a spatial resolution of 0.6-0.7 mm in-plane and 0.4-0.5 mm through-plane and a temporal resolution of 83ms. The radiation doses ranged from 8 to 20 mSv depending on body habitus and table speed.

MSCT protocol post TAVI

The MSCT acquisition protocol has been described before [10]. In brief it was similar to the pre-implantation protocol but with reconstructions of functional MSCT datasets with a slice thickness 0.75 mm; increment 0.4 mm; medium-to-smooth convolution kernel (B26f); sharp kernel (B46f), resulting in a spatial resolution of 0.6-0.7 mm in-plane and 0.4-0.5 mm through-plane

Definition of the aortic annulus on pre-procedural MSCT on an axial image

Siemens Circulation software was used to analyse MSCT images. Axial cuts through the aortic root were obtained by aligning the two longitudinal analysis planes, respectively oblique sagittal and oblique coronal, so that the most caudal attachments of all 3 aortic leaflets could be seen simultaneously in the third (axial) image [9]. The aortic annulus was defined as the base of the aortic root where the nadir of all 3 native leaflets could be seen in one axial image as described before [9] (Figure 1). At the level of the aortic annulus the cross-sectional surface area (CSA) and the smallest (D_{\min}) and largest (D_{\max}) orthogonal diameters were measured on the axial image (Figure 1). The mean diameter (D_{CSA}) was derived from the equation $D_{\text{CSA}} = 20 \times \text{square root} (CSA/\pi)$ as described previously [9]. The interobserver variation of annulus measurements in percent (mean (SD)) as assessed by 2 independent readers blinded to each other's results in 49 patients were as follows: for $D_{\max} = 0.2\%$ (4.1), for $D_{\min} = 3.4\%$ (6.6), and for $D_{\text{CSA}} = 2.1\%$ (5.1).

Evaluation of the CRS frame

MSCT images throughout the cardiac cycle were reviewed (functional datasets) because the motion improved the evaluation of malapposition on the grayscale images. On axial images malapposition of the inflow section of the frame was considered to be present if it was seen over an arc of $\geq 30^\circ$. At the upper level of the skirt covered section of the frame malapposition was considered to be present if an intersinus triangle (IST) was not apposed to the frame even if the arc of malapposition was less than 30° (Figure 2). The location of malapposition was recorded according to a clockface both at the inflow and at the upper level of the sealing skirt of the CRS (generally RC/LC triangle at 1-2 o'clock, LC/NC triangle at 5-6 o'clock and NC/RC triangle at 9 to 10 o'clock) (Figure 2).

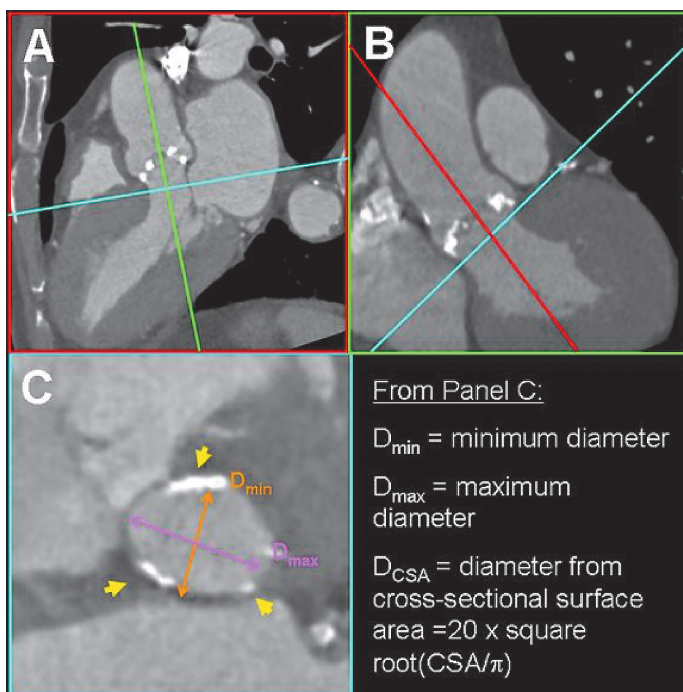


Figure 1: Definition of the aortic annulus and measurements on contrast MSCT.

Axial cuts through the aortic root were obtained by aligning the two longitudinal analysis planes, respectively oblique sagittal (Panel A) and oblique coronal (Panel B), so that the most caudal attachments of all 3 aortic leaflets could be seen simultaneously in the third (axial) image (Panel C) (9). The aortic annulus was defined as the base of the aortic root where the nadir of all 3 native leaflets (Panel C, yellow arrows) could be seen in one axial image. At the level of the aortic annulus the cross-sectional surface area (CSA) and the smallest (D_{\min}) and largest (D_{\max}) orthogonal diameters were measured on the axial image.

Calcium score analysis method

Non-contrast calcium scoring MSCT scans were not always performed in patients with previous CABG or coronary stenting and were available in addition to the contrast scans in 48 out of 56 patients with pre-procedural MSCT. In order to measure aortic root calcification the aortic root was defined as the region stretching from just above the origin of the left main stem to the anterior leaflet of the mitral valve, because these structures could be identified, when calcified, on the non-contrasted MSCT acquisitions. Calcium scoring (Volume, Mass, Agatston score) was limited to the region so defined. In cases where the calcification was confluent to beyond these boundaries the images limited to this region were selectively loaded into the analysis software to avoid overestimation of calcification.

Echocardiography acquisition

TTE was performed with the patient in the left lateral decubitus position, using a Philips iE33 or a Sonos 7500 system (Philips, Best, The Netherlands). Complete echocardiographic studies were performed for all patients in a standard fashion, and were saved as loops or still images for off-line analysis with the QURAD software package (Curad BV, Wijk Bij Duurstede, The Netherlands). Aortic regurgitation was assessed semi-quantitatively based on the vena contracta width to LVOT diameter ratio, Mild: $\leq 25\%$,

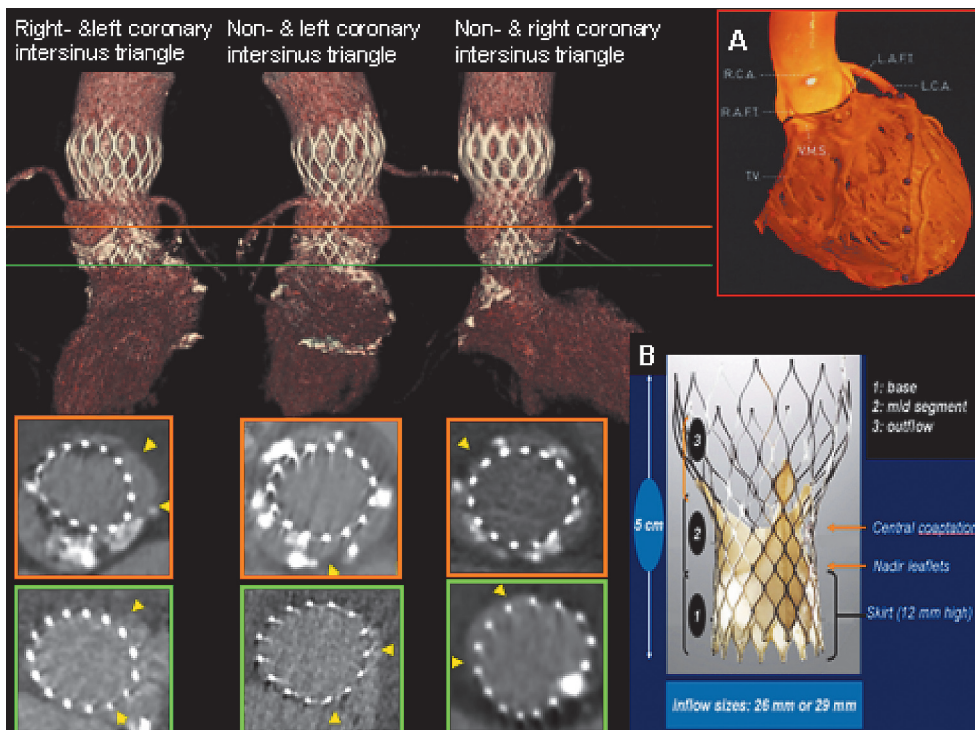


Figure 2: Evaluation of malapposition at the intersinus triangles (IST) at the upper level of the skirt (orange line) and at the inflow (base, green line) of the Medtronic CRS prosthesis.

Inset A demonstrates on an anatomical specimen the location of the right-&left intersinus triangle (Left anterior fibrous trigone or LAFT) and the non-&right intersinus triangle (Right anterior fibrous trigone or RAFT) relative to the ventricular membranous septum (VMS), tricuspid valve (TV), right coronary ostium (RCA) and left coronary artery (LCA). **Inset B** demonstrates the components of the Medtronic CRS prosthesis. A pericardial skirt designed to prevent paravalvular regurgitation covers the lower segment of the CRS from the inflow to the nadir of the leaflets.

The upper row of 3D MSCT images show the intersinus triangles stretching above the upper level of the sealing skirt of the CRS (orange line) and the inflow (green line). The axial images (bottom 2 rows) demonstrate lack of apposition (arrow heads) of the CRS frame at the upper level of the skirt in 3 patients at the corresponding inter-sinus triangle and at the level of the inflow in another 3 patients.

The anatomical image is from W.A. McAlpine, Heart and Coronary Arteries: An Anatomical Atlas for Clinical Diagnosis, Radiological Investigation, and Surgical Treatment, Springer Verlag, October 1974.

Moderate 26-64%, Severe $\geq 65\%$ and was graded as follows: absent or trivial=0, mild=1, moderate=2, severe=3 (Figure 3) [11,12]. PAR was graded by two independent cardiologists who were experienced in TAVI imaging. In case of disagreement, consensus was reached.

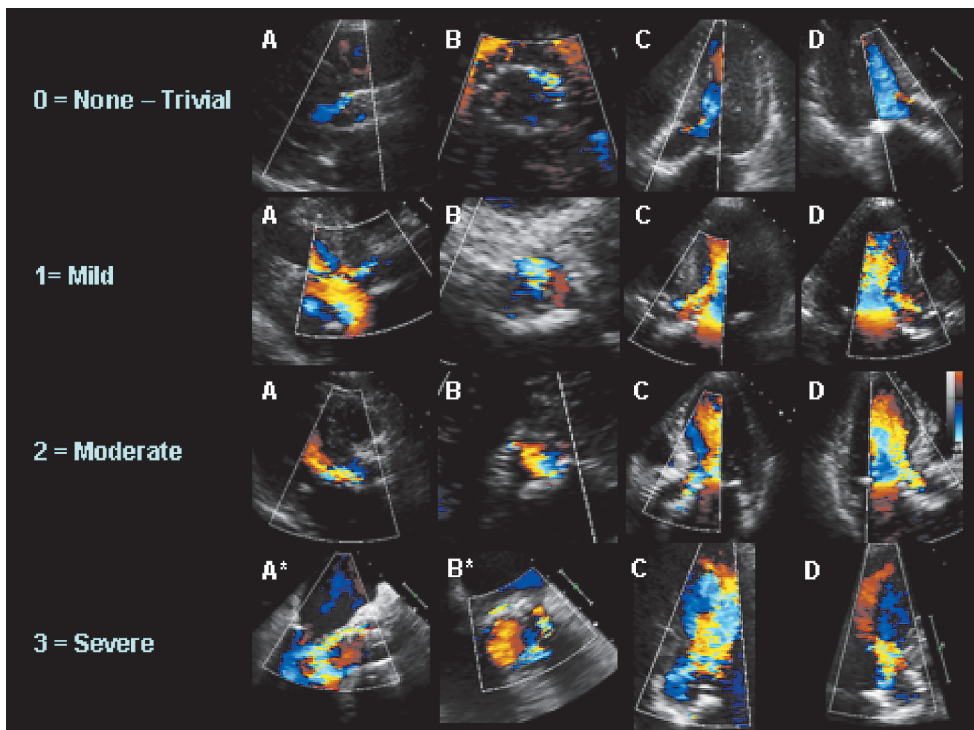


Figure 3: Grading of the severity of paravalvular aortic regurgitation (PAR) on transthoracic echocardiography (TTE).

PAR grading is based on the assessment of the regurgitant jet(s) using multiple echocardiographic views. Column A: parasternal long-axis view; PAR is often underestimated in this view. Column B: parasternal short-axis view; the origins of paravalvular leaks can be identified, especially if the operator slightly modifies the cut-plane in order to capture jets that originate from different levels around the prosthesis. This view may underestimate or overestimate the severity of AR if multiple or eccentric jets are present. Column C: Apical five-chamber view. Column D: Apical three-chamber view. By using apical views the operator can identify and assess the majority of paravalvular jets and then grade the severity of AR. However, exact quantification using the Doppler signal is rarely feasible because commonly jets are multiple and move in a non-parallel direction.

* Images from trans-esophageal echocardiography. Parasternal views on TTE could not be obtained.

Echocardiography analysis method and Comparison of PAR data on TTE with anatomical data from MSCT (Figure 4)

The origin of paravalvular aortic regurgitation (PAR) after TAVI was assessed using the TTE parasternal short axis view, between 5 and 10 days after TAVI. More specifically, a short axis of the Medtronic CRS frame was visible at the level of the native aortic valve, and Color-flow Doppler signals were measured and placed over a clock-face map. In order to increase the precision of measurements, the results of the clock-face map were additionally verified using all TTE views with available Color-flow Doppler signals (parasternal long axis, apical 3-chamber and 5-chamber views).

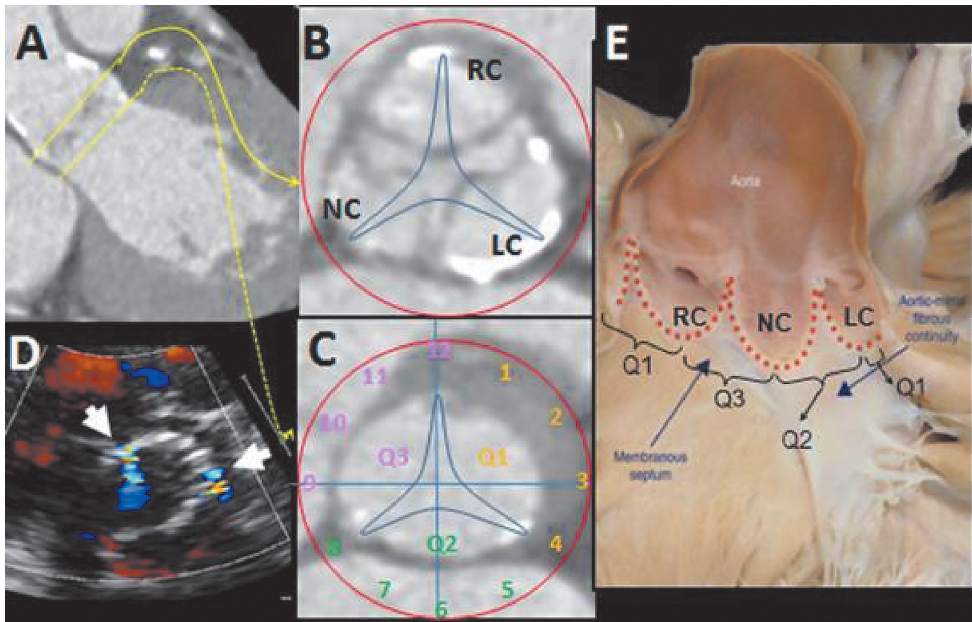


Figure 4. Localisation of paravalvular aortic regurgitation (PAR) on transthoracic echocardiography (TTE) to anatomical structures seen on multislice computer tomography (MSCT).

The coronal view of the aortic root on MSCT (**Panel A**): its relations to cross sectional views of the mid part of the sinus of Valsalva (**Panel B**) and at the base of the aortic root or annulus (**Panel C**) are shown. The presence of PAR localised on a clockface around the inflow of the CRS on TTE (**Panel D**) was simplified to 3 quadrants (Panels B & C). **The first quadrant (Q1)** between 12 o'clock and up to and including 4 o'clock includes the intersinus triangle between the right and left aortic cusps and is illustrated on the anatomic specimen in **Panel E**. This quadrant represents the leftmost aspect of D_{max} adjacent to the right ventricular outflow tract. **The second quadrant (Q2)** between 4 o'clock and up to and including 8 o'clock includes the intersinus triangle between the left and non-coronary aortic cusps and the fibrous section of the annulus confluent with the anterior mitral leaflet (11). **The third quadrant (Q3)** includes the intersinus triangle between the non-coronary and right aortic cusps and the rightmost border of D_{max} adjacent to the membranous inter-ventricular septum. In panel D jets of PAR can be seen at 9 and 2 o'clock which were localised to the junctions of the NC and RC cusps and RC and LC cusps respectively. Some clockwise rotation of the anatomy on TTE relative to that on MSCT is anticipated because MSCT is performed in the supine position whereas TTE is performed with the patient on the left side.

RC=right coronary cusp, LC=left coronary cusp, NC=non-coronary cusp.

Q1: from 12 up to and including 4 o'clock; Q2: from 4 up to and including 8 o'clock;

Q3: from 8 up to and including 12 o'clock.

In order to localise PAR to anatomical structures relevant to TAVI on MSCT the presence of PAR grade ≥ 1 was located to a clockface, in the orientation of the parasternal short axis view on TTE, and was then simplified to 3 quadrants (Figure 4). **The first quadrant (Q1)** between 12 o'clock and up to and including 4 o'clock includes the intersinus triangle between the right and left aortic cusps and the leftmost aspect of D_{max} adjacent to the right ventricular outflow tract. **The second quadrant (Q2)** between 4 o'clock

and up to and including 8 o' clock includes the intersinus triangle between the left and non-coronary aortic cusps and the fibrous section of the annulus confluent with the anterior mitral leaflet [13]. **The third quadrant (Q3)** includes the intersinus triangle between the non-coronary and right aortic cusps and the rightmost border of D_{\max} adjacent to the membranous inter-ventricular septum (Figure 4).

The evaluation of aortic regurgitation after valve implantation was performed by TTE just before discharge.

Statistical methods

The assessment of the determinants of $PAR \geq 1$ was performed by means of an univariate analysis.

Variables that were normally distributed are given as the mean and standard deviation (SD) or otherwise as the median and inter-quartile range (IQ-range). The Student's t-test for independent data and the Mann Whitney U-test were respectively used to compare covariates with Gaussian and non-Gaussian distributions between groups with and without PAR. For the comparison of proportions the Chi-square test was used to determine statistical significance. Statistical analysis was done using SPSS 16.0. Statistical significance was defined as $p < 0.05$.

RESULTS

Clinical characteristics of patients are given in Table 1. The aortic annulus minimum and maximum diameters (D_{\min} , D_{\max}) given in Table 1. The ratio of D_{\max} / D_{\min} was >1.2 in 78% of patients so that the annulus was considered oval in the majority (Table 1). The aortic root was densely calcified (Calcium volume >100) in all but two patients.

Respectively 21 and 35 patients received size 26 and 29 mm inflow CRS's. The nominal size of the prosthesis inflow was on average 38% larger than the CSA of the native annulus.

Invasively measured haemodynamic data both pre- and post TAVI were available in 47 patients. There were no differences in invasively measured haemodynamic data either pre- or post TAVI between patients with or without $PAR \geq 1$ (Table 2).

Prevalence, location and determinants of PAR

Prevalence of PAR

Immediately post implantation contrast aortography was used to evaluate regurgitation. Balloon post dilatation was performed in 4 patients and a valve in valve procedure in one patient. Before hospital discharge PAR grade ≥ 1 was seen in 14 (25%) of the 56 patients. Of the 3 patients (5%) with PAR grade ≥ 2 , one who had severe kiphoscoliosis with an unusual anatomy (compassionate implant) died one week later and two patients with grade 2 PAR despite correctly positioned prostheses remained at the same grading 6 months later and were symptomatically much improved.

Table 1. Patient characteristics.

Mean (SD) or N(%) or Median [IQ-range]	MSCT pre-procedure
Clinical	N=56
Male: N (%)	31 (55)
Age (y)	80 (6)
Height (cm)	167 (9)
Weight (kg)	73 (14)
BMI	26 (4)
BSA (m ²)	1.8 (0.2)
MSCT pre-TAVI	
Diameters in mm	
D _{min}	21 (3)
D _{max}	27 (3)
D _{CSA}	24 (3)
D _{max} /D _{min}	1.28 (0.13)
Calcium score	
Agatston	3337 [2438-4721]*
Mass	752 [507-1250]*
Volume	2649 [1803-4054]*
Procedural factors	
Prosthesis implanted 26:29 (N)	21:35
Ratio of nominal prosthesis CSA at inflow to CSA of the native annulus	1.38 (0.21)

* N=48 patients had non-contrast calcium scoring MSCT in addition to contrast enhanced scans
 BMI: body mass index;
 BSA: body surface area;
 D_{min}: minimum annulus diameter;
 D_{max}: maximum annulus diameter;
 D_{CSA}: diameter from annulus area;
 CSA: cross-sectional surface area.

Table 2. Invasively measured haemodynamic data pre- and post TAVI in patients with and without PAR \geq 1.

Median [IQ-range]	PAR<1 N=36	PAR \geq 1 N=11
Pre TAVI		
LVEDP	16 [11-21]	16 [13-21]
Aorta systolic	122 [105-154]	127 [104-143]
Aorta diastolic	54 [44-65]	50 [44-58]
Peak gradient	46 [31-63]	48 [38-59]
Post TAVI		
LVEDP	17 [13-30]	21 [12-30]
Aorta systolic	136 [120-172]	140 [100-184]
Aorta diastolic	56 [50-63]	49 [41-61]
Peak gradient	1 [0-4]	6 [0-9]

PAR: paravalvular aortic regurgitation;
 LVEDP: Left ventricular end diastolic pressure.

Anatomical location of PAR

PAR \geq 1 was predominantly located at Q1 (20%), which contains the aspect of the largest diameter of the aortic annulus on the inside curve of the ascending aorta, and in Q2 (16%), which contains the aorto-mitral fibrous continuity, and less frequent in Q3 (13%), which contains the ventricular membranous septum and the aspect of the largest diameter of the aortic annulus on the outside curve of the ascending aorta.

Clinical and anatomical determinants of PAR

Patients with PAR \geq 1 were associated with being taller ($p<0.05$), a larger D_{\min} ($p<0.05$), D_{\max} ($p<0.05$) and D_{CSA} ($p<0.01$), a higher calcification score of the aortic root ($p<0.01$), and a smaller ratio of the nominal prosthesis inflow CSA (26mm CRS = 5.32cm²; 29mm CRS=6.62 cm²) to the native pre-implantation aortic annulus CSA ($p<0.05$), when compared to those with PAR $<$ 1 (Table 3). Weight, BSA, BMI, the difference between D_{\min} and D_{\max} or the ratio of D_{\min}/D_{\max} were not significantly different (Table 3). The correlation coefficient of PAR grade (0-3) with the different annulus diameter measurements was strongest for D_{CSA} followed by D_{\min} and D_{\max} (respectively $r=0.43$, $r=0.40$, $r=0.38$, all $p<0.01$).

Table 3. Determinants of PAR \geq 1 in patients with preprocedural MSCT.

Mean (SD) Median [IQ-range] N (%)	AR<1 N=42	AR \geq 1 N=14
Male: N (%)	16 (42)	10 (71)
Age (y)	78 [72-88]	83 [79-85]
Height (cm)	165 (8)	171 (10)*
Weight (kg)	68 [62-82]	72 [63-86]
BMI	26 (4)	25 (4)
BSA (m ²)	1.8 (0.2)	1.9 (0.2)
Diameters in mm		
D_{\min}	21 (2)	23 (3)*
D_{\max}	26 (3)	28 (2)*
D_{CSA}	23 (2)	25 (3)**
Ratio Dmax /Dmin	1.27 (0.09)	1.27 (0.18)
Calcium score		
Agatston	2883[2039-4308]	4083 [3420-5860]*
Mass	621[487-1176]	976[806-1517]**
Volume	2333 [1743-3693]	3449 [2817-4589]*
Ratio of nominal prosthesis CSA at inflow to CSA of the native annulus	1.41 (0.20)	1.28 (0.22)*

* $p<0.05$; ** $p<0.01$

BMI: body mass index; BSA: body surface area; D_{\min} : minimum annulus diameter; D_{\max} : maximum annulus diameter; D_{CSA} : diameter from annulus area; CSA: cross-sectional surface area.

Evaluation of malapposition of the CRS frame post implantation

PAR \geq 1 was present in 8 of 34 (24%) patients with MSCT post-procedure. Malapposition at the inflow of the frame was seen in 51% of patients and was more common at the aspect of the largest diameter of the annulus on the inside curve of the ascending aorta (Q1, 41%) than on the outside curve (Q3, 11%). Malapposition at the inflow of the frame was seen at the aorto-mitral fibrous continuity (Q2) in 38%. A non-apposed intersinus triangle was present in 46% of patients and was more common at the aorto-mitral fibrous continuity in Q2 (44%) than in either Q1 (12%) or Q3 (3%).

DISCUSSION

We observed PAR grade \geq 1 in 25% of patients after TAVI with the Medtronic CRS whereas at least trivial PAR was seen in the majority of patients. We found that PAR grade \geq 1 was predominantly seen in the area of the aorto-mitral fibrous continuity and occurred more often in patients with a larger annulus, more aortic root calcification or in whom there was a lower degree of oversizing of the prosthesis in relation to the native annulus.

Similar rates and severity of PAR were recently reported after TAVI with the Edwards Sapiens prosthesis [7]. Haemodynamically significant PAR (grade \geq 2) is rarely reported after TAVI because it is poorly tolerated peri-procedure in elderly patients with hypertrophied stiff ventricles and is therefore usually corrected during the index procedure either by post dilatation, removal and repositioning of the prosthesis or placement of a second prosthesis [14]. After surgical AVR the reported incidence of PAR ranges from 6% to 48% but in contrast to TAVI it is mostly trivial (rather than mild) and the more recent series report incidences of PAR at the lower end of the range [15-18]. The differences in reported incidence in PAR between surgical AVR and TAVI partly reflect the difficulties in accurately quantifying PAR because signal attenuation from the metal frame obscures the origin of the PAR jet. This factor may affect evaluation of PAR with the Medtronic CRS more than other surgical or TAVI prostheses due to the fact that the frame is much higher (56mm) and may extend deeper below the annulus in a proportion of patients. After surgical AVR mild PAR is usually benign, is only rarely associated with progression in severity in the absence of endocarditis or prosthesis degeneration, and only rarely is associated with significant haemolysis [15-17]. Although there are no randomized comparisons the frequency of mild PAR after TAVI may be higher than after SAVR [19] and long term effects may be unlikely but are yet to be determined.

We report that anatomical factors and sizing may be more important after TAVI whereas the causes of PAR after SAVR are mainly related to technical aspects of the procedure [15,16]. This may in part be because in contrast to SAVR the operator during TAVI can not directly visualize the anatomy but has to rely on imperfect (usually 2D) imaging of the aortic root and clinical data for sizing [20]. Furthermore, as the stenotic valve and

the surrounding root calcifications are not excised during TAVI in addition to the fact that the TAVI prosthesis is not sutured into place but relies on apposition to surrounding tissue inaccurate sizing may be more likely to result in PAR. Two of the factors associated with PAR in our study were related to sizing (prosthesis inflow to native annulus area, annulus diameter). Annulus diameter was also a determinant of PAR as assessed by trans-oesophageal echocardiography (TEE) after TAVI with a balloon expandable prosthesis [7]. In that study only diameter measurements from echocardiography were used [7] which correspond approximately to the D_{\min} in our study [21]. It is now recognized that the aortic annulus is non-circular and that sizing with 2D modalities such as TTE/TEE may lead to undersizing, because 2D TTE/TEE does not allow the measurement of D_{CSA} or D_{\max} [9,22-25]. In the study using TEE a lower degree of oversizing was a determinant of PAR, in addition to annulus diameter, after TAVI with a balloon expandable prosthesis [7]. We confirm this observation using different imaging techniques (MSCT, TEE) and a self expanding prosthesis.

In the present study the association of PAR with D_{\max} and with the ratio of prosthesis inflow to native annulus CSA may indicate that the use of a 3D modality such as MSCT, CMRI or 3D echo would improve size selection for TAVI [9]. The question is how to translate this information into a sizing decision algorithm. The implications of using MSCT for sizing rather than TTE or TEE may be quite different for the Edwards and MCRS prostheses [9,26], in part because the available sizes of Edwards prostheses are designed for smaller annuli and in part due to differences in prosthesis configuration and method of deployment. More sizes of TAVI prostheses may be needed as MSCT provides larger measurements than echocardiography on the basis of which the manufacturer's guidelines of sizing are based.

In the present study the association of PAR grade with D_{CSA} was stronger than for D_{\max} or D_{\min} . We have previously reported that the CRS inflow conforms to the annulus dimensions (i.e. D_{\min} , D_{\max}) when the annulus is non-circular [10]. The best single estimate of the D_{\min} and D_{\max} is the mean of D_{\min} and D_{\max} , which is very similar in magnitude to D_{CSA} [9]. D_{CSA} would also correspond best to operator choice once the operator has taken into account all available clinical data [9]. Therefore if current industry guidelines were to be applied size selection based on D_{CSA} is likely to give the best anatomical match between native annulus dimensions and the prosthesis inflow

In the present study the prosthesis inflow was larger relative to the native annulus area. The Medtronic CRS is self-expanding and is designed to be oversized, within design limits, in order to wedge in the LVOT and under the calcified native leaflets thereby maintaining a stable position and reducing PAR [1]. Nonetheless in the present study a higher grade of PAR was associated with lower degree of oversizing. Deliberate oversizing (implanting a size 29 where a size 26 is indicated according to current guidelines) would likely reduce PAR, but on the other hand may increase the risk of conduction abnormalities due to a theoretical increase of pressure on the thin walled ventricular mem-

branous septum [13], increase the risk of aortic root rupture [27] and potentially also reduce the prosthesis durability due to distortion of leaflet coaptation [28,29]. Alternatively sizing based on mean annulus diameter (either mean of D_{\min} and D_{\max} or D_{CSA}) together with the availability of prosthesis sizes larger than 29 inflow may reduce PAR by reducing undersizing.

In addition to annulus dimensions and sizing the volume of calcium in the aortic root was a determinant of PAR in the present study. MSCT may reproducibly measure aortic root calcification which may facilitate procedural planning before SAVR [30,31]. Whereas the aortic root is decalcified during SAVR the calcium is merely pushed aside during TAVI and has to be overcome by the predilatation balloon and prosthesis frame expansion. The disrupted calcium may contribute to PAR by preventing full or symmetric prosthesis expansion, reducing prosthesis apposition and potentially perforating the sealing skirt or the leaflets. A study of a custom made balloon deployable valve demonstrated that calcium could cause distortion of leaflet coaptation due to under- or asymmetrical expansion of the prosthesis frame [32]. However, due to limitations of current analysis software we were not able to measure the degree of calcification in the 3 quadrants. Interestingly aortic root calcium burden was only associated with AR in Q1.

Due to leverage of the 5cm long prosthesis frame exerted by the leftward curvature of the aorta the force of apposition of the frame to the adjacent tissue of the annulus would be higher in Q3 (outside curve or right-hand side of the annulus) and lower in Q1 (inside curve or left hand side of the annulus). Additionally tension on the delivery catheter during TAVI may push the device toward the outside curve of the aorta. These hypotheses are supported by the higher rate of malapposition in Q1 compared with Q3. Both of these factors would reduce the ability of the frame to overcome the resistance posed by densely calcified tissue and thereby increase the risk of PAR in the presence of a non-apposed frame in Q1. These factors may explain the higher incidence of PAR in Q1 and may suggest that calcification may exacerbate the effects of other determinants of AR such as undersizing. These data may suggest that in cases with substantial curvature of the aorta and a large D_{\max} improvements in the prosthesis delivery technology or less likely a prosthesis with less height may be preferable in order to reduce PAR at the right-left coronary intersinus triangle, although this requires further study.

We also observed a higher incidence of PAR in Q2 when compared to Q3. In Q2 the prosthesis lies adjacent to the aorto-mitral fibrous continuity. This structure is thin walled and may offer less and to some extent a dynamic (anterior mitral valve leaflet) force of apposition to the prosthesis frame. Furthermore due to the oval shape of the aortic annulus the curvature of the CRS frame, when viewed axially, would be flatter along Q2, which may further reduce the ability to ensure apposition in the often densely calcified non- and left coronary intersinus triangle. These anatomical factors may suggest that PAR in Q2 may be a consequence of limitations in prosthesis design.

Limitations

This is a small hypothesis generating study in a selected group of patients and the results require verification. In keeping with the exploratory nature of the study many statistical tests were done relative to study size so that there is a possibility of type 2 error. The severity of PAR is difficult to assess in particular because the point of origin of a regurgitant jet can often not be accurately identified and furthermore there is no consensus or guidelines on how this should be done. TEE is the modality of choice for detecting PAR, but we did not have these data available. Yet by obtaining multiple views on TTE of the prosthesis the under diagnosis of PAR was minimized and it is highly unlikely that any haemodynamically significant PAR (grade 2 or more) was missed on TTE with this approach. Although we have shown that aortic root calcium volume is a significant determinant of PAR we were unable to investigate the contribution of calcification at the various anatomical structures of interest due to limitations in current analysis software. Although the determinants of PAR for the MCRCs in the present study were similar to those seen for the Edwards prosthesis in another study [7], not all these results may not be applicable to other TAVI prostheses due to differences in geometry and implantation method.

CONCLUSIONS

Mild PAR is common after TAVI. PAR was more common at the aorto-mitral fibrous continuity and the left (inside curve of LVOT/ascending aorta) aspect of Dmax. The maximum annulus diameter and a lower degree of prosthesis oversizing were determinants of PAR suggesting that improved sizing based on a 3D imaging modality e.g. MSCT should reduce PAR. The volume of calcification in the aortic root may exacerbate PAR. The availability of additional (larger) prosthesis sizes in combination with improved sizing based on mean annulus diameter (e.g. DCSA) may help to reduce PAR.

REFERENCES

1. Grube E, Laborde JC, Gerckens U, et al., Percutaneous implantation of the CoreValve self-expanding valve prosthesis in high-risk patients with aortic valve disease: the Siegburg first-in-man study; *Circulation*. 2006; 114:1616-24.
2. Cribier A, Eltchaninoff H, Bash A, Borenstein N, Tron C, Bauer F, Derumeaux G, Anselme F, Laborde F, Leon MB. Percutaneous transcatheter implantation of an aortic valve prosthesis for calcific aortic stenosis: first human case description. *Circulation*. 2002;106:3006-8.
3. Fraccaro C, Napodano M, Tarantini G, Gasparetto V, Gerosa G, Bianco R, Bonato R, Pittarello D, Isabella G, Iliceto S, Ramondo A. **Expanding the eligibility for transcatheter aortic valve implantation the trans-subclavian retrograde approach using: the III generation CoreValve revalving system.** *JACC Cardiovasc Interv*. 2009; 2:828-33.
4. Piazza N, Otten A, Schultz C, Onuma Y, Garcia Garcia H, Boersma E, de Jaegere P, Serruys PW. Adherence to patient selection criteria in patients undergoing transcatheter aortic valve implantation with the 18F CoreValve ReValving™ System - Results from a single-center study. *Heart*. 2010; 96:19-26
5. Piazza N, Grube E, Gerckens U, den Heijer P, Linke A, Luha O, Ramondo A, Ussia G, Wenaweser P, Windecker S, Laborde JC, de Jaegere P, Serruys PW. Procedural and 30-day outcomes following transcatheter aortic valve implantation using the third generation (18 Fr) corevalve revalving system: results from the multicentre, expanded evaluation registry 1-year following CE mark approval. *EuroIntervention*. 2008; 4:242-9.
6. Olsen LK, Engstrøm T, Søndergaard L. Transcatheter valve-in-valve implantation due to severe aortic regurgitation in a degenerated aortic homograft. *J Invasive Cardiol*. 2009;21:E197-200.
7. Détaint D, Lepage L, Himbert D, Brochet E, Messika-Zeitoun D, Iung B, Vahanian A. Determinants of significant paravalvular regurgitation after transcatheter aortic valve: implantation impact of device and annulus incongruence. *JACC Cardiovasc Interv*. 2009; 2:821-7.
8. de Jaegere P, van Dijk LC, Laborde JC, Sianos G, Orellana Ramos FJ, Lighthart J, Kappetein AP, Vander Ent M, Serruys PW. True percutaneous implantation of the CoreValve aortic valve prosthesis by the combined use of ultrasound guided vascular access, Prostar(R) XL and the TandemHeart(R). *EuroIntervention*. 2007; 2:500-5.
9. Schultz CJ, Moelker A, Piazza N, Tzikas A, Otten A, Nuis RJ, Neefjes L, van Geuns RJ, de Feyter P, Krestin G, Serruys PW1, de Jaegere PPT. 3D evaluation of the aortic annulus using multislice computer tomography. Are manufacturer's guidelines for sizing for percutaneous aortic valve replacement helpful? *Eur Heart J*. 2010;31:849-56.
10. Schultz CJ, Weustink A, Piazza N, Otten A, Mollet N, Krestin G, van Geuns RJ, de Feyter P, Serruys PW, de Jaegere P. Geometry and degree of apposition of the CoreValve ReValving system with multislice computed tomography after implantation in patients with aortic stenosis. *J Am Coll Cardiol*. 2009;54:911-8
11. Zoghbi WA, Enriquez-Sarano M, Foster M, et al. Recommendations for evaluation of the severity of native valvular regurgitation with two-dimensional and Doppler echocardiography. *J Am Soc Echocardiogr* 2003;16:777– 802.
12. Perry GJ, Helmcke F, Nanda NC, Byard C, Soto B. Evaluation of aortic insufficiency by Doppler color flow mapping. *J Am Coll Cardiol* 1987;9:952–9.

13. Piazza N, de Jaegere P, Schultz C, Becker P, Serruys PWJS, Anderson R; Anatomy of the Aortic Valvar Complex and Its Implications for Transcatheter Implantation of the Aortic Valve. *Circ Cardiovasc Intervent.* 2008;1:74-81.
14. Masson JB, Kovac J, Schuler G, Ye J, Cheung A, Kapadia S, Tuzcu ME, Kodali S, Leon MB, Webb JG. Transcatheter aortic valve implantation: review of the nature, management, and avoidance of procedural complications. *JACC Cardiovasc Interv.* 2009;2:811-20.
15. O'Rourke DJ, Palac RT, Malenka DJ, Marrin CA, Arbuckle BE, Plehn JF. Outcome of mild periprosthetic regurgitation detected by intraoperative transesophageal echocardiography. *J Am Coll Cardiol.* 2001;38:163-6.
16. Ionescu A, Fraser AG, Butchart EG. Prevalence and clinical significance of incidental paraprosthetic valvar regurgitation: a prospective study using transoesophageal echocardiography. *Heart.* 2003;89:1316-21.
17. Rallidis LS, Moysakakis IE, Ikonomidis I, Nihoyannopoulos P. Natural history of early aortic paraprosthetic regurgitation: a five-year follow-up. *Am Heart J.* 1999;138:351-7.
18. Chambers J, Monaghan M, Jackson G. Colour flow Doppler mapping in the assessment of prosthetic valve regurgitation. *Br Heart J.* 1989;62:1-8.
19. Clavel MA, Webb JG, Pibarot P, Altwegg L, Dumont E, Thompson C, De Larocheilière R, Doye D, Masson JB, Bergeron S, Bertrand OF, Rodés-Cabau J. Comparison of the hemodynamic performance of percutaneous and surgical bioprostheses for the treatment of severe aortic stenosis. *J Am Coll Cardiol.* 2009;53:1883-91.
20. Babaliaros VC, Liff D, Chen EP, Rogers JH, Brown RA, Thourani VH, Guyton RA, Lerakis S, Stillman AE, Raggi P, Cheesborough JE, Veladar E, Green JT, Block PC. Can balloon aortic valvuloplasty help determine appropriate transcatheter aortic valve size? *JACC Cardiovasc Interv.* 2008;1:580-6.
21. Tzikas A, Schultz CJ, Piazza N, Moelker A, Van Mieghem NM, Nuis RJ, van Geuns RJ, Geleijnse ML, Serruys PW, de Jaegere PPT. Assessment of the Aortic Annulus by Multi-Slice Computed Tomography, Contrast Aortography and Trans-Thoracic Echocardiography in Patients Referred for Transcatheter Aortic Valve Implantation. *Catheter Cardiovasc Interv.* 2010 (in press)
22. Laurens F, Tops D, David A, Wood, Victoria Delgado, Joanne D. Schuijf, John R. Mayo, Sanjeevan Pasupati, Frouke P.L. Lamers, Ernst E. van der Wall, Martin J. Schalij, John G. Webb, and Jeroen J. Bax. Noninvasive Evaluation of the Aortic Root With Multislice Computed Tomography: Implications for Transcatheter Aortic Valve Replacement *J. Am. Coll. Cardiol. Img.* 2008;1;321-330
23. Doddamani S, Bello R, Friedman MA, Banerjee A, Bowers JH Jr, Kim B, Vennalaganti PR, Ostfeld RJ, Gordon GM, Malhotra D, Spevack DM. Demonstration of left ventricular outflow tract eccentricity by real time 3D echocardiography: implications for the determination of aortic valve area. *Echocardiography.* 2007;24:860-6.
24. Tanaka K, Makaryus AN, Wolff SD. Correlation of aortic valve area obtained by the velocity-encoded phase contrast continuity method to direct planimetry using cardiovascular magnetic resonance. *J Cardiovasc Magn Reson.* 2007;9:799-805.
25. Wood DA, Tops LF, Mayo JR, Pasupati S, Schalij MJ, Humphries K, Lee M, Al Ali A, Munt B, Moss R, Thompson CR, Bax JJ, Webb JG. Role of multislice computed tomography in transcatheter aortic valve replacement. *Am J Cardiol.* 2009;103:1295-301.

26. Messika-Zeitoun D, Serfaty JM, Brochet E, Ducrocq G, Lepage L, Detaint D, Hyafil F, Himbert D, Pasi N, Laissy JP, Iung B, Vahanian A. Multimodal assessment of the aortic annulus diameter: implications for transcatheter aortic valve implantation. *J Am Coll Cardiol.* 2010;55(3):186-94.
27. Lembo NJ, King SB 3rd, Roubin GS, Hammami A, Niederman AL. Fatal aortic rupture during percutaneous balloon valvuloplasty for valvular aortic stenosis. *Am J Cardiol.* 1987;60:733-6.
28. Thubrikar M, Piepgrass WC, Shaner TW, Nolan SP. The design of the normal aortic valve. *Am J Physiol.* 1981;241:H795-801.
29. Thubrikar M, Piepgrass WC, Deck JD, Nolan SP. Stresses of natural versus prosthetic aortic valve leaflets in vivo. *Ann Thorac Surg.* 1980;30:230-9.
30. Mullany CJ. Aortic valve surgery in the elderly. *Cardiol Rev.* 2000;8:333-9.
31. Willmann JK, Weishaupt D, Lachat M, Kobza R, Roos JE, Seifert B, Lüscher TF, Marincek B, Hilfiker PR. Electrocardiographically gated multi-detector row CT for assessment of valvular morphology and calcification in aortic stenosis. *Radiology.* 2002;225:120-8
32. Zegdi R, Ciobotaru V, Noghin M, et al. Is it reasonable to treat all calcified stenotic aortic valves with a valved stent? Results from a human anatomic study in adults. *J Am Coll Cardiol.* 2008;51:579-84.

Chapter 7

Frequency of Conduction Abnormalities Following Transcatheter Aortic Valve Implantation with the Medtronic-CoreValve and the Effect on Left Ventricular Ejection Fraction

Tzikas A
van Dalen BM
Van Mieghem NM
Gutierrez-Chico JL
Nuis RJ
Kauer F
Schultz CJ
Serruys PW
de Jaegere PP
Geleijnse ML

ABSTRACT

New conduction abnormalities occur frequently after TAVI. The relation between new conduction disorders and LV systolic function following TAVI is unknown. The purpose of this prospective single-center study was to investigate the effect of transcatheter aortic valve implantation (TAVI) on left ventricular (LV) systolic function in relation to TAVI-induced conduction abnormalities. Twenty-seven patients had an electrocardiogram and a trans-thoracic echocardiogram the day before and 6 days after TAVI with the Medtronic-CoreValve system. LV ejection fraction (EF) was calculated using the biplane Simpson's method. Systolic mitral annular velocities and longitudinal strain were measured using Speckle Tracking Echocardiography. After TAVI, 18 patients (67%) had new conduction abnormalities; 4 patients (15%) had a new paced rhythm and 14 patients (52%) had a new left bundle branch block. In patients with new conduction abnormalities the EF decreased from 47 ± 12 to 44 ± 10 % whereas in those without new conduction abnormalities the EF increased from 49 ± 12 to 54 ± 12 %. The change in EF was significantly different among patients with and without new conduction abnormalities ($p < 0.05$). In patients without new conduction abnormalities an improvement was found in systolic mitral annular velocities and longitudinal strain ($p < 0.05$), whereas in patients with new conduction abnormalities changes were not significant. In conclusion, the induction of new conduction abnormalities following TAVI with the Medtronic-CoreValve is associated with a lack of improvement in LV systolic function.

INTRODUCTION

Transcatheter aortic valve implantation (TAVI) is a new promising therapeutic option for high-risk patients with severe aortic stenosis. [1-5] Most experience has been achieved with the Medtronic-CoreValve system (Medtronic-CoreValve Inc., Minneapolis, MN, USA) and the Edwards SAPIEN (Edwards Lifesciences, Inc., Irvine, CA, USA) bioprosthetic valve. Both devices have demonstrated favorable hemodynamic results with a significant decrease in trans-aortic gradients and considerable clinical improvement. Despite this immediate decrease in trans-aortic gradient, left ventricular (LV) ejection fraction (EF) has been reported to remain unchanged after TAVI with the Medtronic-CoreValve. [6,7] More subtle measurements of LV systolic function include mitral annular velocities and longitudinal strain (active deformation of the cardiac muscle). Speckle tracking echocardiography (STE) can assess both parameters reliably, independently from the angulation of the transducer and with optimal reproducibility. [8] Following TAVI with the Medtronic-CoreValve, a left bundle branch block (LBBB) or an atrioventricular block needing permanent pacemaker implantation occur in 40-65% and 20-33% of patients, respectively. [9-12] To date the relation between conduction disorders and LV systolic function following TAVI is unknown. The purpose of this prospective single-center study was to investigate the effect of TAVI on LV systolic function in relation to TAVI-induced conduction abnormalities.

METHODS

The study population comprised 27 consecutive patients that underwent TAVI with the Medtronic-CoreValve and had trans-thoracic echocardiograms (TTE) of adequate quality before and after the procedure. The inclusion and exclusion criteria for TAVI have been described in detail elsewhere [3]. Briefly, patients were included if they had severe native aortic valve stenosis with an aortic valve area $<1 \text{ cm}^2$ or $<0.6 \text{ cm}^2/\text{m}^2$, with or without aortic regurgitation and were deemed high risk surgical candidates. Written informed consent was obtained in all patients (post-marketing surveillance registry). The Medtronic-CoreValve System consists of a tri-leaflet porcine pericardial tissue valve, mounted in an hour-glass shaped, self-expanding nitinol frame (50-51 mm high). Currently, the prosthesis is available in sizes of 26 and 29 mm inflow diameter for patient annulus diameters between 20 and 27 mm.

Twelve-lead electrocardiographic tracings were obtained in all patients before and after treatment and were analyzed for rhythm, heart rate, PR interval duration, QRS duration and morphology, and presence of atrioventricular/fascicular block according to recent recommendations [13]. In addition, an electronic single-lead rhythm strip was con-

tinuously recorded during the echocardiographic studies. Patients were considered having new conduction abnormalities when a new LBBB or a new paced rhythm was recorded following the index procedure. Decision to implant a permanent pacemaker was based upon the latest guidelines [14].

Two-dimensional TTE was performed by an independent experienced echocardiographer the day before and one week after the procedure, using a commercially available system (iE33, Philips, Best, The Netherlands) with the patient in a left lateral decubitus position, according to published recommendations [15]. All echocardiograms were saved as video loops or still frames in a digital database and were analyzed by a second independent investigator. LV EF was calculated using the biplane modified Simpson's rule. Trans-aortic peak velocity, peak and mean gradient and velocity-time integral were measured using continuous-wave Doppler through the native or prosthetic aortic valve. The aortic valve area was estimated using the continuity equation approach [$AVA = LVOT_{\text{area}} \times (\text{velocity time integral}_{LVOT} / \text{velocity time integral}_{\text{valve}})$]. Aortic regurgitation and mitral regurgitation were assessed semi-quantitatively according to the current guidelines for the evaluation of native valves [16].

Speckle tracking echocardiography (STE) was performed using 2-dimensional grayscale harmonic images at a frame rate of 70 – 80 frames/s. Datasets were transferred to a QLAB workstation for analysis using QLAB Advanced Quantification Software version 6.0 (Philips, Best, The Netherlands). Details regarding Speckle Tracking analysis have been previously published [8]. For the purpose of this study, systolic mitral annular velocities and longitudinal wall strain were assessed from the infero-septal and antero-lateral sides of the LV (from the base to the distal part of the particular wall) in an apical 4-chamber view. The inter-observer variabilities were $3.7 \pm 3.3\%$ and $4.8 \pm 5.2\%$, respectively [8].

Continuous variables are presented as means (\pm SD) and categorical variables are presented as frequencies and percentages. For comparisons between two time-points, a paired sample *t*-test or a Wilcoxon signed rank test for 2 related samples were used for normally distributed or skewed data, respectively. For ordinal variables (AR and MR grade), a constant difference between values was assumed. A two-sided *p* value < 0.05 was considered statistically significant. All statistical analyses were performed with SPSS 17.0 software (SPSS Inc., Chicago, IL, USA).

RESULTS

Baseline patient characteristics are summarized in Table 1. The study population consisted of elderly patients with a number of co-morbidities. Four patients (15%) had a baseline $EF \leq 35\%$. Eight patients (30%) underwent TAVI using a 26 mm and 19 (70%) using a 29 mm inflow Medtronic-CoreValve. Post – deployment balloon dilatation was performed in 3 patients (11%). No patient required a second bioprosthesis as a valve-in-valve bailout.

Table 1. *Baseline characteristics.*

Variable	Study population (n = 27)
Age (years)	81 (78 – 86)
Male	14 (52%)
Body Mass Index (kg/m ²)	26 ± 4
Body Surface Area (m ²)	1.84 ± 0.19
Antecedents	
Cerebro-vascular events	6 (22%)
Myocardial infarction	6 (22%)
Percutaneous coronary intervention	8 (30%)
Coronary artery bypass	7 (26%)
Co-morbidities	
Chronic obstructive pulmonary disease	8 (30%)
Chronic renal disease	3 (11%)
Peripheral vascular disease	5 (19%)
Atrial fibrillation	6 (22%)
Diabetes mellitus	6 (22%)
Ejection Fraction ≤ 35%	4 (15%)
New York Heart Association status	
I-II	5 (19%)
III-IV	22 (81%)
Logistic EuroSCORE	11 (9 – 22)

Data are presented as mean ± SD, median (IQ range) or number (%).

Before TAVI (1 day before), no patient had a paced rhythm, 1 patient (4%) had an LBBB and 4 patients (15%) a left anterior fascicular block (LAFB). After TAVI (day 6), 4 patients (15%) had a paced rhythm, 15 patients (56%) had an LBBB [14 patients (52%) a new LBBB] and none an LAFB. Therefore, 18 patients (67%) had new conduction abnormalities. With respect to the baseline characteristics, a comparison between patients with and patients without new conduction abnormalities did not reveal statistically significant differences. The indication for permanent pacemaker implantation was (in all 4 cases) a complete heart block.

Echocardiographic changes following TAVI are shown in Table 2. Mean trans-aortic gradient decreased from 44±14 to 9±3 mmHg and aortic valve area increased from 0.62±0.20 to 1.65±0.38 cm² (p<0.001). A small, non-significant decrease in aortic regurgitation and mitral regurgitation severity was observed. Overall, EF and longitudinal strain did not change significantly, whereas systolic mitral annular velocities improved. A subgroup analysis of LV systolic parameters in relation to new conduction abnormalities is shown in Table 3. In patients with new conduction abnormalities the EF decreased from 47±12 to 44±10% whereas in those without new conduction abnormalities the EF

Table 2. *Echocardiographic changes following Transcatheter Aortic Valve Implantation (n=27).*

Variable	Pre-TAVI	Post-TAVI	p value
Peak aortic gradient (mmHg)	75 ± 23	18 ± 7	< 0.001
Mean aortic gradient (mmHg)	44 ± 14	9 ± 3	< 0.001
Peak aortic velocity (cm/sec)	422 ± 58	210 ± 40	< 0.001
Aortic valve area (cm ²)	0.62 ± 0.20	1.65 ± 0.38	< 0.001
Aortic regurgitation grade (1-4)	1.8 ± 1.0	1.6 ± 1.2	0.61
Mitral regurgitation grade (1-4)	1.8 ± 0.7	1.6 ± 0.8	0.06
Ejection Fraction (%)	47 ± 11	48 ± 12	0.94
Mitral annular velocity (cm/sec)			
Infero-septal	4.0 ± 1.2	5.1 ± 1.7	< 0.05
Antero-lateral	4.5 ± 1.4	5.6 ± 1.9	< 0.05
Longitudinal strain (%)	11 ± 3	12 ± 3	0.64

Data are presented as mean ± SD. Sm = peak systolic wave mitral annular velocity.

Table 3. *Left Ventricular systolic function in relation to new conduction abnormalities.*

Variable	New conduction abnormalities			
	No (n = 9)		Yes (n = 18)	
	Pre-TAVI	Post-TAVI	Pre-TAVI	Post-TAVI
Mitral annular velocity (cm/s)				
Infero-septal	4.3 ± 1.4	6.5 ± 2.2*	3.8 ± 1.0	4.4 ± 0.8
Antero-lateral	4.8 ± 1.3	6.6 ± 2.5*	4.4 ± 1.5	5.1 ± 1.4
Longitudinal strain (%)	11 ± 3	13 ± 3*	11 ± 4	11 ± 2
Ejection Fraction (%)	49 ± 12	54 ± 12	47 ± 12	44 ± 10**

*p < 0.05 versus pre-TAVI in patients without new conduction abnormalities.

**p < 0.05 versus post-TAVI in patients without new conduction abnormalities.

increased from 49±12 to 54±12% (Figure 1). The change in EF was significantly different among patients with and without new conduction abnormalities (p<0.05). In addition, in patients without new conduction abnormalities an improvement was found in systolic mitral annular velocities and longitudinal strain (p<0.05), whereas in patients with new conduction abnormalities changes were not significant. In the 4 patients with EF≤35% at baseline the EF increased from 29±6 to 34±8% (p=0.28)

DISCUSSION

The main finding of the present study is that induction of new conduction abnormalities following TAVI with the Medtronic-CoreValve is associated with a lack of improvement in LV systolic function.

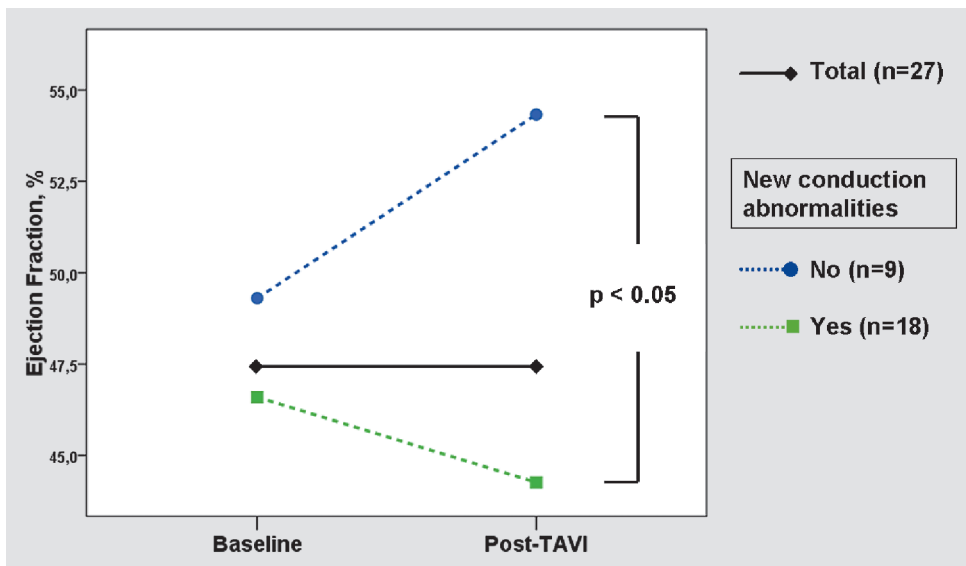


Figure 1. Changes in ejection fraction (EF) following transcatheter aortic valve implantation (TAVI) .

Overall, the EF did not change significantly following TAVI (black line). In patients without new conduction abnormalities (blue dotted line) the EF increased whereas in those with new conduction abnormalities (green dotted line) the EF decreased. The change in EF was significantly different among patients with and without new conduction abnormalities (paired sample t-test, two-sided $p < 0.05$).

After surgical aortic valve replacement the incidence of new LBBB has been reported to be 6% [17], whereas a need for permanent pacing ranged from 3-6% [18]. Conduction disorders have been associated with longer hospital stays and more cardiac adverse events within 1 year following surgical aortic valve replacement [17]. To date, there is no report on the long-term effects of TAVI – induced conduction abnormalities. However, it should be noted that epidemiological studies have shown increased mortality in patients with a combination of complete heart block or LBBB and structural heart disease [19].

Conduction disorders occur frequently after TAVI. The anatomic proximity of the aortic valve to the branching atrioventricular bundle, degeneration and calcification of the conduction system, direct trauma by guidewires and catheters and pre-implantation balloon valvuloplasty may provide possible explanations [9-12]. TAVI using the Medtronic-CoreValve has been associated with a higher incidence of conduction disorders compared to the Edwards SAPIEN valve [10]. This may be explained by the different size of the bioprostheses (height 50-51 mm versus 15-16 mm) and different ways of deployment (self- versus balloon-expandable) [20]. The depth of implantation of the Medtronic-CoreValve within the LV outflow track has been reported to predict the occurrence of new conduction abnormalities, whereas the self-expandable frame per se may produce a more permanent trauma to the adjacent tissue by applying continuous pressure on it [10,20]. Pre-existing conduction disorders such as right bundle branch

block have been found to predict the need for pacemaker implantation following TAVI [10]. In the present study, no patient had a right bundle branch block before or after TAVI. The single patient with baseline LBBB remained in the same status post-TAVI whereas 2 of 4 patients with baseline LAFB developed LBBB and 2 developed complete heart block and received a pacemaker.

Most studies investigating the echocardiographic outcome following TAVI used EF to assess LV systolic function (Table 4). Not all investigators reported the EF after TAVI with the Medtronic-CoreValve [3,4]. It seems reasonable to assume that the reason for not reporting the EF post-TAVI was a lack of significant changes. Nevertheless, in most studies that EF was reported, changes were insignificant, with the exception of subgroup analyses of patients with low baseline EF in whom a significant immediate improvement was found [6,21]. Lack of improvement in EF was also observed by our group in a previous cohort of 74 patients that are not included in the present study [7]. On the contrary, most of the studies on TAVI with the Edwards SAPIEN valve have shown a significant immediate increase in EF, which was more prominent in patients with low EF [1,2,5,22-24]. The results of the present study provide a possible explanation for this discrepancy. Normally, LV and right ventricular contraction is synchronous. In the presence of LBBB or right apical pacing, right ventricular activation/contraction precedes LV activation/contraction. Consequently, this inter-ventricular asynchrony results in paradoxical septal movement that has been associated with a decrease in global EF, even in the absence of heart failure [25]. Lack of improvement in EF following TAVI with the Medtronic-CoreValve may be explained by the higher incidence of new conduction abnormalities, which influence LV synchronous contraction and thus systolic performance. It should

Table 4. Reported immediate changes in left ventricular ejection fraction following Transcatheter Aortic Valve Implantation.

First author [ref #]	Year	Device	Number of patients	Pre-TAVI EF % mean ± SD	Post-TAVI EF % mean ± SD	p value
Bauer et al. [23]	2004	Edwards	8	48 ± 18	57 ± 12	< 0.01
Cribier et al. [1]	2006	Edwards	22	45 ± 18	53 ± 14	0.02
Webb et al. [2]	2007	Edwards	43	53 ± 15	57 ± 13	< 0.0001
Clavel et al. [22]	2009	Edwards	50	54 ± 16	59 ± 12	< 0.05
Ye et al. [5]	2010	Edwards*	71	56 ± 13	61 ± 7	NS
Bauer et al. [24]	2010	Edwards	88	48 ± 17	57 ± 15	< 0.01
Grube et al. [3]	2007	CoreValve	86	54 ± 16	NA	NA
Jilaihawi et al. [21]	2009	CoreValve	50	50 ± 14	56 ± 9	0.001
Tzikas et al. [7]	2010	CoreValve	71	52 ± 15	52 ± 15	NS
Buellesfeld et al. [4]	2010	CoreValve	168	51 ± 16	NA	NA
Gotzmann et al. [6]	2010	CoreValve	39	57 ± 10	59 ± 10	NS

*Transapical

be noted, however, that although EF and/or longitudinal strain measurements are useful for the assessment of LV systolic function they are not synonymous to it. Thereby, results should be interpreted with caution.

LV systolic function following TAVI was evaluated using Doppler tissue imaging in two studies. In the first, involving 8 patients who underwent TAVI with the Edwards SAPIEN valve, Bauer et al. found a significant increase in EF, systolic mitral velocities and longitudinal strain [23]. In the second, involving 39 patients, the EF showed no significant change following TAVI with the Medtronic-CoreValve but there was a small improvement in systolic mitral velocities at 30-day follow-up, similar to our findings [6]. Noteworthy, in our study, systolic mitral velocities and longitudinal strain increased significantly in the group of patients without new conduction abnormalities, whereas in patients with new conduction disorders changes were insignificant, in line with the changes in EF. Systolic mitral velocities and longitudinal strain were assessed using STE, which is more sensitive and reproducible than the EF measurements obtained by conventional echocardiography [8]. In addition, accuracy of STE is higher than Doppler tissue imaging. STE directly tracks the speckles on an echocardiogram and thereby myocardial motion and deformation and is therefore independent of the angle of insonation [8].

This was a single-center prospective study, designed to investigate the immediate effects of TAVI on the LV function. Other studies are needed in order to conclude whether TAVI – induced conduction disorders persist or recover during follow-up. Another limitation is the relatively small number of patients. However, it should be noted that all data (pre- and post-TAVI, including speckle tracking measurements) were 100% complete which allowed a robust paired statistical analysis. Nevertheless, generalizability of our results should be tested in larger scale studies.

Acknowledgement

Dr Tzikas is supported by an unrestricted research grant from the European Association of Percutaneous Cardiovascular Interventions (EAPCI Interventional Cardiology Research Grant 2009).

REFERENCES

1. Cribier A, Eltchaninoff H, Tron C, Bauer F, Agatiello C, Nercolini D, Tapiero S, Litzler PY, Bessou JP, Babaliaros V. Treatment of calcific aortic stenosis with the percutaneous heart valve: mid-term follow-up from the initial feasibility studies: the French experience. *J Am Coll Cardiol* 2006;47:1214-1223.
2. Webb JG, Pasupati S, Humphries K, Thompson C, Altwegg L, Moss R, Sinhal A, Carere RG, Munt B, Ricci D, Ye J, Cheung A, Lichtenstein SV. Percutaneous transarterial aortic valve replacement in selected high-risk patients with aortic stenosis. *Circulation* 2007;116:755-763.
3. Grube E, Schuler G, Buellesfeld L, Gerckens U, Linke A, Wenaweser P, Sauren B, Mohr FW, Walther T, Zickmann B, Iversen S, Felderhoff T, Cartier R, Bonan R. Percutaneous aortic valve replacement for severe aortic stenosis in high-risk patients using the second- and current third-generation self-expanding CoreValve prosthesis: device success and 30-day clinical outcome. *J Am Coll Cardiol*. 2007;50:69-76.
4. Buellesfeld L, Wenaweser P, Gerckens U, Mueller R, Sauren B, Latsios G, Zickmann B, Hellige G, Windecker S, Grube E. Transcatheter aortic valve implantation: predictors of procedural success--the Siegburg-Bern experience. *Eur Heart J* 2010;31:984-991.
5. Ye J, Cheung A, Lichtenstein SV, Nietlispach F, Albugami S, Masson JB, Thompson CR, Munt B, Moss R, Carere RG, Jamieson WR, Webb JG. Transapical transcatheter aortic valve implantation: follow-up to 3 years. *J Thorac Cardiovasc Surg* 2010;139:1107-1113, 1113.e1.
6. Gotzmann M, Lindstaedt M, Bojara W, Mügge A, Germing A. Hemodynamic results and changes in myocardial function after transcatheter aortic valve implantation. *Am Heart J* 2010;159:926-932.
7. Tzikas A, Piazza N, van Dalen BM, Schultz C, Geleijnse ML, van Geuns RJ, Galema TW, Nuis RJ, Otten A, Gutierrez-Chico JL, Serruys PW, de Jaegere PP. Changes in mitral regurgitation after transcatheter aortic valve implantation. *Catheter Cardiovasc Interv* 2010;75:43-49.
8. van Dalen BM, Bosch JG, Kauer F, Soliman OI, Vletter WB, ten Cate FJ, Geleijnse ML. Assessment of mitral annular velocities by speckle tracking echocardiography versus tissue Doppler imaging: validation, feasibility, and reproducibility. *J Am Soc Echocardiogr* 2009;22:1302-1308.
9. Piazza N, Onuma Y, Jesserun E, Kint PP, Maugenest AM, Anderson RH, de Jaegere PP, Serruys PW. Early and persistent intraventricular conduction abnormalities and requirements for pacemaking after percutaneous replacement of the aortic valve. *JACC Cardiovasc Interv* 2008;1:310-316.
10. Erkapic D, Kim WK, Weber M, Möllmann H, Berkowitsch A, Zaltsberg S, Pajitnev DJ, Rixe J, Neumann T, Kuniss M, Sperzel J, Hamm CW, Pitschner HF. Electrocardiographic and further predictors for permanent pacemaker requirement after transcatheter aortic valve implantation. *Europace* 2010 Mar 30. [Epub ahead of print]
11. Jilaihawi H, Chin D, Vasa-Nicotera M, Jeilan M, Spyt T, Ng GA, Bence J, Logtens E, Kovac J. Predictors for permanent pacemaker requirement after transcatheter aortic valve implantation with the CoreValve bioprosthesis. *Am Heart J* 2009;157:860-866.
12. Baan J Jr, Yong ZY, Koch KT, Henriques JP, Bouma BJ, Vis MM, Cocchieri R, Piek JJ, de Mol BA. Factors associated with cardiac conduction disorders and permanent pacemaker implantation after percutaneous aortic valve implantation with the CoreValve prosthesis. *Am Heart J* 2010;159:497-503.

13. Surawicz B, Childers R, Deal BJ, Gettes LS, Bailey JJ, Gorgels A, Hancock EW, Josephson M, Kligfield P, Kors JA, Macfarlane P, Mason JW, Mirvis DM, Okin P, Pahlm O, Rautaharju PM, van Herpen G, Wagner GS, Wellens H; American Heart Association Electrocardiography and Arrhythmias Committee, Council on Clinical Cardiology; American College of Cardiology Foundation; Heart Rhythm Society. AHA/ACCF/HRS recommendations for the standardization and interpretation of the electrocardiogram: part III: intraventricular conduction disturbances: a scientific statement from the American Heart Association Electrocardiography and Arrhythmias Committee, Council on Clinical Cardiology; the American College of Cardiology Foundation; and the Heart Rhythm Society: endorsed by the International Society for Computerized Electrocardiology. *Circulation* 2009;119:e235-240.
14. Epstein AE, DiMarco JP, Ellenbogen KA, Estes NA 3rd, Freedman RA, Gettes LS, Gillinov AM, Gregoratos G, Hammill SC, Hayes DL, Hlatky MA, Newby LK, Page RL, Schoenfeld MH, Silka MJ, Stevenson LW, Sweeney MO, Smith SC Jr, Jacobs AK, Adams CD, Anderson JL, Buller CE, Creager MA, Ettinger SM, Faxon DP, Halperin JL, Hiratzka LF, Hunt SA, Krumholz HM, Kushner FG, Lytle BW, Nishimura RA, Ornato JP, Page RL, Riegel B, Tarkington LG, Yancy CW; American College of Cardiology/American Heart Association Task Force on Practice Guidelines (Writing Committee to Revise the ACC/AHA/NASPE 2002 Guideline Update for Implantation of Cardiac Pacemakers and Antiarrhythmia Devices); American Association for Thoracic Surgery; Society of Thoracic Surgeons. ACC/AHA/HRS 2008 Guidelines for Device-Based Therapy of Cardiac Rhythm Abnormalities: a report of the American College of Cardiology/American Heart Association Task Force on Practice Guidelines (Writing Committee to Revise the ACC/AHA/NASPE 2002 Guideline Update for Implantation of Cardiac Pacemakers and Antiarrhythmia Devices) developed in collaboration with the American Association for Thoracic Surgery and Society of Thoracic Surgeons. *J Am Coll Cardiol* 2008;51:e1-62.
15. Lang RM, Bierig M, Devereux RB, Flachskampf FA, Foster E, Pellikka PA, Picard MH, Roman MJ, Seward J, Shanewise J, Solomon S, Spencer KT, St John Sutton M, Stewart W; American Society of Echocardiography's Nomenclature and Standards Committee; Task Force on Chamber Quantification; American College of Cardiology Echocardiography Committee; American Heart Association; European Association of Echocardiography, European Society of Cardiology. Recommendations for chamber quantification. *Eur J Echocardiogr* 2006;7:79-108.
16. Zoghbi WA, Enriquez-Sarano M, Foster E, Grayburn PA, Kraft CD, Levine RA, Nihoyanopoulos P, Otto CM, Quinones MA, Rakowski H, Stewart WJ, Waggoner A, Weissman NJ, American Society of Echocardiography. Recommendations for evaluation of the severity of native valvular regurgitation with two-dimensional and Doppler echocardiography. *J Am Soc Echocardiogr* 2003;16:777-802.
17. El-Khally Z, Thibault B, Staniloae C, Theroux P, Dubuc M, Roy D, Guerra P, Macle L, Talajic M. Prognostic significance of newly acquired bundle branch block after aortic valve replacement. *Am J Cardiol* 2004;94:1008-1011.
18. Huynh H, Dalloul G, Ghanbari H, Burke P, David M, Daccarett M, Machado C, David S. Permanent pacemaker implantation following aortic valve replacement: current prevalence and clinical predictors. *Pacing Clin Electrophysiol* 2009;32:1520-1525.
19. Shen WK, Hammill SC, Hayes DL, Packer DL, Bailey KR, Ballard DJ, Gersh BJ. Long-term survival after pacemaker implantation for heart block in patients > or=65 years. *Am J Cardiol* 1994;74:560-564.

20. Gutiérrez M, Rodés-Cabau J, Bagur R, Doyle D, DeLarochellière R, Bergeron S, Lemieux J, Villeneuve J, Côté M, Bertrand OF, Poirier P, Clavel MA, Pibarot P, Dumont E. Electrocardiographic changes and clinical outcomes after transapical aortic valve implantation. *Am Heart J* 2009;158:302-308.
21. Jilaihawi H, Chin D, Spyt T, Jeilan M, Vasa-Nicotera M, Bence J, Logtens E, Kovac J. Prosthesis-patient mismatch after transcatheter aortic valve implantation with the Medtronic-Core-valve bioprosthesis. *Eur Heart J* 2010;31:857-864.
22. Clavel MA, Webb JG, Pibarot P, Altwegg L, Dumont E, Thompson C, De Larochellière R, Doyle D, Masson JB, Bergeron S, Bertrand OF, Rodés-Cabau J. Comparison of the hemodynamic performance of percutaneous and surgical bioprostheses for the treatment of severe aortic stenosis. *J Am Coll Cardiol* 2009;53:1883-1891.
23. Bauer F, Eltchaninoff H, Tron C, Lesault PF, Agatiello C, Nercolini D, Derumeaux G, Cribier A. Acute improvement in global and regional left ventricular systolic function after percutaneous heart valve implantation in patients with symptomatic aortic stenosis. *Circulation* 2004;110:1473-1476.
24. Bauer F, Lemercier M, Zajarias A, Tron C, Eltchaninoff H, Cribier A. Immediate and long-term echocardiographic findings after transcatheter aortic valve implantation for the treatment of aortic stenosis: the Cribier-Edwards/Edwards-Sapien valve experience. *J Am Soc Echocardiogr* 2010;23:370-376.
25. Melek M, Esen O, Esen AM, Barutcu I, Onrat E, Kaya D. Tissue Doppler evaluation of intra-ventricular asynchrony in isolated left bundle branch block. *Echocardiography* 2006;23:120-126.

**Prosthesis-Patient Mismatch
after Transcatheter Aortic Valve Implantation
with the Medtronic CoreValve System
in Patients with Aortic Stenosis**

Tzikas A

Piazza N

Geleijnse ML

van Mieghem N

Nuis RJ

Schultz C

van Geuns RJ

Galema TW

Kappetein AP

Serruys PW

de Jaegere PP

ABSTRACT

A prosthesis-patient mismatch (PPM) is present when the prosthetic valve is too small in relation to the patient's body size. The purpose of the present study was to investigate the frequency of PPM after the implantation of the Medtronic CoreValve System, and its relation to the clinical outcome. The indexed effective orifice area (EOA) was measured in 74 patients with symptomatic severe aortic stenosis, who had undergone successful trans-catheter aortic valve implantation with the Medtronic CoreValve System, at baseline and discharge. PPM was defined as severe (indexed EOA $<0.65 \text{ cm}^2/\text{m}^2$) or moderate (indexed EOA 0.65 to $0.85 \text{ cm}^2/\text{m}^2$). The indexed EOA increased from 0.35 ± 0.13 to $0.97 \pm 0.34 \text{ cm}^2/\text{m}^2$ after transcatheter aortic valve implantation ($p < 0.001$) and was accompanied by significant clinical improvement. Severe and moderate PPMs were found in 16% and 23% of patients, respectively. Patients with severe PPM were more symptomatic and had a smaller indexed EOA at baseline than those with moderate or no PPM (0.28 ± 0.09 vs $0.36 \pm 0.12 \text{ cm}^2/\text{m}^2$, $p < 0.05$). Functional status and mortality at 30 days and 6 months was not significantly different between the patients with severe PPM and those with moderate or no PPM. In conclusion, the indexed EOA increased significantly after transcatheter aortic valve implantation. Severe PPM was observed in 16% of the patients and was not associated with the clinical outcome.

INTRODUCTION

Prosthesis-patient mismatch (PPM) is present when the prosthetic valve is too small in relation to the patient's body size [1]. PPM is associated with a greater than expected transprosthetic gradient and increased left ventricular after-load, which, in turn, can adversely affect the immediate and long-term clinical outcome [2]. PPM is considered severe when the indexed effective orifice area (EOA) is $<0.65 \text{ cm}^2/\text{m}^2$ and moderate when the indexed EOA is 0.65 to $0.85 \text{ cm}^2/\text{m}^2$ [3]. After surgical aortic valve replacement, PPM has been reported to range from 20% to 70% and to be severe in 2% to 28% of patients [2,4,5]. Notwithstanding the conflicting reports of the effect of PPM on outcome, the general concept has been that PPM should be avoided by the careful selection of the prosthesis type and size and possibly by the use of additional surgical techniques, such as aortic root enlargement, to accommodate a larger prosthesis [2,4]. Recently, in a study investigating the incidence and predictors of PPM after Medtronic CoreValve System (Medtronic, Minneapolis, Minnesota) implantation in 50 patients, Jilaihawi et al [6], reported that severe PPM was present at discharge in 2% of patients. In a series of 50 patients who had received the Edwards SAPIEN bioprosthetic valve (Edwards Lifesciences, Irvine, California), Clavel et al [7], reported that severe PPM was present in 11% of patients at discharge. The effect of PPM after transcatheter aortic valve implantation (TAVI) on the clinical outcome is unknown. We investigated the frequency of PPM after the implantation of the Medtronic CoreValve System and its relation to 30-day and 6-month mortality and functional status.

METHODS

The study population included a series of 74 of 96 consecutive patients with symptomatic severe aortic stenosis who had undergone successful TAVI with the Medtronic CoreValve System and were discharged alive and in whom the image quality of transthoracic echocardiography allowed accurate measurements of the EOA at baseline and discharge. The inclusion and exclusion criteria for Medtronic CoreValve implantation have been previously described in detail [8,9]. In brief, the patients were eligible for TAVI in the case of severe valvular aortic stenosis ($\text{EOA} < 1 \text{ cm}^2$ or $< 0.6 \text{ cm}^2/\text{m}^2$) and considered at high or prohibitive operative risk.

The Medtronic CoreValve System consists of a trileaflet porcine pericardial tissue valve, mounted in a self-expanding nitinol frame [8,9]. The selection of the size of the prosthesis was determined by the assessment of the aortic annulus using transthoracic echocardiography and/or multislice computed tomography before the procedure. With increasing operator experience, the latter technique became the single most important method for selecting the valve size [10,11].

Transthoracic Echocardiography was performed at baseline and before discharge using a Philips iE33 or a Sonos 7500 system (Philips, Best, The Netherlands). Complete echocardiographic studies were performed in a standard fashion and analyzed by an experienced echocardiographer. During the studies, patients had a normal at rest heart rate (60 to 90 beats/min) and blood pressure within normal limits. The left ventricular (LV) ejection fraction was calculated using the Teichholz method. Low-gradient aortic stenosis was defined by a mean transaortic gradient of <40 mm Hg and a LV ejection fraction of <35% [12]. The EOA was estimated using the continuity equation approach ($EOA = LV \text{ outflow tract [LVOT]}_{\text{area}} \times \text{velocity time integral}_{\text{LVOT}} / \text{velocity time integral}_{\text{valve}}$). According to the published guidelines, the LVOT area was measured just underneath the prosthesis, assuming a circular geometry. In addition, the pulse wave Doppler sample volume was located in the LVOT, adjacent to the in-flow segment of the prosthesis but not inside it, avoiding the region of subvalvular acceleration [13]. The indexed EOA was calculated by dividing the EOA by the patient's body surface area. The PPM was defined as follows: no PPM if the indexed EOA was $>0.85 \text{ cm}^2/\text{m}^2$, moderate PPM if the indexed EOA was $0.65 \text{ to } 0.85 \text{ cm}^2/\text{m}^2$, and severe PPM when the indexed EOA was $<0.65 \text{ cm}^2/\text{m}^2$ [3].

For the purposes of the present study, functional status (New York Heart Association) and mortality data were collected at baseline and 30 days and 6 months and were complete for all patients. Early and short-term mortality was defined by all-cause mortality at 30 days and 6 months after TAVI, respectively (for patients who were discharged alive).

Continuous variables are presented as the mean \pm SD. The mean values of the continuous variables were compared using the *t* test. Categorical variables are presented as frequencies and percentages and were compared using the chi-square test or Fisher's exact test. The significance of the differences among the 3 groups (severe PPM, moderate PPM, no PPM) was tested using 1-way analysis of variance, followed by the Bonferroni method for post hoc comparisons of the mean values. Univariate analysis was performed to delineate the differences between the patients with severe PPM and those without or with moderate PPM. Statistical significance was assumed at $p < 0.05$. All statistical analyses were performed using the Statistical Package for Social Sciences, version 15.0, software (SPSS, Chicago, Illinois).

RESULTS

The baseline characteristics are summarized in Table 1. The study population consisted of 74 elderly patients with significant comorbidities. Of the 96 patients who had undergone successful TAVI with the Medtronic CoreValve System during the study period, 22 were excluded from the analysis but had baseline characteristics similar to those of the study population. The reasons for exclusion were procedural death (3 patients), in-hospital death (6 patients), and suboptimal image quality on transthoracic echocardiography (13 patients). None of the deaths was related to the prosthesis. For patients discharged alive, the median length of stay was 10 days (interquartile range 7 to 18 days).

Table 1. *Baseline characteristics of study population and excluded patients.*

Variable	Study Population (n=74)	Excluded Patients (n=22)	p Value
Age (years)	81±7	82±4	0.51
Men	35 (47%)	8 (36%)	0.37
Weight (kg)	71±12	74±15	0.30
Height (cm)	166±8	167±9	0.91
Body mass index (kg/m ²)	26±4	27±4	0.36
Body surface area (m ²)	1.81±0.18	1.85±0.23	0.37
Antecedents			
Cerebrovascular events	18 (24%)	5 (23%)	1.00
Acute myocardial infarction	15 (20%)	6 (27%)	0.56
Percutaneous coronary intervention	18 (24%)	3 (14%)	0.39
Coronary artery bypass	21 (28%)	6 (27%)	0.91
Co-morbidities			
Chronic obstructive pulmonary disease	22 (30%)	2 (9%)	0.06
Chronic renal disease	11 (15%)	4 (18%)	0.74
Peripheral vascular disease	4 (5%)	1 (5%)	1.00
Atrial fibrillation	17 (23%)	9 (41%)	0.10
Diabetes mellitus	12 (16%)	6 (27%)	0.35
New York Heart Association class			
I–II	15 (20%)	2 (9%)	0.34
III–IV	59 (80%)	20 (91%)	
Logistic EuroSCORE	15±8	19±10	0.08
Medtronic CoreValve sizes available (mm)			
26	20 (27%)	4 (18%)	0.52
26 or 29	54 (73%)	18 (82%)	

Data are presented as mean±SD or numbers (%).

Of the 74 patients, 59 (80%) had New York Heart Association class III to IV at baseline. Twenty patients (27%) were treated during a period when only the 26-mm inflow Medtronic CoreValve System was available. TAVI was associated with a significant improvement in EOA (from 0.62±0.20 to 1.74±0.59 cm², p<0.001), indexed EOA (from 0.35±0.13 to 0.97±0.34 cm²/m², p<0.001), and mean transaortic gradient (from 47±16 to 9±5mmHg, p<0.001). Moreover, TAVI was accompanied by significant clinical improvement. The percentage of patients with New York Heart Association class I to II increased from 20% at baseline to 66% at discharge. Severe and moderate PPM, however, was identified in 16% and 23% of patients, respectively (Table 2).

Univariate analysis was performed to delineate the differences between patients with severe PPM and those without or with moderate PPM (Tables 3 and 4). Patients with severe PPM had a greater prevalence of a history of myocardial infarction. All patients with

Table 2. Frequency of prosthesis–patient mismatch (PPM) at discharge.

Variable	Total	PPM			p Value
		Severe	Moderate	Absent	
Patients	74 (100%)	12 (16%)	17 (23%)	45 (61%)	
Effective orifice area (cm ²)	1.74±0.59	1.02±0.17	1.34±0.14	2.08±0.49	<0.001*
Effective orifice area indexed (cm ² /m ²)	0.97±0.34	0.56±0.08	0.74±0.06	1.17±0.04	<0.001*
Mean gradient (mm Hg)	9±5	14±6	10±4	8±4	<0.001**

Data are presented as mean±SD or number (%).

* Between group without PPM and groups with severe or moderate PPM.

** Between group without PPM and group with severe PPM.

Table 3. Severe prosthesis–patient mismatch (PPM), relation to baseline characteristics.

Variable	Severe PPM			p Value
	Yes (n=12)	No (n=62)		
Age (years)	82±6	81±7		0.73
Men	7 (58%)	28 (45%)		0.40
Weight (kg)	72±12	71±12		0.69
Height (cm)	168±6	166±9		0.45
Body mass index (kg/m ²)	26±4	26±4		0.94
Body surface area (m ²)	1.83±0.17	1.80±0.18		0.59
Antecedents				
Cerebrovascular events	3 (25%)	15 (24%)		0.60
Acute myocardial infarction	7 (58%)	8 (13%)		<0.001
Percutaneous coronary intervention	4 (33%)	14 (23%)		0.32
Coronary artery bypass	3 (25%)	18 (29%)		0.54
Co-morbidities				
Chronic obstructive pulmonary disease	4 (33%)	18 (29%)		0.51
Chronic renal disease	2 (18%)	9 (15%)		0.57
Peripheral vascular disease	0 (0%)	4 (6%)		0.48
Atrial fibrillation	2 (18%)	15 (24%)		0.44
Diabetes mellitus	2 (18%)	10 (16%)		0.62
New York Heart Association class				
I–II	0 (0%)	15 (24%)		0.05
III–IV	12 (100%)	47 (76%)		
Logistic EuroSCORE	15±7	15±9		0.83
Medtronic CoreValve sizes available (mm)				
26	5 (42%)	15 (24%)		0.18
26 or 29	7 (58%)	47 (76%)		

Data are presented as mean±SD or number (%).

Table 4. Severe prosthesis–patient mismatch (PPM), Echocardiography, and procedure-related indexes.

Variable	Total	Severe PPM		
		Yes (\pm 12)	No ($n\pm 62$)	p Value
Baseline	(n=74)	(n=12)	(n=64)	
Ejection fraction (%)	52 \pm 16	49 \pm 18	53 \pm 16	0.50
Ejection fraction <35%	9(12%)	3 (25%)	6 (10%)	0.16
Low-gradient aortic stenosis*	3 (4%)	1 (8%)	2 (3%)	0.07
Aortic annulus diameter (mm)	22 \pm 2	22 \pm 2	23 \pm 2	0.13
Peak gradient (mm Hg)	81 \pm 26	92 \pm 31	78 \pm 25	0.10
Mean gradient (mm Hg)	47 \pm 16	56 \pm 17	46 \pm 15	0.05
Peak velocity (cm/s)	438 \pm 72	469 \pm 84	433 \pm 69	0.11
Effective orifice area (cm ²)	0.62 \pm 0.20	0.52 \pm 0.16	0.64 \pm 0.20	<0.05
Effective orifice area indexed (cm ² /m ²)	0.35 \pm 0.12	0.28 \pm 0.09	0.36 \pm 0.12	<0.05
Discharge				
Peak gradient (mm Hg)	18 \pm 9	26 \pm 10	17 \pm 8	<0.001
Mean gradient (mm Hg)	9 \pm 5	14 \pm 6	8 \pm 4	<0.001
Peak velocity (cm/s)	206 \pm 53	252 \pm 52	197 \pm 48	<0.001
Effective orifice area (cm ²)	1.74 \pm 0.59	1.02 \pm 0.17	1.88 \pm 0.54	<0.001
Effective orifice area indexed (cm ² /m ²)	0.97 \pm 0.34	0.56 \pm 0.08	1.05 \pm 0.31	<0.001
Aortic regurgitation grade				0.44
None to mild	57 (77%)	10 (83%)	47 (76%)	
Moderate to severe	17 (23%)	2 (17%)	15 (24%)	
Medtronic CoreValve size (mm)				0.06
26	37 (50%)	9 (75%)	28 (45%)	
29	37 (50%)	3 (25%)	34 (55%)	
Outcome				
At 30 days				
New York Heart Association class				1.00
I–II	49 (66%)	8 (67%)	41 (66%)	
III–IV	24 (33%)	4 (33%)	20 (32%)	
Mortality**	1 (1%)	0 (0%)	1 (2%)	0.84
At 6 months				
New York Heart Association status				0.45
I–II	49 (66%)	6 (50%)	43 (69%)	
III–IV	19 (26%)	4 (33%)	15 (24%)	
Mortality**	6 (8%)	2 (17%)	4 (7%)	0.25

Data are presented as mean \pm SD or number (%).

* Mean gradient <40 mm Hg and ejection fraction <35%.

** For patients who were discharged alive.

severe PPM had New York Heart Association class III to IV at baseline. Furthermore, patients with severe PPM had a greater severity of aortic stenosis at baseline (indexed EOA 0.28 ± 0.09 vs 0.36 ± 0.12 cm^2/m^2 , $p < 0.05$). No difference was seen in LV function or aortic annulus size. Patients with severe PPM were more likely to have received a 26-mm inflow CoreValve (75% vs 25%, $p = 0.06$). Clinical improvement was found in most patients after TAVI that was maintained at 6 months. We found no difference in functional status or mortality between patients with severe PPM and those without or with moderate PPM (Table 4). An inverse exponential relation was found between the indexed EOA and the mean transprosthetic gradient at discharge ($r^2 = 0.38$; Figure 1).

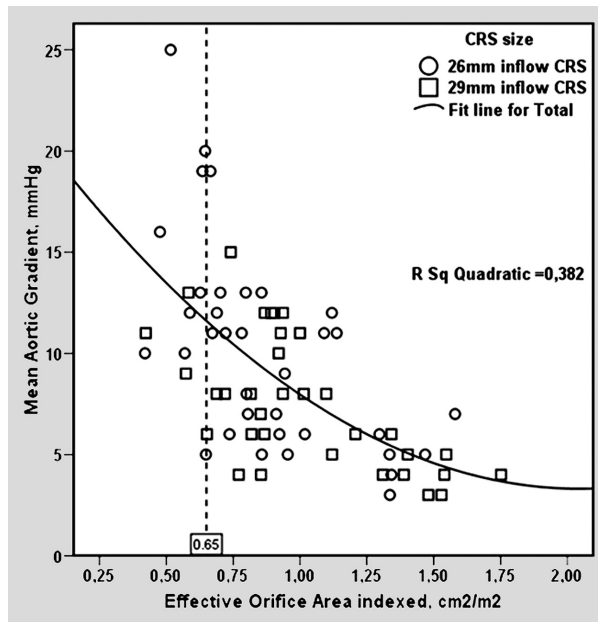


Figure 1. Correlation between mean aortic gradient and indexed EOA at discharge.

DISCUSSION

In the present study, we found a significant increase in the indexed EOA after TAVI. Severe and moderate PPM, however, was identified in 16% and 23% of patients, respectively. Severe PPM at discharge was observed more often in patients with a greater severity of aortic stenosis at baseline, in patients who had received a smaller (26-mm inflow) Medtronic CoreValve, and in those with a history of myocardial infarction. No association was found between severe PPM and the clinical outcome.

To date, the indexed EOA and the prevalence of PPM after TAVI have been reported in 2 studies. In a series of 50 patients, reported by Jilalihawi et al [6], the frequency of

PPM after TAVI with the Medtronic CoreValve System was 32%, comparable to the 39% found in our study. However, the frequency of severe PPM was significantly different (2% vs 16%). This could be explained in part by the differences in method. The measurement of the LVOT area after TAVI was obtained “just below hinge points of the visible prosthetic leaflets ... and from inner edges of the stent” (eg, within the Medtronic CoreValve frame). If the velocity time integral_{LVOT} was also obtained at that location, it would have been overestimated owing to the subvalvular acceleration effect and would lead to an overestimation of the EOA. Also, that study did not investigate the severity of aortic stenosis at baseline as a predictor of PPM.

In another study, comparing the hemodynamic performance of the balloon expandable Edwards SAPIEN valve with 2 surgically implanted bioprostheses, Clavel et al [7] reported a frequency of severe PPM of 11% at discharge after TAVI, significantly lower than the frequency observed in 2 matched groups of patients who had undergone surgical aortic valve replacement (26% to 28%). It is questionable whether the differences in the design between the Medtronic CoreValve and the Edwards SAPIEN and the level at which the bioprostheses were implanted (intra-vs supra-annularly) explain the differences in PPM thus far reported.

The Medtronic CoreValve System consists of an hourglass-shaped, self-expanding nitinol frame (50 to 51 mm high), in which a trileaflet porcine pericardial valve is mounted. After implantation, the frame extends from the LVOT up to the ascending aorta. However, the bioprosthetic leaflets are mounted in the constraint mid-portion, which is located above the native aortic annulus; therefore, the device functions supra-annularly [8,9]. The Medtronic CoreValve is implanted in patients with an aortic annulus of 20 to 23 mm (26-mm inflow bioprosthesis) and 23 to 27 mm (29-mm inflow bioprosthesis). In the present study, 1/3 of the patients were treated before October 2007 when only the 26-mm inflow Medtronic CoreValve was available. Even though patients with a large annulus were excluded, a number of patients might have received a prosthesis that was too small during that period (inappropriate patient and valve selection could be explained by the absence of a multislice computed tomographic reading of the annulus). This could explain the greater frequency of severe PPM (42% vs 24%) observed in the first period when only the 26-mm inflow valve was available compared to the period when the 2 sizes were available (58% vs 76%).

The LV ejection fraction did not differ between patients with severe PPM and those with moderate or without PPM, whether examined as a categorical or a continuous variable. Low-gradient aortic stenosis can lead to an underestimation of the EOA, because the LV outflow is too low to open the valve cusps. As a result, low gradient aortic stenosis could lead to an overestimation of the incidence and severity of PPM. In addition, we found a greater frequency of PPM in patients with a history of acute myocardial infarction. However, the relatively small number of patients in our study did not allow us to draw any firm conclusions. Finally, the calculation of the ejection fraction using the Teichholz method can be influenced by wall motion abnormalities.

The general consensus among surgical aortic valve replacement studies has been to try to avoid PPM by selecting the most appropriate type and size of valve and by eventually performing additional surgical procedures such as aortic root enlargement [2]. TAVI differs from surgical valve replacement in that we cannot intervene with the patient's anatomy and only 2 sizes of valves are available. Moreover, the operator cannot measure the dimensions of the annulus directly, such as is done during surgical aortic valve replacement, and the manufacturer's proposal of sizing has not been validated [11]. In general, operators try to oversize the prosthesis to avoid paravalvular aortic regurgitation. Given the role of valve size selection and valve performance, the manufacturers of catheter-based aortic bioprostheses are developing a wider range of valve sizes, similar to surgical aortic valve replacement.

The clinical effect of PPM is still a matter of debate, in the elderly in particular. We found an improvement in functional status and New York Heart Association class after TAVI for most patients. However, it was not significantly different between patients with severe PPM and those without or with moderate PPM. In accordance with recent observations after surgical aortic valve replacement in patients >70 years old, we found no association between PPM and early and short-term mortality after TAVI [14,15]. The patients undergoing TAVI were not only older than their surgical counterparts, but also had more co-morbidities. Therefore, it is possible that, with respect to the outcomes, PPM is an "innocent bystander," as has been suggested by Monin [3]. The logistic EuroSCORE of our study population was not very high. However, the EuroSCORE does not take into account several important risk factors such as frailty, liver cirrhosis, previous chest radiation, and so forth.

PPM is generally defined by the projected indexed EOA, which is the ratio between the projected EOA provided by the manufacturer for each type and size of prosthetic valve and the patient's body surface area. The projected indexed EOA might help the surgeon to select the valve size and thereby prevent PPM. However, the projected indexed EOA differs from the actual or measured indexed EOA (i.e., after valve insertion) because of a combination of valve- and patient-related properties, such as the morphology of the outflow tract and the base of the aortic root, which, in turn, could affect the angle of the valve in the aortic root and, thus, performance [3,4]. Florath et al [5], who demonstrated a weak correlation between the projected indexed EOA and the actual indexed EOA measured by echocardiography, have recently corroborated this. In the present study, we used the actual indexed EOA, measured by transthoracic echocardiography, to define PPM. In accordance with the study by Pibarot et al [2], we found a similar correlation between the indexed EOA and the mean gradient in patients who underwent TAVI (Figure 1).

The main limitations of the present study were its sample size, the selected population (elderly patients), and the duration of follow-up. These factors precluded a precise estimation of the incidence of PPM, an in-depth analysis of its determinants, and the relation to the outcome.

REFERENCES

1. Rahimtoola SH. The problem of valve prosthesis–patient mismatch. *Circulation* 1978;58:20-24.
2. Pibarot P, Dumesnil JG. Prosthesis–patient mismatch: definition, clinical impact, and prevention. *Heart* 2006;92:1022–1029.
3. Monin JL. Prosthesis–patient mismatch: myth or reality? *Heart* 2009; 95:948-952.
4. Mohty D, Malouf JF, Girard SE, Schaff HV, Grill DE, Enriquez-Sarano ME, Miller FA Jr. Impact of prosthesis–patient mismatch on long-term survival in patients with small St Jude Medical mechanical prostheses in the aortic position. *Circulation* 2006;113:420-426.
5. Florath I, Albert A, Rosendahl U, Ennker IC, Ennker J. Impact of valve prosthesis–patient mismatch estimated by echocardiographic determined effective orifice area on long-term outcome after aortic valve replacement. *Am Heart J* 2008;155:1135-1142.
6. Jilaihawi H, Chin D, Spyt T, Jeilan M, Vasa-Nicotera M, Bence J, Logtens E, Kovac J. Prosthesis–patient mismatch after transcatheter aortic valve implantation with the Medtronic-Core-Valve bioprosthesis. *Eur Heart J Epub* 2009 Dec 25.
7. Clavel MA, Webb JG, Pibarot P, Altwegg L, Dumont E, Thompson C, De Larochelli re R, Doye D, Masson JB, Bergeron S, Bertrand OF, Rodés-Cabau J. Comparison of the hemodynamic performance of percutaneous and surgical bioprostheses for the treatment of severe aortic stenosis. *J Am Coll Cardiol* 2009;53:1883-1891.
8. Piazza N, Grube E, Gerckens U, den Heijer P, Linke A, Luha O, Ramondo A, Ussia G, Wenaweser P, Windecker S, Laborde JC, de Jaegere P, Serruys PW. Procedural and 30-day outcomes following transcatheter aortic valve implantation using the third generation (18 Fr) CoreValve ReValving System: results from the multicentre, expanded evaluation registry 1-year following CE mark approval. *EuroIntervention* 2008;4:242-249.
9. Grube E, Laborde JC, Gerckens U, Felderhoff T, Sauren B, Buellesfeld L, Mueller R, Menichelli M, Schmidt T, Zickmann B, Iversen S, Stone GW. Percutaneous implantation of the Core-Valve self-expanding valve prosthesis in high-risk patients with aortic valve disease: the Siegburg first-in-man study. *Circulation* 2006;114:1616-1624.
10. Schultz C, Weustink A, Piazza N, Otten A, Mollet N, Krestin G, van Geuns RJ, de Feyter P, Serruys PW, de Jaegere P. Geometry and degree of apposition of the CoreValve ReValving system with multi-slice computed tomography after implantation in patients with aortic stenosis. *J Am Coll Cardiol* 2009;54:911–918.
11. Schultz C, Moelker A, Piazza N, Tzikas A, Otten A, Nuis RJ, van Geuns RJ, de Feyter P, Krestin G, Serruys PW, de Jaegere P. 3D evaluation of the aortic annulus using multislice computer tomography: are manufacturer’s guidelines for sizing helpful? *Eur Heart J Epub* 2009 Dec 7.
12. Monin JL, Monchi M, Kirsch ME, Petit-Eisenmann H, Baleynaud S, Chauvel C, Metz D, Adams C, Quere JP, Gueret P, Tribouilloy C. Low-gradient aortic stenosis: impact of prosthesis–patient mismatch on survival. *Eur Heart J* 2007;28:2620–2626.
13. Zoghbi WA, Chambers JB, Dumesnil JG, Foster E, Gottdiener JS, Grayburn PA, Khandheria BK, Levine RA, Marx GR, Miller FA Jr, Nakatani S, Qui-ones MA, Rakowski H, Rodriguez LL, Swaminathan M, Waggoner AD, Weissman NJ, Zabalgoitia M; American Society of Echocardiography’s Guidelines and Standards Committee; Task Force on Prosthetic Valves; American College of Cardiology Cardiovascular Imaging Committee; Cardiac Imaging Committee of the American Heart Association; European Association of Echocardiography; European Society of Cardiology; Japanese Society of Echocardiography; Canadian Society of

Echocardiography; American College of Cardiology Foundation; American Heart Association; European Association of Echocardiography; European Society of Cardiology; Japanese Society of Echocardiography; Canadian Society of Echocardiography. Recommendations for evaluation of prosthetic valves with Echocardiography and Doppler ultrasound: a report from the American Society of Echocardiography's Guidelines and Standards Committee and the Task Force on Prosthetic Valves, developed in conjunction with the American College of Cardiology Cardiovascular Imaging Committee, Cardiac Imaging Committee of the American Heart Association, the European Association of Echocardiography, a registered branch of the European Society of Cardiology, the Japanese Society of Echocardiography and the Canadian Society of Echocardiography, endorsed by the American College of Cardiology Foundation, American Heart Association, European Association of Echocardiography, a registered branch of the European Society of Cardiology, the Japanese Society of Echocardiography, and Canadian Society of *Echocardiography*. *J Am Soc Echocardiogr* 2009;22: 975–1014.

14. Mohty D, Dumesnil JG, Echahidi N, Mathieu P, Dagenais F, Voisine P, Pibarot P. Impact of prosthesis–patient mismatch on long-term survival after aortic valve replacement: influence of age, obesity, and left ventricular dysfunction. *J Am Coll Cardiol* 2009;53:39–47.
15. Moon MR, Lawton JS, Moazami N, Munfakh NA, Pasque MK, Damiano RJ Jr. POINT: prosthesis–patient mismatch does not affect survival for patients greater than 70 years of age undergoing bioprosthetic aortic valve replacement. *J Thorac Cardiovasc Surg* 2009;137:278–283.

Chapter 9

Changes in Mitral Regurgitation after Transcatheter Aortic Valve Implantation

Tzikas A
Piazza N
van Dalen BM
Schultz C
Geleijnse ML
van Geuns RJ
Galema TW
Nuis RJ,
Otten A
Gutierrez-Chico JL
Serruys PW
de Jaegere PP

ABSTRACT

Objectives: To assess the acute and intermediate changes in mitral regurgitation (MR) severity after transcatheter aortic valve implantation (TAVI) with the CoreValve Revalving SystemTM (CRS).

Background: Following surgical aortic valve replacement, improvement in MR is reported in 27-82% of the patients. The changes in MR severity following CRS implantation are unknown.

Methods: Transthoracic echocardiography was performed in 79 consecutive patients before and after treatment, and at the first outpatient visit. Left ventricular dimensions and ejection fraction (LVEF), left atrial (LA) size, and aortic gradient were measured. MR was assessed by color flow mapping and was graded as none, mild, moderate, or severe. It was defined as organic or functional. The depth of CRS implantation was measured by angiography.

Results: Post-treatment, the mean gradient decreased from 48 ± 16 mmHg to 9 ± 5 mmHg ($P < 0.0001$). There was no significant change in the left ventricular dimensions, LA size, and LVEF. MR pretreatment was mild, moderate, or severe in 57%, 18%, and 1% of the patients, respectively. It was defined as organic in 27 patients (36%) and functional in 27 patients (36%). The degree of MR remained unchanged in 61% of the patients, improved in 17%, and worsened in 22%. MR improvement was associated with a lower baseline LVEF ($P = 0.02$). There was no association between the changes in MR severity and the depth of CRS implantation.

Conclusions: Most patients who underwent TAVI had some degree of MR. Overall there was no change in the degree of MR post-treatment. Patients in whom MR improved had a lower LVEF at baseline.

INTRODUCTION

Mitral regurgitation (MR) is present in approximately two-thirds of patients with aortic stenosis (AS) [1]. It may be secondary to AS (functional) or due to intrinsic pathology of the mitral apparatus itself (organic) [2,3]. Moderate to severe MR is observed in 27-48% of patients undergoing transcatheter aortic valve implantation (TAVI) [4,5].

Following surgical aortic valve replacement (SAVR), improvement in MR is reported in 27-82% of patients [3,6-17]. Given the inherent differences in the technique of valve replacement between SAVR and TAVI, one may question whether MR will improve or worsen after TAVI. In TAVI, the prosthesis is implanted intraannular, with some part extending into the left ventricular outflow tract (LVOT) [18]. This may be, in particular, the case with the CoreValve Revalving System™ (CRS), because the average depth of implantation is ~8 mm below the base of the aortic root (Figure 1) [19]. Even more, it is postulated that the impact of the ventricular end of the CRS frame on the motion of the anterior mitral leaflet may induce or adversely affect MR [20].

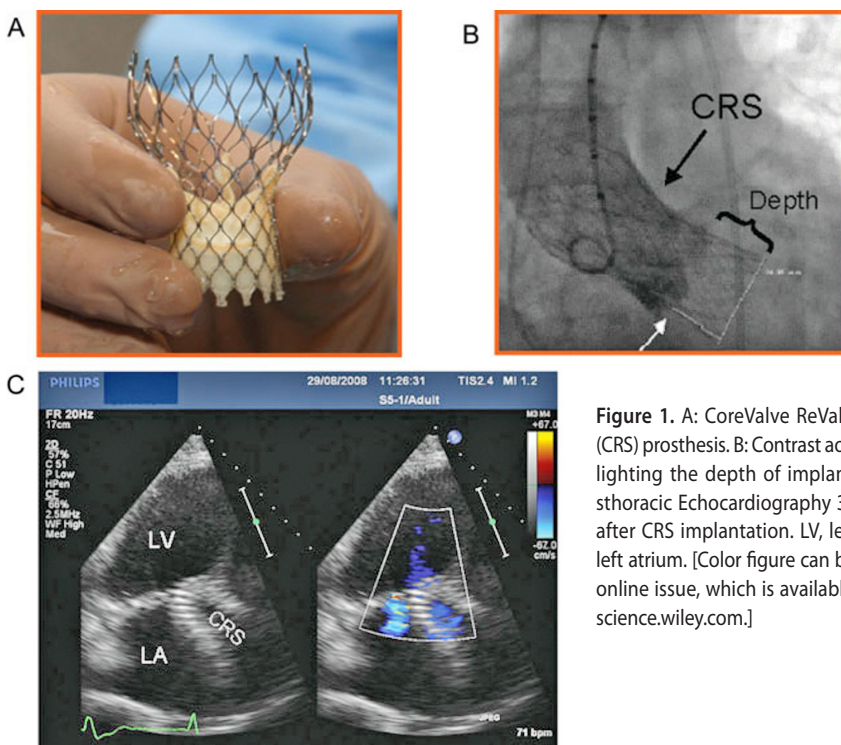


Figure 1. A: CoreValve ReValving System™ (CRS) prosthesis. B: Contrast aortography highlighting the depth of implantation. C: Trans-thoracic Echocardiography 3-chamber view after CRS implantation. LV, left ventricle; LA, left atrium. [Color figure can be viewed in the online issue, which is available at www.interscience.wiley.com.]

We investigated, therefore, by means of 2D transthoracic echo-Doppler-cardiography (TTE) the acute and intermediate temporal changes in MR severity after TAVI.

METHODS

Patient Population

The study population consists of 79 consecutive patients with severe symptomatic AS, considered to be at high or prohibitive surgical risk, who underwent TAVI with the CRS (CoreValve, Irvine, CA) between November 2005 and March 2009 at the Thoraxcenter, Rotterdam. Before the procedure, consensus was achieved between a cardiologist and a cardiac surgeon regarding surgical risk, and all patients provided informed written consent. The inclusion and exclusion criteria have been described in detail elsewhere [18]. Briefly, patients were included if they had severe native valvular AS with an area $<1 \text{ cm}^2$ or $<0.6 \text{ cm}^2/\text{m}^2$, with or without aortic regurgitation; aortic valve annulus diameter $\geq 20 \text{ mm}$ and $\leq 27 \text{ mm}$; and a diameter of sinutubular junction $\leq 43 \text{ mm}$, measured by echocardiography.

Device Description and Procedure

The Core Valve aortic valve prosthesis consists of a trileaflet bioprosthetic porcine pericardial tissue valve, which is sutured in a self-expanding nitinol tri-level frame (Figure 1). Details regarding the device and technical aspects of the procedure have been previously described [18]. TAVI was carried out under general anesthesia via transfemoral approach. All patients were extubated immediately after TAVI, in the catheterization laboratory. The selection of the size of the CRS prosthesis was based on the measurements of the aortic valve annulus obtained by angiography, multislice computed tomography, and/or TTE. CRS positioning and deployment were performed under fluoroscopic guidance.

Echocardiography

TTE was performed pretreatment (last echo study before TAVI), post-treatment (at discharge), and post-discharge (first outpatient clinic visit), using a Philips Ie33 or a Sonos 7500 system (Philips, Best, The Netherlands).

Complete echocardiographic studies were performed for each patient in a standard fashion. Using the parasternal long-axis view and either M-mode or 2D echocardiography, left ventricular end-diastolic (LVEDD) and end-systolic (LVESD) dimensions and left atrial (LA) size measurements were obtained. The diameter of LVOT was also obtained in the parasternal long-axis view, by using the zoom mode and standard 2D calliper measurements. Quantification of LVEF was performed by using the equation $\text{LVEF} = (\text{LVEDD}^2 - \text{LVESD}^2) / \text{LVEDD}^2$ [21].

To assess the severity of AS peak aortic velocity, peak instantaneous gradient, mean transaortic gradient, and velocity-time integral were measured. A peak instantaneous valve gradient was derived from the continuous-wave Doppler velocity across the aortic valve, by using the modified Bernoulli equation ($dP = 4v^2$). Aortic valve area was estimated using the continuity equation approach [$AVA = LVOT_{area} (\text{velocity time integral}_{LVOT} / \text{velocity time integral}_{valve})$].

The color-flow Doppler signal was used to assess aortic and mitral regurgitation. According to the European Society of Cardiology guidelines and American Society of Echocardiography recommendations, valvular insufficiency was graded as none, mild, moderate, or severe [22,23]. More specifically, MR was assessed by visual inspection and by using color-flow mapping of the regurgitant jet as described by Helmcke et al. [24]. The maximum jet area was measured by planimetry where it reached its greatest percentage of LA area, in the four-chamber apical view, with the use of Curad off-line analysis package. MR was then expressed as jet area as a percentage of left atrium area (MR percentage), and its severity was graded as follows: none $\leq 5\%$, mild = 5 to 20%, moderate = 20 to 40%, and severe $\geq 40\%$.

MR was defined as organic in the presence of calcifications or myxomatous degeneration of the mitral annulus and/or leaflets and functional in case of LV dysfunction and absence of morphological abnormalities of the mitral apparatus [12,13].

All echocardiograms were obtained with the patient in a stable hemodynamic condition, with blood pressure within normal limits. No patient was on mechanical ventilation during the studies. Two independent experienced cardiologists, blinded to the patient clinical status, graded MR. In case of discrepancies in MR grading between the two cardiologists consensus was achieved.

Angiography

To examine the association between the depth of implantation of the CRS and the severity of MR following CRS implantation, the distance of the ventricular end of the CRS within the LVOT (depth of implantation) was assessed by using quantitative angiographic measurements (CASS 5.0). More specifically, we estimated the distance between the lower edge of: (1) the right coronary cusp (or the noncoronary cusp) and (2) the left coronary cusp and the ventricular end of the frame (Figure 1) [19].

Statistical Analysis

Categorical variables are expressed as frequencies and continuous variables are expressed as mean \pm SD. For comparison between categorical variables a chi-square test was used. A one-way ANOVA test was used for comparison between continuous variables. A Bonferroni test was used to define statistical difference between groups at each time point. A *P*-value of <0.05 was considered statistically significant.

RESULTS

The baseline clinical and echo characteristics are summarized in Tables 1 and 2. Successful valve implantation was achieved in 78 out of 79 patients (99%). One patient died during induction of anesthesia and did not receive a valve. A 26-mm inflow CRS was implanted in 40 patients, and 38 patients received a 29-mm inflow CRS. Completeness and reasons for missing echocardiographic studies is shown in the patient flow diagram (Figure 2).

Table 1. *Baseline Characteristics (n=74).*

Age (yr), mean \pm SD	81 \pm 7
Male, n (%)	34 (46%)
Atrial fibrillation, n (%)	20 (27%)
Diabetes, n (%)	16 (22%)
Acute myocardial infarction, n (%)	18 (24%)
Percutaneous coronary intervention, n (%)	18 (24%)
Coronary artery bypass, n (%)	22 (30%)
Cerebrovascular events, n (%)	17 (23%)
Peripheral vascular disease, n (%)	15 (20%)
Renal disease, n (%)	15 (20%)
NYHA Class, n (%)	
I	0(0%)
II	9 (12%)
III	51 (69%)
IV	14 (19%)
COPD, n (%)	19 (26%)
Logistic EuroScore, mean \pm SD	16 \pm 8

COPD, chronic obstructive pulmonary disease; NYHA, New York Heart Association.

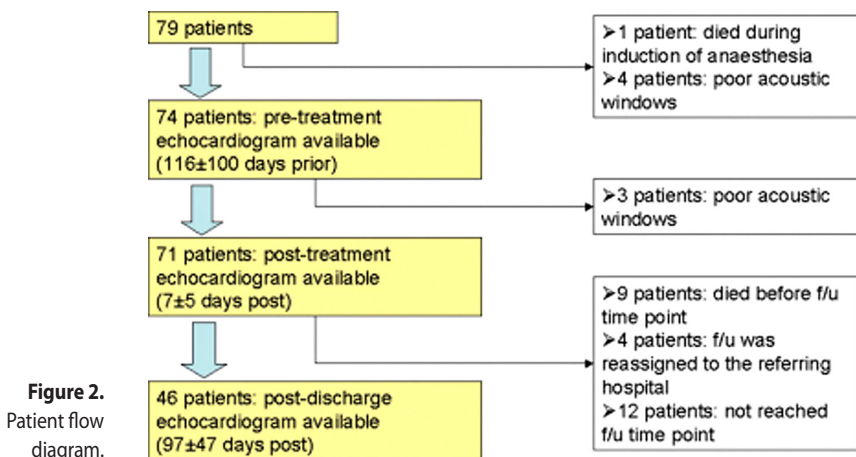


Table 2. Mean Echocardiographic Indices Before and After TAVI.

Measurement	Pretreatment n = 74	Posttreatment n = 71	Follow-up n = 46	P-value
LV end-diastolic dimensions (mm)	50 ± 7	49 ± 7	50 ± 7	0.90
LV end-systolic dimensions (mm)	35 ± 9	34 ± 9	35 ± 9	0.98
LV ejection fraction (%)	52 ± 15	52 ± 15	52 ± 14	0.98
Left atrial size (mm)	46 ± 7	46 ± 7	46 ± 7	0.99
Peak AV gradient (mm Hg)	80 ± 28	18 ± 9	18 ± 9	<0.0001
Mean AV gradient (mm Hg)	48 ± 16	10 ± 5	9 ± 5	<0.0001
Aortic valve area (cm ²)	0.62 ± 0.20	1.71 ± 0.61	1.60 ± 0.52	<0.0001
Aortic regurgitation grade (1–4)	2.27	2.08	2.07	0.29
Mitral regurgitation grade (1–4)	1.91	1.89	1.98	0.89
Type of MR				
Organic MR, n (%)	27 (36%)			
Functional MR, n (%)	27 (36%)			
Prosthetic MV, n (%)	2 (3%)			
No MR, n (%)	18 (25%)			

LV, left ventricle; AV, aortic valve; MR, mitral regurgitation; MV, mitral valve.

Echocardiographic Evaluation

The echocardiographic findings are summarized in Table 2. There was a statistically significant decrease in the peak and mean gradient after CRS implantation (from 80±28 mm Hg to 18±9 mm Hg and from 48±16mm Hg to 9±5 mm Hg, respectively), which was associated with an increase in the aortic valve area (pretreatment 0.62±0.20 cm² vs. post-treatment 1.71±0.61 cm² vs. postdischarge 1.60±0.52 cm², *P*<0.0001). LVEF, LA size, aortic regurgitation grade, and MR grade did not change significantly during follow-up. MR was organic in 27 patients (34%) and functional in another 27 patients (34%). Two patients (3%) had a prosthetic mitral valve, precluding precise assessment of the cause of eventual MR. Eighteen patients (26%) did not have MR at baseline.

The degree of MR before and after CRS implantation is shown in Figure 3. Overall, there was no change in the degree of MR (*P* =0.89). Figure 4 summarizes the changes in MR in the individual patients in whom an echocardiogram was available at all three time points (46 patients); the degree of MR did not change after CRS implantation in 28 patients (61%), it improved in eight patients (17%), and worsened in 10 patients (22%) (Figure 5). Patients in whom an improvement in MR was found had a lower LVEF (Table 3, *P*=0.017). We found no association between the changes in MR and baseline LA size and atrial fibrillation. There was also no association with the depth of CRS implantation or the cause of MR (organic, functional) (Table 3).

Table 4 summarizes the changes in MR in the 14 patients with moderate-severe MR at baseline. An improvement in MR after CRS implantation was observed in most patients, in particular those with functional MR. In one patient there was a worsening of MR.

Table 3. *Changes in Mitral Regurgitation in Relation to Patient and Procedural Variables (n=46).*

	Overall (n = 46)	Improved (n = 8)	Unchanged (n = 28)	Worsened (n = 10)	P-value
Left ventricular ejection fraction (mm), mean ± SD	53±15	40±13	57±15	50±14	0.017*
Left atrial size (mm), mean ± SD	46±8	49±7	45±7	45±9	0.403
Atrial fibrillation at baseline, n (%)	12 (26%)	4 (50%)	6 (21%)	2 (20%)	0.249
Distance between device end and left coronary cusp (mm), mean ± SD	8.8±3.7	9.6±2.2	8.2±4.1	9.9±3.4	0.212
Distance between device end and right coronary cusp (mm), mean ± SD	8.2±2.8	8.9±0.9	8.1±3.1	7.8±3.3	0.062
Type					
Organic MR at baseline, n (%)	15 (33%)	3 (38%)	11 (39%)	1 (10%)	0.225
Functional MR at baseline, n (%)	19 (41%)	5 (62%)	10 (36%)	4 (40%)	0.396
No MR at baseline, n (%)	12 (26%)	0 (0%)	7 (25%)	5 (50%)	–

*P value = 0.017 between the group that improved and the group that remained unchanged (Bonferroni test).

Table 4. *Patients with Moderate-Severe MR at Baseline.*

Pt No	LVEF (%)	LA size (mm)	Depth of right (mm)	Depth of left (mm)	MR grade pretreatment	MR grade posttreatment	MR grade postdischarge	Type of MR	Postdischarge change in MR
1	34	57	NA	NA	3	2	2	Functional	Improved
3	32	36	9.8	10.5	3	1	1	Functional	Improved
9	21	59	9.5	12.5	3	3	(3) ^a	Functional	(Unchanged) ^a
18	45	46	7.8	8.1	3	2	2	Functional	Improved
30	32	53	8.7	7.3	3	3	2	Functional	Improved
32	75	47	7.1	6.6	3	3	3	Organic	Unchanged
33	24	60	4.9	2.5	3	3	3	Organic	Unchanged
36	32	53	8.4	9.6	4	3	3	Organic	Improved
42	47	43	8.2	13.8	3	3	4	Functional	Worsened
44	69	31	NA	NA	3	3	2	Organic	Improved
51	44	39	3.5	4.3	3	3	3	Organic	Unchanged
66	49	45	9.6	11.5	3	2	NA ^b	Organic	–
69	66	44	NA	NA	3	3	NA ^b	Organic	–
72	47	54	NA	NA	3	3	NA ^b	Functional	–

LVEF, left ventricular ejection fraction; LA, left atrium; Depth of right/left, read definition on text; MR grade: 1=none, 2=mild, 3=moderate, 4=severe.

^aFollow-up reassigned to another hospital. ^bDid not reach follow-up time point.

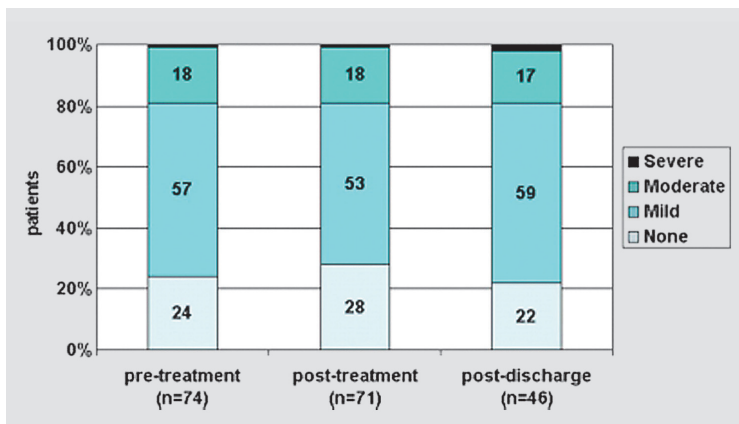


Figure 3. Degree of mitral regurgitation pretreatment, post-treatment, and at the first outpatient visit (postdischarge). There was no significant change in mean MR severity after CRS implantation ($P=0.89$).

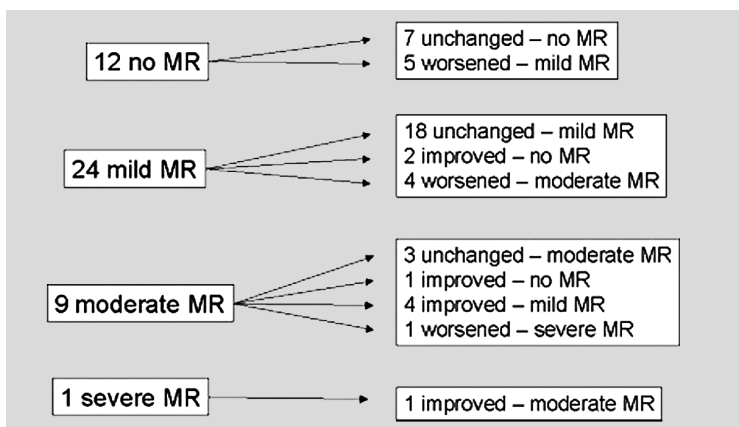


Figure 4. Changes in MR before and after treatment in patients with available pre and postdischarge echocardiography ($n=46$).

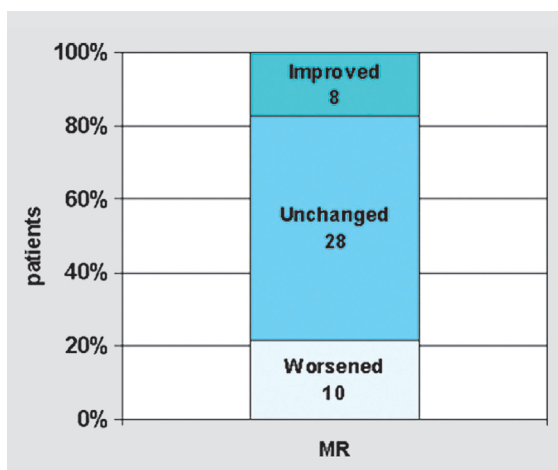


Figure 5. Proportion of patients who experienced an improvement, no change, or worsening in MR severity after CRS implantation ($n=46$).

DISCUSSION

In this series of 74 elderly patients with severe AS, we found that the majority of patients (76%) had some degree of MR at baseline. Overall, there was no change in MR after CRS implantation. We found no correlation between the change in MR and the depth of CRS implantation or the type of MR at baseline (organic, functional).

The absence of improvement in MR after CRS implantation in this study may be explained by the fact that only 19% of the patients had moderate to severe MR (e.g., a greater potential for improvement). The low number of patients with moderate to severe MR is in accordance with the inclusion and exclusion criteria of the Safety and Feasibility studies and Expanded Evaluation Registry after obtaining CE mark (April 2007). Webb et al. reported an improvement in MR in 24 out of the 50 patients (48%) with moderate to severe MR following the implantation of the EDWARDS Sapien valve [5]. Of note, we found an improvement in MR in 6 out of the 10 patients who had moderate to severe MR before CRS implantation (Table 4).

The relatively small number of patients with moderate-severe MR may also explain the fact that no relation was found between the cause and the changes in MR. In accordance with previous studies, improvement was predominantly seen in patients with functional MR at baseline (Table 4) [8-11,13-17].

Noteworthy, we found that patients in whom MR improved after CRS had a lower LVEF at baseline in comparison with those in whom no improvement was observed. This is consistent with the observations of Brener et al. who found that in longstanding AS left ventricular dilation and dysfunction is a maladaptive response to pressure overload that causes MR [2]. It is also consistent with the finding that following SAVR MR improves in patients with a low LVEF [8,13]. At variance with a surgical series reported by Tassan-Mangina et al., we found no relation between changes in MR and LA size or atrial fibrillation [13]. This is most likely explained by our small sample size and the limitation of a single anterior-posterior dimensional estimation of LA size.

No relation was found between the depth of CRS implantation and the outcome of MR. This appears to be a true observation considering the values of the depth of implantation summarized in Table III. The average depth was ~8 mm but considering the SD, in a number of patients the depth exceeded 8 mm. One may argue that longer follow-up is needed to rule out any detrimental effects on the mitral valve, especially in patients with an implantation exceeding 6-8 mm below the base of the aortic root.

The findings of this study need to be interpreted in light of the sample size, the type of patients treated, and the variability in the assessment of the severity of MR. Color-flow mapping is a qualitative method for the assessment of MR and despite the fact that it has been used by the majority (9 out of 12) of SAVR studies in the past, it is not ideal. We, therefore, cannot propose recommendations on the management of elderly patients with combined AS and MR. Neither this study nor the literature provide data to decide whether such patients should be excluded from TAVI or whether they should undergo a com-

bined aortic and mitral valve treatment. For that purpose, more detailed pathophysiologic data on the effects of TAVI on MR are needed in addition to longer-term clinical follow-up. As TAVI and catheter-based mitral repair are still in the experimental phase, it is too early to consider a combined percutaneous aortic and mitral treatment.

CONCLUSIONS

Most patients who underwent TAVI had some degree of MR. Overall, there was no change in the degree of MR after CRS implantation. Patients in whom MR improved had a lower LVEF at baseline. There was no association between the changes in MR severity and either the cause of MR (organic, functional) or the depth of CRS implantation.

REFERENCES

1. Come PC, Riley MF, Ferguson JF, Morgan JP, McKay RG. Prediction of severity of aortic stenosis: Accuracy of multiple noninvasive parameters. *Am J Med* 1988;85:29–37.
2. Brener SJ, Duffy CI, Thomas JD, Stewart WJ. Progression of aortic stenosis in 394 patients: Relation to changes in myocardial and mitral valve dysfunction. *J Am Coll Cardiol* 1995;25:305–310.
3. Unger P, Dedobbeleer C, Van Camp G, Plein D, Cosyns B, Lancellotti P. Mitral regurgitation in patients with aortic stenosis undergoing valve replacement. *Heart* (in press).
4. Cribier A, Eltchaninoff H, Tron C, Bauer F, Agatiello C, Nercolini D, Tapiero S, Litzler PY, Bessou JP, Babaliaros V. Treatment of calcific aortic stenosis with the percutaneous heart valve: Mid-term follow-up from the initial feasibility studies— The French experience. *J Am Coll Cardiol* 2006;47:1214– 1223.
5. Webb JG, Pasupati S, Humphries K, Thompson C, Altwegg L, Moss R, Sinhal A, Carere RG, Munt B, Ricci D, Ye J, Cheung A, Lichtenstein SV. Percutaneous transarterial aortic valve replacement in selected high-risk patients with aortic stenosis. *Circulation* 2007;116:755–763.
6. Adams PB, Otto CM. Lack of improvement in coexisting mitral regurgitation after relief of valvular aortic stenosis. *Am J Cardiol* 1990;66:105–107.
7. Tunick PA, Gindea A, Kronzon I. Effect of aortic valve replacement for aortic stenosis on severity of mitral regurgitation. *Am J Cardiol* 1990;65:1219–1221.
8. Harris KM, Malenka DJ, Haney MF, Jayne JE, Hettleman B, Plehn JF, Griffin BP. Improvement in mitral regurgitation after aortic valve replacement. *Am J Cardiol* 1997;80:741–745.
9. Christenson JT, Jordan B, Bloch A, Schmuziger M. Should a regurgitant mitral valve be replaced with a stenotic aortic valve? *Tex Heart Inst J* 2000;27:350–355.
10. Brasch AV, Khan SS, DeRobertis MA, Kong JH, Chiu J, Siegel RJ. Change in mitral regurgitation severity after aortic valve replacement for aortic stenosis. *Am J Cardiol* 2000;85:1271–1274.
11. Tassan-Mangina S, Codorean D, Metivier M, Costa B, Himberlin C, Jouannaud C, Blaise AM, Elaerts J, Nazeyrollas P. Factors determining early improvement in mitral regurgitation after aortic valve replacement for aortic valve stenosis: A transthoracic and transesophageal prospective study. *Eur J Echocardiogr* 2006;7:141–146.
12. Moazami N, Diodato MD, Moon MR, Lawton JS, Pasque MK, Herren RL, Guthrie TJ, Damiano RJ. Does functional mitral regurgitation improve with isolated aortic valve replacement? *J Card Surg*. 2004;19:444–448.
13. Barreiro CJ, Patel ND, Fitton TP, Williams JA, Bonde PN, Chan V, Alejo DE, Gott VL, Baumgartner WA. Aortic valve replacement and concomitant mitral valve regurgitation in the elderly: Impact on survival and functional outcome. *Circulation* 2005;112:I443–I447.
14. Ruel M, Kapila V, Price J, Kulik A, Burwash IG, Mesana TG. Natural history and predictors of outcome in patients with concomitant functional mitral regurgitation at the time of aortic valve replacement. *Circulation* 2006;114:I541–I546.
15. Vanden Eynden F, Bouchard D, El-Hamamsy I, Butnaru A, Demers P, Carrier M, Perrault LP, Tardif JC, Pellerin M. Effect of aortic valve replacement for aortic stenosis on severity of mitral regurgitation. *Ann Thorac Surg* 2007;83:1279–1284.
16. Waisbren EC, Stevens LM, Avery EG, Picard MH, Vlahakes GJ, Agnihotri AK. Changes in mitral regurgitation after replacement of the stenotic aortic valve. *Ann Thorac Surg* 2008;86:56–62.

17. Caballero-Borrego J, Gómez-Doblas JJ, Cabrera-Bueno F, García-Pinilla JM, Melero JM, Porras C, Olalla E, De Teresa Galván E. Incidence, associated factors and evolution of non-severe functional mitral regurgitation in patients with severe aortic stenosis undergoing aortic valve replacement. *Eur J Cardiothorac Surg* 2008;34:62-66.
18. Piazza N, Grube E, Gerckens U, den Heijer P, Linke A, Luha O, Ramondo A, Ussia G, Wenaweser P, Windecker S, Laborde JC, de Jaegere P, Serruys PW. Procedural and 30-day outcomes following transcatheter aortic valve implantation using the third generation (18 Fr) corevalve revalving system: Results from the multicentre, expanded evaluation registry 1-year following CE mark approval. *EuroIntervention* 2008;4:242-249.
19. Piazza N, Onuma Y, Jesserun E, Kint PP, Maugenest A, Anderson RH, de Jaegere P, Serruys PW. Early and persistent intraventricular conduction abnormalities and requirements for pacemaking after percutaneous replacement of the aortic valve. *JACC Cardiovasc Interv* 2008;1:310-316.
20. Chin D. Echocardiography for transcatheter aortic valve implantation. *Eur J Echocardiogr* 2009;10:i21-i29.
21. Oh JK, Seward JB, Tajik AJ. *The Echo Manual*, 3rd ed. Philadelphia: Lippincott Williams & Wilkins; 2006.
22. Vahanian A, Baumgartner H, Bax J, Butchart E, Dion R, Filippatos G, Flachskampf F, Hall R, Iung B, Kasprzak J, Nataf P, Tornos P, Torracca L, Wenink A; Task Force on the Management of Valvular Heart Disease of the European Society of Cardiology; ESC Committee for Practice Guidelines. Guidelines on the management of valvular heart disease: The Task Force on the Management of Valvular Heart Disease of the European Society of Cardiology. *Eur Heart J* 2007;28:230-268.
23. Zoghbi WA, Enriquez-Sarano M, Foster E, Grayburn PA, Kraft CD, Levine RA, Nihoyanopoulos P, Otto CM, Quinones MA, Rakowski H, Stewart WJ, Waggoner A, Weissman NJ, American Society of Echocardiography. Recommendations for evaluation of the severity of native valvular regurgitation with two-dimensional and Doppler echocardiography. *J Am Soc Echocardiogr* 2003;16:777-802.
24. Helmcke F, Nanda NC, Hsiung MC, Soto B, Adey CK, Goyal RG, Gatewood RP Jr. Color Doppler assessment of mitral regurgitation with orthogonal planes. *Circulation* 1987;75:175-183.

Chapter 10

Left Ventricular Mass Regression One Year After Transcatheter Aortic Valve Implantation

Tzikas A
Geleijnse ML
Van Mieghem NM
Schultz CJ
Nuis RJ
van Dalen BM
Sarno G
van Domburg RT
Serruys PW
de Jaegere PP

ABSTRACT

Background. Left ventricular (LV) hypertrophy is associated with LV diastolic dysfunction and constitutes a risk factor for cardiac morbidity and mortality. The objective of this study was to investigate the degree of LV mass regression and the changes of LV diastolic function one year after transcatheter aortic valve implantation (TAVI).

Methods. Echocardiography was performed at baseline, before discharge, and at one-year follow-up in 63 consecutive patients with severe aortic stenosis who underwent TAVI with the Medtronic CoreValve System (Medtronic Inc, Minneapolis, MN). The LV mass was calculated using the Devereux formula and indexed to body surface area.

Results. One-year all-cause mortality was 29%. The LV mass index decreased from 126 ± 42 g/m² at baseline to 110 ± 30 g/m² at one-year follow-up ($p<0.001$). Left ventricular ejection fraction and LV diastolic function did not change significantly. Mean transaortic gradient decreased from 47 ± 19 mm Hg at baseline to 9 ± 5 mm Hg at discharge and 9 ± 4 mm Hg at one year ($p<0.001$), and was accompanied by significant clinical improvement. More than mild paravalvular aortic regurgitation was found in 24% and 15% of patients at discharge and one-year follow-up, respectively.

Conclusions. A significant regression in LV mass was found one year after TAVI. However, regression was incomplete and was not accompanied by an improvement in LV diastolic function.

INTRODUCTION

Left ventricular (LV) hypertrophy is associated with LV diastolic dysfunction and constitutes a risk factor for cardiac morbidity and mortality [1,2]. Within one year after surgical aortic valve replacement for aortic stenosis, LV afterload reduction results in regression of LV mass in the majority of patients. However, in some patients regression is incomplete and diastolic dysfunction does not improve [3,4]. Transcatheter aortic valve implantation (TAVI) is a feasible alternative for high-risk patients with aortic stenosis. Preliminary early and midterm results after TAVI have been promising, with significant reduction in transaortic gradient and clinical improvement [5-9]. Unlike surgical valve replacement, during TAVI the native aortic valve is left in place leading sometimes to underexpansion and (or) incomplete apposition of the prosthetic stent frame and secondary paravalvular aortic regurgitation (AR) [9-11]. In addition, patient selection for TAVI has led to treat very old patients with several comorbidities. The long-term impact of TAVI on LV mass and LV diastolic function is unknown. Therefore, the objective of this study was to investigate the degree of LV mass regression and the changes of LV diastolic function one year after TAVI.

PATIENTS AND METHODS

Patient Population, Procedure, and Outcome

The study population comprised 63 consecutive patients with symptomatic, severe aortic stenosis who underwent TAVI with the CoreValve system (Medtronic Inc, Minneapolis, MN) and reached at least one-year follow-up. The study had the approval of The Institutional Ethics Committee and all patients signed an informed consent form before TAVI. The inclusion and exclusion criteria for TAVI have been described in detail elsewhere [5,6]. Briefly, patients were included if they had severe native valvular aortic stenosis with an aortic valve area less than 1 cm^2 or less than $0.6 \text{ cm}^2/\text{m}^2$, with or without aortic regurgitation, and were deemed high-risk surgical candidates by the heart team (specifically, an interventional cardiologist and a cardiothoracic surgeon). The CoreValve system consists of a trileaflet porcine pericardial tissue valve, mounted in a self-expanding nitinol frame [5,6]. The selection of the size of the prosthesis was based on the assessment of the aortic annulus by transthoracic echocardiography (TTE) and (or) multislice computed tomography before the procedure. For the purpose of this study, functional status (New York Heart Association class) was assessed at baseline, at discharge, and at one-year follow-up. Mortality was defined as all-cause mortality one year after TAVI. No patient was lost to follow-up.

Transthoracic Echocardiography

Two-dimensional TTE was performed at baseline, before discharge, and at one-year follow-up using a Philips iE33 or a Sonos 7500 system (Philips, Best, The Netherlands) with the patient in the left lateral decubitus position. Echocardiographic studies were performed by an independent experienced echocardiographer, blinded to the patient's clinical status. All echocardiograms were saved as video loops or still frames in a digital database and were reanalyzed retrospectively by an experienced cardiologist. Left ventricular dimensions were obtained from the parasternal long-axis view, with measurement of end-diastolic interventricular septum thickness, LV posterior wall thickness, and LV end-diastolic and endsystolic internal diameters just below the tips of the anterior mitral leaflet. The LV mass was calculated using the Devereux formula [12] and indexed to body surface area (LV mass index, LVMI). The LV hypertrophy was defined by LVMI greater than 115 g/m² for males and LVMI greater than 95 g/m² for females. Relative wall thickness (RWT) was calculated ($RWT = 2 \times \text{LV posterior wall thickness} / \text{LV end-diastolic diameter}$), and considered abnormal when RWT was greater than 0.42 [13]. The RWT and LVMI were used to assess LV geometry. Patients were categorized as having the following: normal geometry (normal RWT-normal LVMI); concentric remodeling (increased RWT-normal LVMI); eccentric hypertrophy (normal RWT-increased LVMI); and concentric hypertrophy (increased RWT-increased LVMI). Left ventricular end-diastolic and end-systolic volumes were obtained from the apical view and indexed to body surface area. The LV ejection fraction was calculated using the biplane modified Simpson rule. The mitral inflow velocity profile (E:A wave ratio, E wave deceleration time) and tissue Doppler imaging (septal annular early diastolic mitral annular motion, e' wave, E:e' wave ratio) were used to determine the diastolic function grade [14]. If the e' or A wave was not available (eg, poor quality signal, atrial fibrillation), diastolic grade was assessed using the remaining available parameters. Patients were categorized as having mild (grade 1, impaired relaxation), moderate (grade 2, pseudonormal), or severe (grade 3, restrictive) LV diastolic dysfunction. Transaortic peak velocity, peak and mean gradient, and velocity-time integral were measured using continuous-wave Doppler through the native or prosthetic aortic valve. The Doppler signal was acquired from multiple views after achieving optimal alignment with the direction of transaortic blood flow. The AVA (aortic valve area), was estimated using the continuity equation approach ($AVA = LVOT_{\text{area}} \times [\text{velocity time integral}_{LVOT} / \text{velocity time integral}_{\text{valve}}]$). Aortic regurgitation and mitral regurgitation were assessed semiquantitatively according to the current guidelines for the evaluation of native valves [15].

For hypertensive patients, medical therapy was instituted in-hospital in order to achieve a systemic blood pressure less than 140 over 90 mm Hg, and was reassessed and modified in each follow-up visit. Angiotensin-converting enzyme inhibitors were prescribed as the treatment of choice in all hypertensive patients, in the absence of contraindications.

Statistical Analysis

Continuous variables are presented as means (\pm SD) and categorical variables are presented as frequencies and percentages. In order to assess differences between baseline, discharge, and one-year follow-up for continuous variables, a one-way analysis of variance for repeated measurements was used, followed by a post hoc Bonferroni method of multiple comparisons. The same strategy was used for ordinal variables, assuming a constant difference between values. If variables were not normally distributed, differences were assessed using nonparametric tests for three related samples (Friedman test). For comparisons between two time points, a paired sample t test or a Wilcoxon signed rank test was used for normally distributed or skewed data, respectively. A Cox regression univariate analysis on death as a time-related response was performed to investigate predictors of mortality. A two-sided p value less than 0.05 was considered statistically significant. All statistical analyses were performed with SPSS 15.0 software (SPSS Inc, Chicago, IL).

RESULTS

Baseline patient characteristics are summarized in Table 1. The study population consists of elderly patients with important comorbidities. Thirty-three patients (54%) underwent TAVI using a 26-mm and 30 patients (46%) using a 29-mm inflow CoreValve bioprosthesis. A post-deployment balloon dilatation was performed in 16 patients (25%) and a second CoreValve was implanted in 8 patients (13%). Eight patients (13%) underwent a permanent pacemaker implantation. Eighteen patients (29%) died within the first year after the index procedure (4 in hospital, 14 after discharge). Completeness of the echocardiographic studies is shown in Figure 1. A TTE was not available in 5 patients; 2 patients had TTE of inadequate quality and 3 patients refused to come for one-year follow-up TTE. None of them reported a bad clinical status as the reason for not coming. Forty patients had a TTE available for repeated measurements at baseline, discharge (median [interquartile range] 6 [4 to 8] days post-TAVI), and one-year follow-up (median [interquartile range] 383 [356 to 419] days post-TAVI).

Changes in LV dimensions, mass, and geometry are shown in Table 2. Interventricular septum and LV posterior wall thickness decreased significantly at one year. Also, at one-year follow-up the LV mass index decreased from 126 ± 42 to 110 ± 30 g/m² ($p<0.001$; Fig 2) and RWT decreased from 0.51 to 0.45 ($p<0.001$). However, the percentage of patients with LV hypertrophy and (or) RWT greater than 0.42 did not change significantly. Concentric remodeling and concentric hypertrophy were the predominant LV geometry patterns and remained unchanged one year after TAVI. The LV systolic and diastolic function did not change significantly (Table 3). However, after TAVI, a significant clinical improvement was observed in the majority of patients that was sustained at one-year follow-up. Also, TAVI resulted in a significant decrease in transaortic gradient that was sustained at one-year follow-up (Table 4). The AR post-TAVI was invariably paravalvular in origin; more than mild AR

Table 1.
Baseline
Characteristics.

Variable	Study population (n=63)
Age (years)	82 (78-86)
Male	27 (43%)
Weight (kg)	73±13
Height (cm)	167±8
Body mass index (kg/m ²)	26±4
Body surface area (m ²)	1.84±0.19
Antecedents	
Cerebrovascular events	15 (24%)
Myocardial infarction	18 (29%)
Percutaneous coronary intervention	16 (25%)
Coronary artery bypass	20 (32%)
Comorbidities	
Hypertension	36 (57%)
Chronic obstructive pulmonary disease	16 (25%)
Chronic renal disease	13 (21%)
Peripheral vascular disease	3 (5%)
Atrial fibrillation	18 (29%)
Diabetes	14 (22%)
Ejection fraction < 0.35	12 (19%)
New York Heart Association status	
I-II	5 (8%)
III-IV	58 (92%)
STS score	5 (3-8)
Logistic EuroSCORE	15 (11-19)

Data are presented as mean±SD, median (interquartile range), or number (%).

EuroSCORE = European system for cardiac operative risk evaluation;
STS = Society of Thoracic Surgeons.

Figure 1.
Flow diagram.
Completeness of echocardiographic studies at baseline, discharge, and one-year follow-up. (TTE=transthoracic echocardiography.)

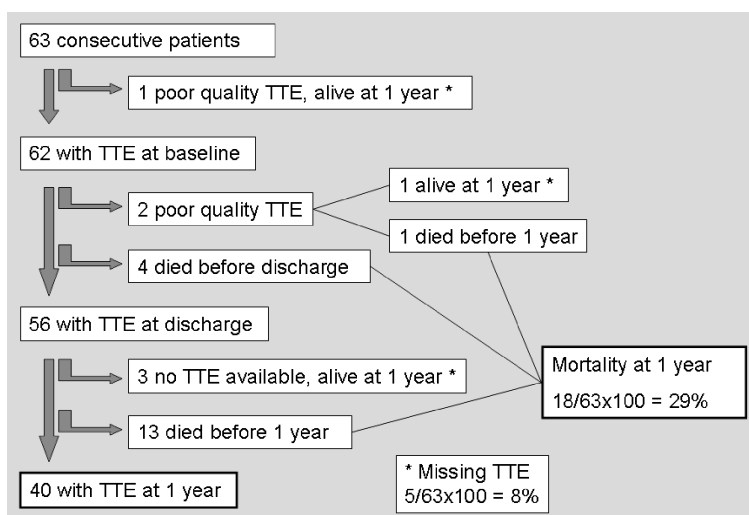


Table 2. Left Ventricular Dimensions, Mass and Geometry.

Variable	Baseline (n=40)	Discharge (n=40)	One Year (n=40)	p value ^a		
				Baseline Versus Discharge	Discharge Versus One Year	Baseline Versus One Year
LV dimensions						
Interventricular septum (mm)	13.5±2.6	13.3±2.4	12.0±2.0	0.15	< 0.001	< 0.001
Posterior wall (mm)	11.6±2.4	11.3±2.3	10.4±1.8	0.08	< 0.001	< 0.001
LV end-diastolic diameter (mm)	47±8	47±7	48±8	1.00	0.28	0.95
LV end-systolic diameter (mm)	32±10	32±9	34±9	1.00	0.09	0.42
LV end-diastolic volume index (cm ³ /m ²)	116±29	121±31	122±33	0.06	1.00	0.21
LV end-systolic volume index (cm ³ /m ²)	60±26	64±26	67±27	0.10	1.00	0.13
LV mass						
LV mass (g)	232±85	222±76	201±60	0.11	< 0.05	< 0.001
LV mass regression (g)	0	10±29	31±46	0.11	< 0.05	< 0.001
LV mass regression (%)	0	3±12	10±16	0.52	< 0.05	< 0.05
LV mass index (g/m ²)	126±42	121±38	110±30	0.11	< 0.05	< 0.001
LV mass index regression (g/m ²)	0	5±16	17±24	0.11	< 0.05	< 0.001
LV hypertrophy ^b	23 (58%)	26 (65%)	23 (58%)	0.55	0.79	1.00
Relative wall thickness ^c	0.51	0.49	0.45	0.66	< 0.001	< 0.001
Relative wall thickness >0.42	33(83%)	33(83%)	31(78%)	1.00	0.97	0.48
LV geometry						
Normal geometry	2 (5%)	3 (7%)	5 (13%)	1.00	0.59	1.00
Concentric remodeling	15 (38%)	11 (28%)	12 (30%)			
Eccentric hypertrophy	6 (15%)	7 (17%)	7 (17%)			
Concentric hypertrophy	17 (43%)	19 (48%)	16 (40%)			

^a Analysis of variance for repeated measurements with Bonferroni correction. ^b LV hypertrophy: LV mass index males >115 g/m², females >95 g/m². ^c Relative wall thickness: 2 × (posterior wall)/(LV end-diastolic diameter). Data are presented as mean ± SD, or number (%). LV = left ventricular.

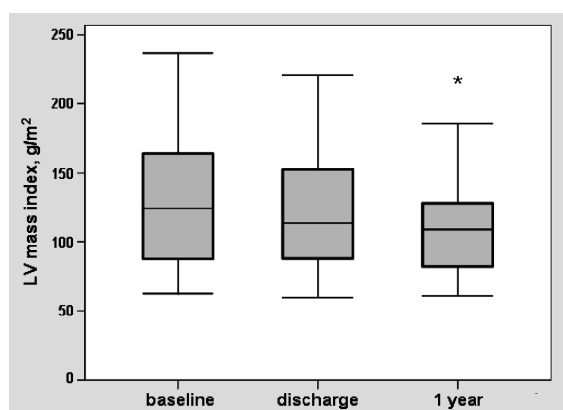


Figure 2. Changes in left ventricular mass index. Box-plot indicating the changes in left ventricular mass index between and baseline, discharge and 1 year follow-up (* p<0.001).

Table 3. *Left Ventricular Function and Clinical Status.*

Variable	Baseline (n=40)	Discharge (n=40)	One year (n=40)	p value ^a		
				Baseline Versus Discharge	Discharge Versus One Year	Baseline Versus One Year
Ejection fraction	0.49±0.14	0.48±0.13	0.46±0.13	1.00	1.00	0.37
Diastolic dysfunction grade (0-3)	1.59±0.79	1.62±0.71	1.54±0.68	1.00	1.00	1.00
0 – none	0 (0%)	0 (0%)	0 (0%)			
1 – mild	23 (59%)	20 (51%)	22 (57%)			
2 – moderate	9 (23%)	14 (36%)	13 (33%)			
3 – severe	7 (18%)	5 (13%)	4 (10%)			
NYHA class (1-4)	3.1±0.6	1.9±0.7	1.8±0.9	< 0.001	1.00	< 0.001
I	0 (0%)	11 (28%)	18 (45%)			
II	4 (10%)	22 (55%)	12 (30%)			
III	27 (68%)	6 (15%)	9 (23%)			
IV	9 (23%)	1 (2%)	1 (2%)			

^a Analysis of variance for repeated measurements with Bonferroni correction.
Data are presented as mean ±SD or number (%). NYHA = New York Heart Association.

Table 4. *Aortic Valve and Mitral Valve Function.*

Variable	Baseline (n=40)	Discharge (n=40)	One Year (n=40)	p value ^a		
				Baseline Versus Discharge	Discharge Versus One Year	Baseline Versus One Year
Aortic valve function						
Peak aortic gradient (mm Hg)	79±32	17±9	17±8	< 0.001	1.00	< 0.001
Mean aortic gradient (mm Hg)	47±19	9±5	9±4	< 0.001	1.00	< 0.001
Peak aortic velocity (cm/sec)	432±90	198±57	199±48	< 0.001	1.00	< 0.001
Aortic regurgitation grade (1-4)	2.25±0.84	2.10±0.71	1.58±1.04	1.00	< 0.05	< 0.05
None - trivial	9 (22%)	7 (18%)	19 (47%)			
Mild	13 (33%)	23 (58%)	15 (38%)			
Moderate	17 (43%)	9 (22%)	4 (10%)			
Severe	1 (2%)	1 (2%)	2 (5%)			
Mitral valve function						
Mitral regurgitation grade (1-4)	2.03±0.66	1.98±0.77	1.93±0.66	1.00	1.00	1.00
None - trivial	8 (20%)	11 (28%)	8 (20%)			
Mild	23 (58%)	20 (50%)	26 (65%)			
Moderate	9 (22%)	8 (20%)	6 (15%)			
Severe	0 (0%)	1 (2%)	0 (0%)			

^a Analysis of variance for repeated measurements with Bonferroni correction.
Data are presented as mean ±SD or number (%).

was observed in 22% of patients. At one-year follow-up the degree of AR decreased, with 15% of patients having more than mild AR ($p < 0.05$). More specifically, between discharge and one-year follow-up, AR grade remained the same in 19 patients (47%), it improved in 18 patients (45%), and got worse in 3 patients (8%). There was no association between the change in AR grade and the degree of LV mass regression. Overall, mitral regurgitation grade did not change. Between discharge and one-year follow-up, MR grade remained the same in 25 patients (62%), improved in 8 patients (20%), and got worse in 7 patients (18%). Similarly to AR, no association was found between the change in MR grade and the degree of LV mass regression. Finally, LV mass regression was not found to be significantly different in patients who underwent a permanent pacemaker implantation after the index procedure. Survival after TAVI is shown in Figure 3. In Cox regression univariate analysis, a history of myocardial infarction (hazard ratio [HR] 2.56; 95% confidence interval [CI], 1.14 to 5.74; $p = 0.02$), a history of renal insufficiency (HR 2.63; 95% CI, 1.15 to 6.04; $p = 0.02$), Society of Thoracic Surgeons score (HR 1.07; 95% CI, 1.02 to 1.12; $p = 0.003$), and logistic European system for cardiac operative risk evaluation score (HR 1.06; 95% CI, 1.02 to 1.10; $p = 0.003$) were identified as prognostic factors of mortality. Age, gender, New York Heart Association class, history of hypertension, diabetes, atrial fibrillation, pulmonary disease, previous bypass surgery, baseline LV ejection fraction, LV mass index and LV hypertrophy, and AR grade or MR grade post-TAVI were not found to be predictors of mortality.

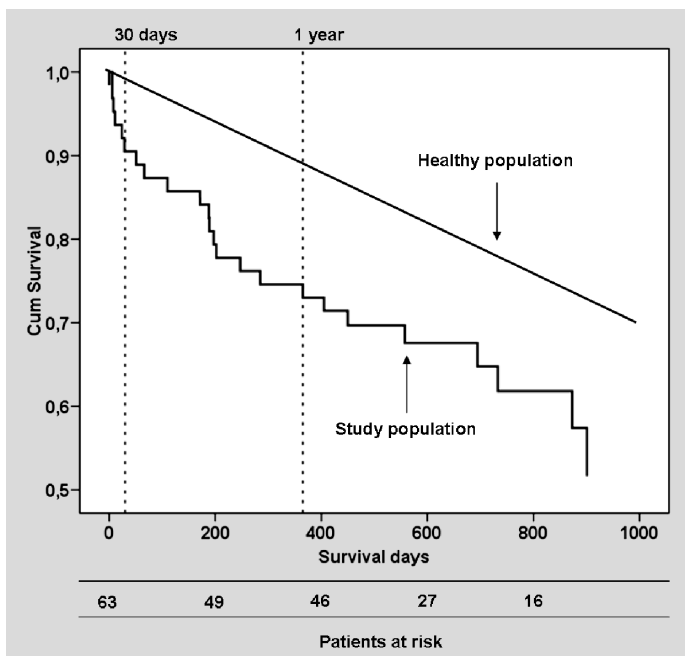


Figure 3. Cumulative survival curves. The stepped regression line indicates cumulative survival of the study population. The straight line indicates cumulative survival of a matched healthy Dutch population (age 82 years).

COMMENT

In the present study a significant regression in LV mass was found one year after TAVI. However, regression was incomplete and was not accompanied by an improvement in LV diastolic function.

Incomplete LV mass regression can be explained by several factors. Due to restrictions in inclusion criteria for TAVI, the study population represents the most morbid cluster of patients with severe aortic stenosis [5-7]. One fifth of patients had an LV ejection fraction less than 0.35, which is usually found at the latest stages of aortic stenosis. Moreover, due to their advanced age, patients were exposed to the harmful effects of severe aortic stenosis for many years, suffering from long-standing LV hypertrophy, which eventually becomes irreversible due to myocardial fibrosis [16,17]. In addition, 57% of patients had a history of hypertension. Despite optimal medical treatment, reduced systemic arterial compliance may have contributed to the incomplete LV mass regression [18]. Finally, genetic factors may have played a role [19].

In this study, in accordance with previous reports, concentric hypertrophy and remodeling were the most frequent LV geometry patterns [20]. Although concentric anatomy is a risk factor for mortality in patients with severe aortic stenosis, our study was underpowered to detect its prognostic impact on one-year mortality. In a recent publication, Gotzmann and colleagues [9] reported a significant decrease in LV mass index 6 months after TAVI using the Medtronic CoreValve, whereas LV ejection fraction and E:e' ratio did not change significantly. As mentioned above, LV dysfunction may be more persistent in the elderly. After valve replacement, even though relief of the valvular afterload, LV is still facing an increased "vascular afterload" due to reduced systemic arterial compliance [18, 20-24]. Nevertheless, in our cohort, as in previous reports, clinical status improved considerably.

Paravalvular AR is a common finding after TAVI and has been characterized as one of the main problems of the technology [25]. However, the degree of AR remains stable or even improves slightly over time [9-11]. In the present study more than mild AR was found in 24% and 15% of patients at discharge and at one-year follow-up, respectively. Although preliminary data suggest AR is a benign bystander, medium and long-term results are still missing. In addition, assessment of the severity of AR after TAVI is complicated, mainly because of the common presence of multiple, eccentric regurgitant jets that originate from different levels around the bioprosthesis. For that reason the differences in AR severity between baseline and discharge that are presented in this and other studies should be interpreted with caution. In addition, one might argue that our reported frequency of more than mild AR of 24% at discharge is high and can be attributed to methodologic issues. Even so, AR grade was assessed (blindly) by the same cardiologist, using the same method both at discharge and at one-year followup. Therefore, the significant improvement in AR severity at one year can be considered as a valid observation. Continuing expansion of the prosthetic frame over time, remodeling of the base of the aortic root, and gradual coverage of paravalvular spaces with tissue (pannus) are possible explanations. Mitral regurgitation

is a common finding in patients with severe aortic stenosis. In the present study the overall severity of MR remained unchanged at discharge and at one year after TAVI, which is consistent with previous observations published by our group [26].

One-year mortality after TAVI was analogous to reports of other groups [5-7]. Univariate analysis revealed a history of myocardial infarction, renal insufficiency, Society of Thoracic Surgeons' score, and logistic European system for cardiac operative risk evaluation score as potential prognostic factors for mortality. However, the number of observations does not allow firm conclusions; larger studies are needed for this purpose.

Acknowledgement

Dr Tzikas is supported by an unrestricted research grant which is provided by the European Association of Percutaneous Cardiovascular Interventions (EAPCI Interventional Cardiology Research Grant 2009).

REFERENCES

1. Devereux RB, Wachtell K, Gerds E, et al. Prognostic significance of left ventricular mass change during treatment of hypertension. *JAMA* 2004;292:2350-6.
2. Kupari M, Turto H, Lommi J. Left ventricular hypertrophy in aortic valve stenosis: preventive or promotive of systolic dysfunction and heart failure? *Eur Heart J* 2005;26:1790-6.
3. Monrad ES, Hess OM, Murakami T, Nonogi H, Corin WJ, Krayenbuehl HP. Time course of regression of left ventricular hypertrophy after aortic valve replacement. *Circulation* 1988;77:1345-55.
4. Villa E, Troise G, Cirillo M, et al. Factors affecting left ventricular remodeling after valve replacement for aortic stenosis. An overview. *Cardiovasc Ultrasound* 2006;4:25.
5. Grube E, Buellesfeld L, Mueller R, et al. Progress and current status of percutaneous aortic valve replacement: results of three device generations of the CoreValve Revalving system. *Circ Cardiovasc Interv* 2008;1:167-75.
6. Piazza N, Grube E, Gerckens U, et al. Procedural and 30-day outcomes following transcatheter aortic valve implantation using the third generation (18 Fr) corevalve revalving system: results from the multicentre, expanded evaluation registry 1-year following CE mark approval. *EuroIntervention* 2008;4:242-9.
7. Cribier A, Eltchaninoff H, Tron C, et al. Treatment of calcific aortic stenosis with the percutaneous heart valve: mid-term follow-up from the initial feasibility studies: the French experience. *J Am Coll Cardiol* 2006;47:1214 -23.
8. Rodés-Cabau J, Webb JG, Cheung A, et al. Transcatheter aortic valve implantation for the treatment of severe symptomatic aortic stenosis in patients at very high or prohibitive surgical risk: acute and late outcomes of the multicenter Canadian experience. *J Am Coll Cardiol* 2010;55:1080 -90.
9. Gotzmann M, Lindstaedt M, Bojara W, Mügge A, Germing A. Hemodynamic results and changes in myocardial function after transcatheter aortic valve implantation. *Am Heart J* 2010;159:926 -32.
10. Rajani R, Kakad M, Khawaja MZ, et al. Paravalvular regurgitation one year after transcatheter aortic valve implantation. *Catheter Cardiovasc Interv* 2010;75:868 -72.
11. Bauer F, Lemercier M, Zajarias A, Tron C, Eltchaninoff H, Cribier A. Immediate and long-term echocardiographic findings after transcatheter aortic valve implantation for the treatment of aortic stenosis: the Cribier-Edwards/Edwards- Sapien valve experience. *J Am Soc Echocardiogr* 2010;23: 370-6.
12. Devereux RB, Alonso DR, Lutas EM, et al. Echocardiographic assessment of left ventricular hypertrophy: comparison to necropsy findings. *Am J Cardiol* 1986;57:450-8.
13. Lang RM, Bierig M, Devereux RB, et al. Recommendations for chamber quantification. *Eur J Echocardiogr* 2006;7:79- 108.
14. Lester SJ, Tajik AJ, Nishimura RA, Oh JK, Khandheria BK, Seward JB. Unlocking the mysteries of diastolic function: deciphering the Rosetta Stone 10 years later. *J Am Coll Cardiol* 2008;51:679-89.
15. Zoghbi WA, Enriquez-Sarano M, Foster E, et al. American Society of Echocardiography. Recommendations for evaluation of the severity of native valvular regurgitation with two-dimensional and Doppler echocardiography. *J Am Soc Echocardiogr* 2003;16:777- 802.

16. Hanayama N, Christakis GT, Mallidi HR, et al. Determinants of incomplete left ventricular mass regression following aortic valve replacement for aortic stenosis. *J Card Surg* 2005;20:307-13.
17. Lund O, Emmertsen K, Dørup I, Jensen FT, Flø C. Regression of left ventricular hypertrophy during 10 years after valve replacement for aortic stenosis is related to the preoperative risk profile. *Eur Heart J* 2003;24:1437-46.
18. Dumesnil JG, Pibarot P, Carabello B. Paradoxical low flow and/or low gradient severe aortic stenosis despite preserved left ventricular ejection fraction: implications for diagnosis and treatment. *Eur Heart J* 2010;31:281-9.
19. Dellgren G, Eriksson MJ, Blange I, Brodin LA, Rådegran K, Sylvén C. Angiotensin-converting enzyme gene polymorphism influences degree of left ventricular hypertrophy and its regression in patients undergoing operation for aortic stenosis. *Am J Cardiol* 1999;84:909-13.
20. Duncan AI, Lowe BS, Garcia MJ, et al. Influence of concentric left ventricular remodeling on early mortality after aortic valve replacement. *Ann Thorac Surg* 2008;85:2030-9.
21. Chahal NS, Lim TK, Jain P, Chambers JC, Kooner JS, Senior R. New insights into the relationship of left ventricular geometry and left ventricular mass with cardiac function: a population study of hypertensive subjects. *Eur Heart J* 2010;31:588-94.
22. Gjertsson P, Caidahl K, Bech-Hanssen O. Left ventricular diastolic dysfunction late after aortic valve replacement in patients with aortic stenosis. *Am J Cardiol* 2005;96: 722-7.
23. Kühl HP, Franke A, Puschmann D, Schöndube FA, Hoffmann R, Hanrath P. Regression of left ventricular mass one year after aortic valve replacement for pure severe aortic stenosis. *Am J Cardiol* 2002;89:408 -13.
24. Lund O, Flø C, Jensen FT, et al. Left ventricular systolic and diastolic function in aortic stenosis. Prognostic value after valve replacement and underlying mechanisms. *Eur Heart J* 1997;18:1977- 87.
25. Walther T, Falk V. Hemodynamic evaluation of heart valve prostheses paradigm shift for transcatheter valves? *J Am Coll Cardiol* 2009;53:1892-3.
26. Tzikas A, Piazza N, van Dalen BM, et al. Changes in mitral regurgitation after transcatheter aortic valve implantation. *Catheter Cardiovasc Interv* 2010;75:43-9.

Summary and Conclusions

Transcatheter aortic valve implantation (TAVI) is a new treatment strategy for aortic stenosis. This thesis has evaluated the role of advanced imaging in the pathophysiology of aortic stenosis as well as in the planning, performance and evaluation of TAVI. In the introduction, the background and the outline of the thesis were brought into attention.

PART I. PATHOPHYSIOLOGY OF AORTIC STENOSIS

In Chapter 2, using speckle tracking echocardiography, we showed that LV twist increases proportionally to the severity of aortic stenosis, which might serve as a compensatory mechanism to maintain systolic LV function. In addition, we found that, in aortic stenosis, LV diastolic untwisting is delayed and the untwisting rate is reduced. In Chapter 3, this Thesis provides evidence that LV twist and LV twist-to-shortening ratio are increased in patients with aortic stenosis and are related to symptoms (angina) or electrocardiographic signs (strain) compatible with subendocardial ischemia.

PART II. IMAGING OF THE AORTIC ROOT IN THE PLANNING AND DURING TRANSCATHETER AORTIC VALVE IMPLANTATION

Precise measurement of the aortic annulus is very important for TAVI. In Chapter 4 we found significant differences in the assessment of the aortic annulus by multi slice computed tomography (MSCT), contrast aortography and trans-thoracic echocardiography. MSCT had considerably lower inter-observer variability in comparison with the other two techniques. During TAVI, it is crucial to achieve an optimal fluoroscopic working view projection, with all three aortic cusps depicted in one line. In Chapter 5, the validation of the new software C-THV (Paieon), designed to estimate the optimal projection for TAVI, showed good accuracy when compared to MSCT or to the final operator's choice.

PART III. ADVANCED IMAGING IN THE EVALUATION OF TRANSCATHETER AORTIC VALVE IMPLANTATION

Paravalvular aortic regurgitation and conduction abnormalities are common complications following TAVI. In Chapter 6, we found that TAVI with the Medtronic CoreValve resulted in some degree of paravalvular aortic regurgitation in the majority of patients. Significant regurgitation was associated with a larger aortic annulus, more aortic root calcification and with less oversizing of the prosthesis in relation to the native annulus. In Chapter 7, we reported the frequency of conduction abnormalities following TAVI with the Medtronic CoreValve and its association with the lack of improvement of LV systolic function. Sometimes a prosthetic valve maybe too small in relation to the patient's body size, a condition called prosthesis-patient mismatch. In Chapter 8, we showed that

the indexed effective orifice valve area is increased significantly following TAVI with the Medtronic CoreValve. Although severe prosthesis-patient mismatch was observed in 16% of the patients it was not associated with the clinical outcome. In Chapter 9, we found that, alike patients with severe aortic stenosis that are treated surgically, most patients who undergo TAVI have some degree of mitral regurgitation, which generally remains unchanged post-treatment. Patients in whom mitral regurgitation improved had a lower LV ejection fraction at baseline. Finally, relief of the obstruction caused by the stenotic aortic valve and the normalization of LV afterload is expected to lead in regression of LV mass. In Chapter 10, a significant regression of LV mass was found one year after TAVI. However, regression was incomplete and was not accompanied by an improvement in LV diastolic function.

FUTURE DIRECTIONS

During the last decades, interventional cardiology has been driven by the need for less invasive treatment options. Similarly to the introduction of percutaneous coronary interventions, transcatheter valve therapies have created a lot of enthusiasm in the scientific community. Although the number of TAVI procedures is increasing exponentially year by year, surgical aortic valve replacement remains the “gold standard” treatment. In order for TAVI to become available to all patients suffering from aortic stenosis several issues have to be addressed. With respect to patient safety, the rate of vascular complications, stroke, paravalvular aortic regurgitation and permanent pacemaker implantation has to decrease. In addition, long term durability of the bioprostheses used in TAVI has to be confirmed. The knowledge and experience that has been achieved so far has to be applied in the design and development of new devices. Finally, TAVI-specific cardiovascular imaging techniques should be further developed and tested. In the light of the first randomized clinical trials comparing TAVI with surgery we anticipate that in the near future TAVI is going to become a routine procedure and thousand of patients are going to benefit from it.

Transkatheter aortaklep vervanging (TAVI) is een nieuwe behandelmethode voor patiënten met aorta stenose. Dit proefschrift evalueert de rol van geavanceerde beeldvorming ten aanzien van de pathofysiologie van aorta stenose alsmede de planning, uitvoering en evaluatie van TAVI. De achtergrond en structuur van deze scriptie komen aan bod in de introductie.

DEEL 1. PATHOFYSIOLOGIE VAN AORTA STENOSE

In hoofdstuk 2 is met behulp van speckle tracking echocardiografie aangetoond dat linker ventrikel twist proportioneel toeneemt met de ernst van aorta stenose, wat mogelijk een compensatoir mechanisme weerspiegelt om de systolische linker ventrikel (LV) functie te behouden. Ook vonden we dat bij aorta stenose de LV diastolische untwisting vertraagd is en dat de untwisting snelheid is verminderd. Hoofdstuk 3 van deze scriptie laat zien dat LV twist en de LV twist-to-shortening ratio zijn toegenomen in patiënten met aorta stenose en dat deze zijn gerelateerd aan symptomen als angina of bevindingen op het electrocardiogram die wijzen op subendocardiale ischemie.

DEEL 2. BEELDVORMING VAN DE AORTA WORTEL VOOR DE PLANNING VAN EN GE- DURENDE TRANSCATHETER AORTAKLEP VERVANGING.

Nauwkeurige metingen van de aorta annulus zijn van belang voor TAVI. Hoofdstuk 4 toont dat wij een significant verschil vonden in de annulus dimensies gemeten volgens multi slice computed tomography (MSCT), contrast aortografie en transthoracale echocardiografie. MSCT was geassocieerd met een lagere inter-observer variabiliteit in vergelijking met de andere twee beeldvormende technieken. Tijdens TAVI is het van cruciaal belang om een optimale projectie te verkrijgen bij fluoroscopie, waarbij alle drie de aorta klep bladen in één lijn worden geprojecteerd. In hoofdstuk 5 is aangetoond dat de validiteit van de nieuwe software C-THV (Paieon), ontworpen om een optimale projectie te schatten voor TAVI, nauwkeurig is als deze vergeleken wordt met MSCT of de projectie keuze van de behandelaar.

DEEL 3. GEAVANCEERDE BEELDVORMING IN DE EVALUATIE VAN TAVI

Para-prothetische aorta insufficiëntie en geleidingsstoornissen vormen een frequente complicatie na TAVI. In hoofdstuk 6 is aangetoond dat TAVI met de Medtronic Core-Valve prothese resulteerde in para-prothetische aorta insufficiëntie in het merendeel van de patiënten. Ernstige aorta insufficiëntie was geassocieerd met een grote aorta annulus, meer aorta wortel calcificatie en met minder 'oversizing' van de prothese in vergelijking met de natieve annulus. Hoofdstuk 7 beschrijft de frequentie van geleidingsstoornissen

na TAVI met de Medtronic CoreValve prothese, alsmede de relatie met verminderde verbetering van de LV systolische functie. Soms is de prothese te klein in vergelijking tot de afmetingen van de patiënt ('prosthesis-patient mismatch'). In hoofdstuk 8 is aangetoond dat de geïndexeerde effectieve aortaklep oppervlakte significant is toegenomen na TAVI met de Medtronic CoreValve prothese. Hoewel ernstige 'prosthesis-patient mismatch' was geobserveerd in 16% van de patiënten na TAVI werden er geen klinische symptomen geobserveerd. In hoofdstuk 9 vonden we dat de meeste patiënten die TAVI ondergaan in beperkte mate een mitralis klep insufficiëntie hebben, hetgeen eveneens bekend is bij chirurgische klepvervanging, die meestal onveranderd blijft na de ingreep. Patiënten met een verbetering van de mitralis insufficiëntie hadden een lagere LV ejectie fractie voor de procedure. Het verhelpen van de door aorta stenose veroorzaakte obstructie en daarmee normalisatie van de LV afterload leidt naar verwachting tot regressie van de LV massa. In hoofdstuk 10 vonden wij een significante regressie van de LV massa 1 jaar na TAVI. De regressie was echter incompleet en niet geassocieerd met een verbetering van de LV diastolische functie.

TOEKOMSTVISIE

Gedurende de laatste decennia is de interventie cardiologie enorm beïnvloed door de vraag naar minimaal invasieve behandelmethoden. Evenals bij de introductie van de percutane coronaire interventie heeft de transkatheter klep therapie veel enthousiasme te weeggebracht in 'de wetenschappelijke wereld'. Hoewel het aantal TAVI procedures exponentieel is toegenomen, blijft de conventionele chirurgische aortaklep vervanging de gouden standaard. Voordat TAVI toegepast kan worden in alle patiënten met aorta stenose, dient de patiënt veiligheid verder verzekerd te worden door periprocedurele problemen, zoals vasculaire complicaties, beroerte, para-prothetische aorta insufficiëntie en de noodzaak tot pacemaker implantatie, te beperken. Eveneens dient de duurzaamheid van de bioprothesen die momenteel gebruikt worden voor TAVI, aangetoond te worden. De huidige kennis en ervaring moet daarom efficiënt worden gebruikt voor nieuwe ontwerpen en de ontwikkeling van toekomstige prothesen. Tot slot is het van belang om de voor TAVI specifieke beeldvormingstechnieken verder te ontwikkelen en testen. In het licht van de eerste trials die TAVI met chirurgische klepvervanging vergelijken is het waarschijnlijk dat TAVI in de nabije toekomst een routine behandeling zal worden waarbij tal van patiënten gebaat zullen zijn.

It was a cold morning in January 2008 when I entered the office of Professor Patrick W. Serruys, on the fifth floor of the Thoraxcenter, to be interviewed for the Fellowship position I had applied for. It was this half hour conversation which gave birth to this thesis. I can honestly say, that conversation changed the course of my career. I still vividly remember the Professor telling me, “Thirty years ago, when interventional cardiology was in its infancy, we were developing our technical skills in an empirical way, and at the same time we were struggling to understand and establish the basic principles for percutaneous interventions on the human heart. Today, things have changed dramatically, and relevant scientific knowledge is growing exponentially. If you want to become a good interventionalist, besides developing your technical skills, you must dig into this knowledge. By learning how to design, conduct and publish a research assignment, besides discovering new findings, you will be able to judge for yourself and choose the information you need in order to provide high quality treatment to your patients.” I listened to him, and he guided me well. I would like to thank Professor Serruys for, among many other things, teaching me how to approach scientific judgment, for his generous interest in my research inquiries, for the time we spent together reviewing my work, and for his kind help and advice with my future plans. Most of all, however, I would like to thank Professor for inciting my inspiration!

When I first met Marcel Geleijnse in his office, I felt him to be somewhat distant. He may very well have thought, “What is an interventional cardiology Fellow doing at the echocardiography department?” First impressions, however, are sometimes mistaken, and this was one of those times. It didn’t take us very long to build a good collaborative relationship. Within a week of our first meeting, a detailed protocol concerning echocardiography for the patients referred for TAVI was created and applied. The results were immediate with regard to the completeness and quality of the studies. As our working relationship grew, so did the fruitfulness of our scientific discussions, which I found to be succinct and level-headed. Of course, there were heated discussions as well, but these revolved around European politics. I would like to thank Marcel for his intelligent and sharp comments, for his frankness and for his wonderful ability to start a meaningful debate out of the blue.

Bas van Dalen was finishing his thesis when I met him. Despite the fact that he was overburdened with assignments - the most challenging being having Marcel as boss - he did not mince his time and effort when it came to my research projects, and always guid-

ed me patiently through the misty paths of advanced echocardiographic analysis. I thank him for his invaluable help and for his steadfast kind, decent and friendly manners.

Nicolas Van Mieghem was introduced to me in late August of 2009 as the new Fellow of the valve program. He was inadvertently assigned my desk and computer in the Fellows' room; it was not the most auspicious manner in which to begin collaboration as Fellows at the Thoraxcenter. However, as it turned out, Nicolas and I made a great team. We worked together on many projects and steadily developed a solid working and personal relationship. I thank him for being such an ideal roommate and colleague.

My relationship with Nicolo Piazza, a.k.a. Nick, was, and is, reflective of our Mediterranean origins. Our interactions (and antics) were varied - from silly fights, to sophisticated "brainstorming" sessions, from the ABCs of statistics, to joint research achievements. I shall miss our coffee meetings across the Kunsthal museum on those (rare) Rotterdam sunny days. I thank him for introducing me to the Montreal Heart Institute, which has been the latest step in my career; and, most of all, I thank him for being a wonderfully playful co-voyager in our Thoraxcenter "adventure." It was fun!

Rutger-Jan Nuis, a medical student who was involved in the valve program, is a brilliant young man. Without having previous experience in research, he worked hard on the clinical database, providing valuable information for the majority of my research projects. I want to thank Rutger for his genuine spirit of collaboration, his sense of humour, and his open-mindedness. I would also like to thank Amber Otten, the medical student who was succeeded by Rutger and who helped me in my initial research projects.

An important part of this Thesis resulted from my collaboration with Carl Schultz. I would like to thank him for his sharp and creative commentary that helped me improve my scientific methodology and thinking. I would also like to thank Chris Gyrisis for guiding me through my first steps in Rotterdam and the Thoraxcenter. Although my area of research did not allow me to work closely with most of the interventional cardiology Fellows, I would like to mention and to thank all the Fellows at the Thoraxcenter for helping to create an exceptional working environment: Scot Garg, Yoshinobu Onuma, Hector Garcia-Gracia, Takayuki Okamura, Joanna Wykrzykowska, Zhu Jun Shen, Eun-Seok Shin, Josep Gomez, Salvatore Brugaletta, Roberto Diletti and Bill Gogas.

I would like to thank Giovanna Sarno and Juan-Luis Gutierrez Chico who became my closest friends in Rotterdam. On many occasions, and especially when things were getting bumpy, they helped me "decompress" and move on with my work. I miss their company, but I am confident that we will keep in close touch, as we have done since leaving Rotterdam.

During the TAVI procedures, I had the opportunity to work in the catheterization laboratory. I want to express my gratitude to all the nurses, technicians, and anesthesiologists who kindly supported my efforts. I would also like to thank the staff of the echocardiography department, especially Vim Vletter, for their help in the pre-procedural and follow-up studies. I would like to thank Ron van Domburg for his advice on statistical analyses, as well as the administrative personnel of the Erasmus Medical Center for their kind sup-

port whenever I needed them. I would especially like to thank Willeke Tomasouw and Kim Levisson for helping me with the arrangements for the defense of my thesis. During my stay in Rotterdam, I participated in the editorial board meetings of the EuroIntervention Journal. I would like to thank Paul Cummins, Sylvie Lhoste, and the associate editors, with whom I sat in the editorial board meetings of the Journal. The experience was invaluable.

Before coming to Rotterdam, I trained in cardiology at the First Cardiology Department of the Georgios Papanikolaou Hospital in Thessaloniki, Greece. It was there that the bases of my career as a cardiologist were founded. I would like to thank the Chief of the Department, Dr. Zarifis, the physicians and staff of the Department. I especially like to thank Dr. Vasilis Stravelas for his help and support through my first steps in the Cath Lab.

It is not easy for parents to have their children living abroad. I want to thank my father, Giannis, and my mother, Zoi, for their love and support during my Fellowship in Rotterdam. I am grateful for being their son; their role in my personal development has been determinant. I would also like to thank my younger sister, Danai, for her love and generous spirit; she has always been there for me.

Back in 2008, when my wife Katerina and I were discussing our future plans, it was her who insisted that we move to Rotterdam. During our first months in Holland, while I was trying to find my pace at the Thoraxcenter, Katerina managed to overcome a number of challenges in order to provide our two-year old daughter, Zoi, and me a warm home environment. She has been a loving partner, a wonderful mother, and a wise advisor. By seeing things from a different perspective, she helped me to find the personal balance I needed in order to be efficient and productive in my work. I would not have succeeded without her. She has also put great effort in editing this book, which is axiomatically dedicated to her. I want to thank Katerina for bringing light into my life, for the years that have passed and for the years that are coming. I would also like to thank my young daughter, Zoi, who has spent half her life in Holland, and who, without knowing it, helped me tremendously just by making me happy!

When I met Dr. Peter de Jaegere a few months before starting my Fellowship, I expressed my strong interest in transcatheter valve therapies. The idea of focusing on the role of imaging - especially echocardiography - in TAVI, was entirely his. He helped me prepare a research proposal with which I won the EAPCI Research Grant for 2009. From the first day I joined the TAVI team at the Thoraxcenter, Dr. de Jaegere was unwavering in his efforts to teach me all that he could about clinical research. He was always generous in his support, but he was also quite demanding. I remember his corrections on my first manuscript; the paper had so many red spots that I told him it looked like it developed a rash. Fortunately, in the subsequent manuscripts the red spots were fewer and a period of vigorous scientific development began; we spent hundreds of hours reviewing my papers and presentations, and although those hours spent together were always amicable, they were not without differences of opinion. At the end of each session I felt exhausted but satisfied because the quality of my work was clearly improving, and improving fast. I

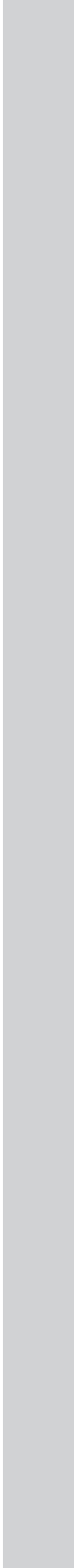
would like to thank Dr. de Jaegere for being a spirited scientist, a vigilant supervisor, and a great teacher. I would like to thank Peter for his compassionate and insightful character. I was, indeed, very lucky to have him as a supervisor, and I am truly grateful for being his friend. The cover of this book is dedicated to him.

1. **Tzikas A**, van Dalen BM, Van Mieghem NM, Gutierrez-Chico JL, Nuis RJ, Kauer F, Schultz CJ, Serruys PW, de Jaegere PP, Geleijnse ML. Frequency of conduction abnormalities after transcatheter aortic valve implantation with the Medtronic-CoreValve and the effect on left ventricular ejection fraction. *Am J Cardiol.* 2011;107:285-9.
2. **Tzikas A**, Geleijnse ML, Van Mieghem NM, Schultz CJ, Nuis RJ, van Dalen BM, Sarano G, van Domburg RT, Serruys PW, de Jaegere PP. **Left ventricular mass regression** one year after transcatheter aortic valve implantation. *Ann of Thorac Surg.* 2011 Mar;91(3):685-91
3. **Tzikas A**, Piazza N, Geleijnse ML, van Mieghem N, Nuis RJ, Schultz C, van Geuns RJ, Galema TW, Kappetein AP, Serruys PW, de Jaegere PP. Prosthesis-patient mismatch following transcatheter aortic valve implantation with the CoreValve Revalving System in patients with aortic stenosis. *Am J Cardiol.* 2010;106:255-60.
4. **Tzikas A**, Piazza N, van Dalen BM, Schultz C, Geleijnse ML, van Geuns RJ, Galema TW, Nuis RJ, Otten A, Gutierrez-Chico JL, Serruys PW, de Jaegere PP. Changes in mitral regurgitation after transcatheter aortic valve implantation. *Catheter Cardiovasc Interv.* 2010;75:43-9.
5. **Tzikas A**, Schultz C, Van Mieghem NM, de Jaegere PP, Serruys PW. **Optimal projection estimation** for transcatheter aortic valve implantation based on contrast aortography: validation of a prototype software. *Catheter Cardiovasc Interv.* 2010;76:602-7.
6. Van Mieghem NM, Piazza N, Anderson RH, **Tzikas A**, Nieman K, McGhie JS, Geleijnse ML, Feldman T, Serruys PW, de Jaegere PP. Anatomy of the mitral valvar complex and its implications for transcatheter interventions for mitral regurgitation. *J Am Coll Cardiol.* 2010;56:617-26.
7. Van Mieghem N, Nuis R, Piazza N, **Tzikas A**, Ligthart J, Schultz C, de Jaegere PP, Serruys PW. Vascular complications with transcatheter aortic valve implantation using the 18 Fr Medtronic CoreValve System®: the Rotterdam experience. *EuroIntervention* 2010;5:673-679.
8. **Tzikas A**, Schultz CJ, Piazza N, Moelker A, Van Mieghem NM, Nuis RJ, van Geuns RJ, Geleijnse ML, Serruys PW, de Jaegere PPT. Assessment of the aortic annulus by multislice computed tomography, contrast aortography and trans-thoracic echocardiography in patients referred for transcatheter aortic valve implantation. *Catheter Cardiovasc Interv.* 2010 (in press)

9. Van Mieghem NM, **Tzikas A**, Nuis RJ, Schultz C, de Jaegere PP, Serruys PW. How should I treat a staggering TAVI procedure? *EuroIntervention*. 2010;6:418-423.
10. **Tzikas A**, Piazza N, Serruys PW, de Jaegere P. Transcatheter Mitral Valve Repair: Is there a future? *Hospital Chronicles* 2010; Suppl. 149-50.
11. Piazza N, **Tzikas A**, Van Mieghem NM, Lange R, de Jaegere P, Serruys PW. Interpreting the current data on transcatheter aortic valve implantation: a difficult task. *Eur Heart J* 2010;12 Suppl E:E41-E45.
12. Schultz C, Moelker A, **Tzikas A**, Piazza N, de Feyter P, van Geuns RJ, Serruys PW, Krestin G, de Jaegere P. The use of MSCT for the evaluation of the aortic root before transcatheter aortic valve implantation: the Rotterdam approach. *EuroIntervention*. 2010;6:505-511.
13. Piazza N, Nuis RJ, **Tzikas A**, Schultz C, Onuma Y, Otten A, Garcia Garcia H, van Domburg R, van Es GA, van Geuns RJ, de Jaegere PP, Serruys PW. Persistent conduction abnormalities and requirements for pacemaking 6 months after transcatheter aortic valve implantation. *EuroIntervention* 2010;6:475-484.
14. Schultz CJ, Moelker A, **Tzikas A**, Rossi A, van Geuns RJ, P de Feyter, Serruys PW, de Jaegere PP. Cardiac CT: necessary for precise sizing for transcatheter aortic valve implantation. *EuroIntervention*. 2010;6 Suppl G:G6-G13.
15. Schultz CJ, Papadopoulou SL, Moelker A, **Tzikas A**, Nuis RJ, Gutiérrez Chico JL, Rossi A, ten Kate GJR, Dijkshoorn M, Mollet N, Geleijnse ML, de Feyter P, de Jaegere PP, Serruys PW. Transaortic flow velocity from dual source MDCT for the diagnosis of aortic stenosis severity. Proof of concept. (submitted)
16. Schultz CJ, **Tzikas A**, Moelker A, Rossi A, Nuis RJ, Piazza N, Mollet N, Krestin G, de Feyter P, Serruys PW, de Jaegere PP. Determinants on MSCT of paravalvular aortic regurgitation after transcatheter aortic valve implantation. (submitted)
17. Nuis RJ, Van Mieghem NM, **Tzikas A**, Piazza N, Otten A, Cheng JM, van Domburg RT, Betjes M, Serruys PW, de Jaegere PP. Frequency, determinants and prognostic effects of acute kidney injury and red blood cell transfusion in patients undergoing transcatheter aortic valve implantation. *Catheter Cardiovasc Interv*. 2010 (in press)
18. van Dalen BM, **Tzikas A**, Soliman OI, Kauer F, Heuvelman HJ, Vletter WB, Ten Cate FJ, Geleijnse ML. Assessment of subendocardial ischemia in aortic stenosis: a study using speckle tracking echocardiography. (submitted)
19. Schultz C, **Tzikas A**, Nuis RJ, Brada R, Moelker A, Rossi A, Van Mieghem NM, van Geuns RJ, Krestin GP, de Feyter P, de Jaegere PT, Serruys PW. Sizing for percutaneous valve replacement based on aortic sinus dimensions and clinical parameters – a feasibility study using MSCT. (submitted)
20. Van Mieghem NM, Nuis RJ, **Tzikas A**, Piazza N, Schultz C, Serruys PW, Jaegere PP. Prevalence and prognostic implications of baseline anemia in patients undergoing transcatheter aortic valve implantation. (submitted)

21. Nuis RJ, Piazza N, Otten A, **Tzikas A**, Van Mieghem NM, Schultz C, van Geuns RJ, Serruys PW, de Jaegere PP. In-hospital complications after transcatheter aortic valve implantation revisited according to the Valve Academic Research Consortium definitions. (submitted)
22. **Tzikas A**, Schultz C, Piazza N, van Geuns RJ, Serruys PW, Jaegere PP. Perforation of the membranous inter-ventricular septum following transcatheter aortic valve implantation. *Circulation Cardiovasc Interv.* 2009;2:582-3.
23. van Dalen BM, **Tzikas A**, Soliman OI, Kauer F, Heuvelman HJ, Vletter WB, Ten Cate FJ, Geleijnse ML. Left ventricular twist and untwist in aortic stenosis. *Int J Cardiol.* 2009 (in press)
24. Schultz C, Moelker A, Piazza N, **Tzikas A**, Otten A, Nuis RJ, van Geuns RJ, de Feyter P, Krestin G, Serruys PW, de Jaegere PP. 3D evaluation of the aortic annulus using multislice computer tomography. Are manufacturer's guidelines for sizing helpful? *Eur Heart J.* 2010;31:849-56.
25. Piazza N, **Tzikas A**, de Jaegere PP, Serruys PW. Transcatheter aortic valve implantation: what lies ahead? *Confluence – Issues in Interventional Cardiology* 2009;1:1-7.
26. Piazza N, Wenaweser P, van Gameren M, Pilgrim T, **Tzikas A**, Otten A, Nuis R, Onuma Y, Cheng JM, Kappetein AP, Boersma E, Juni P, de Jaegere P, Windecker S, Serruys PW. Relationship between the logistic EuroSCORE and the Society of Thoracic Surgeons Predicted Risk of Mortality score in patients implanted with the CoreValve ReValving System-A Bern-Rotterdam Study. *Am Heart J.* 2010;159:323-329.
27. de Jaegere P, Piazza N, **Tzikas A**, Scultz C, Serruys PW. Steps in CoreValve Implantation. In Serruys PW, Piazza N, Cribier A, Webb J, Laborde JC, de Jaegere P, eds. Transcatheter aortic valve implantation. Tips and tricks to avoid failure. New York: *Informa Healthcare*, 2009.

Apostolos Tzikas was born on December 5th, 1974, in Thessaloniki, Greece. After graduating from secondary school in 1992, he started his studies in medicine, at the Aristotle University of Thessaloniki. Upon graduation in 1999, he started his training in General Practice in Chios General Hospital, Chios Island, Greece. Later, he trained in Aviation Medicine and worked as a doctor for the Hellenic Military Air Force, both in Athens and Thessaloniki. As part of his training in Cardiology, he was a resident at the 1st Department of Internal Medicine, in AHEPA University Hospital, Aristotle University of Thessaloniki from 2002 to 2004. He did his main Cardiology training at the 1st Cardiology Department of the “George Papanikolaou” Hospital in Thessaloniki, from 2004 to 2008. He obtained his Cardiology Degree in 2008. In 2009, he started working as a Research Fellow in Interventional Cardiology, at the Transcatheter Valve Program, at the Thoraxcenter, Erasmus Medical Center, in Rotterdam, the Netherlands. Under the supervision of Dr. P.P.T de Jaegere he focused on the role of advanced imaging in transcatheter aortic valve implantation, resulting in this thesis. Apostolos Tzikas is currently working as a Clinical Fellow, in Interventional Cardiology for Structural Heart Disease, at the Montreal Heart Institute, in Montreal, Canada.



Additional Financial Support for this Thesis
was generously provided by:

Erasmus University Rotterdam

Netherlands Heart Foundation

Psimitis S.A.

Medtronic Hellas S.A.

Cardialysis B.V.

